Hawaiian montane peatland ecology and history through analysis of testate amoebae and Cladocera

By

Kevin D. Barrett

A dissertation submitted in partial fulfillment of

the requirements for the degree of

Doctor of Philosophy

(Botany)

at the

UNIVERSITY OF WISCONSIN-MADISON

2019

Date of final oral examination: 8/26/2019

This dissertation is approved by the following members of the Final Oral Committee:

Dr. Sara C. Hotchkiss, Professor, Botany

Dr. Thomas Givnish, Professor, Botany

Dr. Bret Larget, Professor, Botany

Dr. Jack W. Williams, Professor, Geography

Dr. Robert K. Booth, Professor, Earth and Environmental Science, Lehigh University

Acknowledgements

This research is the result of several important contributions. I am indebted to the support from mentors, collaborators, donors, agencies, cowboys, ranchers, neighbors, friends, and family.

First, and emphatically, I thank my advisor Sara Hotchkiss who has been the biggest advocate of this research and is a role model of the scientist, teacher, and mentor I aim to be.

I thank my thesis committee Tom Givnish, Bret Larget, Jack Williams, and Bob Booth for their mentorship, constructive feedback, and for challenging me to meet a high standard of scholarship. I want to thank Bob Booth in particular for his mentorship over the past decade. Bob introduced me to ecology, which was a watershed moment. Bob also introduced me to my first peatland. He put faith in me as an undergraduate and taught me the techniques I use in this research. The skills I learned with the Booth Lab, at the bench and in the field, made this research endeavor possible, so I also thank Michael Clifford and Eric Klein.

Members of the Hotchkiss Lab have been the nuts and bolts of the progress I have been able to make. I thank my co-author Patricia Sanford who first spotted cladocerans in my peat samples and taught me cladoceran identification. Patricia continues to inspire and amaze me with her knowledge of the microscopic universe. She is an encyclopedia of paleoecological and paleolimnological remains and has saved me uncountable hours of researching the source of the fragments on slides. I thank my colleague and friend Soo Hyun Kim whose contributions to this research deserve a chapter of their own. And I thank Kristin Michels, Michael Peyton, Lisa Schomaker, Danielle Gygi, Bridget Gilmore, and the rest of members of the Hotchkiss Lab and Paleotea for their important feedback over the years.

I thank my collaborators at the Beilman Lab, Dave Beilman and Olivia Mahronic, and the University of Hawai‘i – Mānoa for analyses and sharing peat sediment from Kohala, and for welcoming me into their group to study the history of Hawaiian peatlands.

Mahalo to the scientists in Hawai‘i, and especially Peter Vitousek, for establishing the foundation of research that I am humbled to contribute to. Mahalo nui loa to Kahua Ranch, Ponoholoholo Ranch, and Parker Ranch for their generous accessibility to field sites, and to the Kohala Forest Reserve System and Natural Area Reserve System for their continued stewardship of these lands.

Thank you Diana, Gary, Eliza, Rebecca, Keenan, Kaija, Stacy, and Rachel for the warmth and laughs along the way.

This research was possible possible thanks to a Flora Aeterna Research Fellowship, Davis Award, and Demeter Award from the UW-Madison Botany Department, a visiting student award from LacCore of the University of Minnesota, and a student research award from the Palynological Society.

Table of Contents

Hawaiian montane peatland ecology and history through analysis of testate amoebae and Cladocera

By Kevin D. Barrett

Abstract

Tropical montane peatlands in Hawai‘i are important repositories of biodiversity and water resources, and paleoenvironmenal archives preserved in Hawaiian peatland deposits are a rare cache of past terrestrial environments and climate in the middle of the North Pacific. I researched the distribution and ecology of testate amoebae, single-celled protists that produce their own shells (“tests”) and Cladocera (water fleas) in montane peatlands on Kohala and on windward Mauna Loa on Hawai‘i Island to 1) describe the spatial distribution of testate amoebae diversity in relation to Hawaiian peatland envirnmental gradients, 2) develop a new approach for peatland paleoecology that integrates testate amoebae (TA) and Cladocera data as proxies for peatland water-table depth, and 3) produce new paleorecords of peatland paleohydrology based on subfossil TA and Cladocera in Hawaiian peat cores.

I analyzed correlations between peatland environmental gradients and testate amoebae by using taxonomic and functional trait approaches. TA are sensitive to biotic and abiotic peatland variations in Hawai‘i, including composition of peatland surface vegetation, soil bulk density, water table depth, and pH. *Sphagnum palustre* L. in Kohala generates vertical and chemical gradients on the peatland surface that resemble peatland environmental gradients in temperate and boreal regions. TA taxonomic diversity was greatest in habitats dominated by emergent rushes in the genus *Juncus* L. and lowest in *Sphagnum* hummocks.

Peatland hydrology, measured as water-table depth, was the dominant environmental control on TA distribution in Kohala. Transfer functions relating species assemblage data to water-table depth performed well under leave-one-site-out cross-validation (RMSEP = 9.75 cm, $r^2 = 0.62$). A peat core spanning the last 300 years shows that peatland water tables dropped from 1700 to 1850 CE, then rose to a near-surface level between 1900 and 1930 CE, a period characterized by anomalously high rainfall in Hawai‘i. A 4000-yr peat record had evidence of abrupt peatland drying and a shift to an oxidizing state from 2.7 to 1.6 thousand years ago (ka) that interrupted two periods of high and stable water tables, from 3.3 to 2.7 ka and 1.6 to 1.2 ka. The period of drying overlaps with a period of increased aridity inferred from paleorecords on Oahu, Maui, and Moloka‘i (from 2.2 to 1.5 ka) and occurred during a period of increased El Niño acitivity. These results provide evidence for a centuries-long period of increased aridity in Hawai‘i and point to the occurrence of statewide drought, likely associated with El Niño-like conditions in the North Pacific, between 2.2 and 1.5 ka.

Introduction

Peatland services

Peatlands are globally important terrestrial ecosystems. While covering less than 3% of the earth's land surface, peatlands contain more than 25% of the total terrestrial soil carbon stock (Page *et al.* 2011). This massive carbon stock is credited to the accumulation of partiallydecayed and carbon-dense layers of peat. On average, peatlands in the boreal zone hold up to seven times more carbon per hectare than neighboring ecosystems on mineral soils; in the tropics they hold up to 10 times more carbon than mineral soils (Joosten and Couwenberg 2008). Since living peatlands accumulate and store carbon underground over long timescales, and also emit mehane (CH_4), and because carbon dioxide (CO_2) and CH_4 are greenhouse gases, peatlands are also crucial regulators of global climate.

But the value of peatlands extends beyond their role in the global carbon cycle. Peatlands improve drinking water (Van der Wall *et al*. 2011) and regulate local watersheds by storing water and reducing overland surface-flow rates during floods (Munang *et al.* 2014). Due to often extreme environmental conditions (anoxia, and in many cases acidity and low nutrients), peatland biota can be highly specialized with many species that are found only in peatlands, so peatlands represent important reserves of biodiversity. One consequence of anoxia and slow decomposition is that peatlands also have the ability to store records of past climate, vegetation, and environment within waterlogged soils. Studies of peat archives have greatly contributed to our understanding of environmental changes, including the timing and drivers of regional vegetation change (Booth *et al*. 2012), and regional to global climate variability (Booth *et al*. 2006, Chambers *et al*. 2007).

Tropical peatlands

Peatlands also occur broadly in the humid tropics where rainfall is abundant and topographic (*e.g.* flat) and edaphic (*e.g.* presence of confining layer, such as clay) features result in waterlogged soil conditions (Page *et al.* 2011). Much of the attention on tropical peatlands has been focused on their role in the global carbon cycle. This is appropriate given ongoing trends of tropical peatland draining and degradation, primarily for agriculture and extraction services, that have contributed to alarming amounts of greenhouse gas emissions in recent decades (Hooijer *et al.* 2010), resulting in new multi-national frameworks to mitigate peatland losses and conserve existing peatland area (IPCC Special Report, Climate Change and Land, 2019).

In addition to direct modification of tropical peatlands through land use, anthropogenic influence can damage tropical peatland ecological services indirectly through introductions of exotic plants and animals, at times intentionally (*e.g.* domestic animals). For example, the humid, high-altitude Andean páramo ecosystem, a biodiverse grassland with numerous wetlands and peatlands, contains areas that have been exploited for cattle grazing for > 200 years (Salvador *et al.* 2014). In Hawai‘i, non-native feral ungulates cause considerable damage to montane peatlands, which has prompted major efforts to exclude or curtail ungulate expansion into those areas (Medeiros *et al*. 1991). These disturbances can degrade peatlands as a result of trampling and nutrification from animal waste (Sjögersten *et al.* 2011), which can in turn provide opportunities for exotic plant species.

High-altitude tropical peatlands (hereafter tropical montane peatlands), may be especially sensitive to climate change because these ecosystems often occupy a narrow band of suitable climate along or atop mountains where changes in precipitation, temperature, and relative humidity are expected to be pronounced (Loope & Giambelluca 1998, Buytaert *et al.* 2011).

Crucial ecological services provided by tropical peatlands—carbon storage, water regulation, and biodiversity conservation—may be altered or degraded by these climate changes. It is therefore imperative to develop a dense network of spatial and temporal environmental biomonitoring datasets dedicated to understanding environmental trajectories of tropical peatlands. This can be accomplished because these ecosystems retain information about past environments preserved in underlying peat.

Bioindicators

The application of bioindicators is an efficient way to study peatland environmental change (Bonn *et al.* 2016). A bioindicator in this context is a species whose presence and abundance require, and can therefore be used to infer, the presence of particular ecological or environmental conditions. A useful suite of bioindicators is taxonomically (and morphologically) diverse, and each indicator taxon will occupy discrete environmental conditions. Useful bioindicators should also be sensitive to environmental perturbations and have rapid generation times so that their occurence or absence reflects environmental changes. A group of organisms that is abundant in peatlands and has been exceptionally useful as bioindicators in contemporary and paleoecological studies of peatlands is the testate amoebae (Mitchell *et al.* 2008).

Testate amoebae are free-living, single-celled protists that produce their own shells ("tests"). While they are often treated as a uniform ecological group, testate amoebae include members from at least three distantly related phylogenetic groups that have distinct morphologies: Arcellenida, Euglyphida, and Amphitremida (Kosakyan *et al.* 2016). Testate amoeba species are morphologically discrete and taxonomically diverse. As a functional group, testate amoebae are the top predators in the soil microbial loop, and their species assemblages are

correlated with differences in availability of the microbial food they prey on (Jassey *et al.* 2013, Krashevska *et al.* 2008). Testate amoebae are also sensitive to peatland environmental conditions, chiefly moisture and pH, which renders the group useful to peatland biomonitoring around the globe, including studies in North America (Booth 2008), Europe (Amesbury *et al*. 2016), Russia (Bobrov *et al*. 1999), China (Qin *et al*. 2013), New Zealand (Charman 1997), Patagonia (Van Bellen *et al*. 2014), and Australia (Zheng *et al*. 2019). Lastly, the shells of testate amoebae are resistant to decay and many tests preserve well in anoxic underground peat. Consequently, the testate amoebae assemblage in any given layer of peat is a clue to the peatland surface conditions that existed when those individuals were alive, after considering the effects of taphonomy, sediment accumulation, and time-averaging.

Testate amoebae in Hawaiian montane peatlands

Here I focus on testate amoebae as bioindicators in montane peatlands in Hawai‘i. Testate amoebae research in the tropics is not as extensive as for higher latitudes, however the research is expanding and the initial results are promising. Testate amoebae have been extensively studied as bioindicators in tropical montane cloud forest soils in Ecuador (Krashevska *et al.* 2007, 2008, 2014), and experiments have shown that testate amoebae responded more strongly to precipitation exclusion than other soil microorganisms (Krashevska *et al*. 2012). Peatland testate amoebae have now been characterized in both lowland (Peruvian Amazon, Swindles *et al.* 2014) and montane tropical peatlands (Columbian páramo, Liu *et al.* 2019) and these studies confirmed that tropical testate amoebae were reliable environmental and paleoenvironmental indicators.

Hawai‘i is an excellent location to extend testate amoebae-based approaches, for several reasons. First, montane peatlands exist on all five major Hawaiian islands. Second, the

vegetation structure of Hawaiian montane peatlands (*i.e. Sphagnum* hummock-hollow microtopography and sedge tussocks) shares striking similarities with temperate and boreal peatlands (Vogl & Henrickson 1971, Canfield 1986), which have been extensively studied through analysis of testate amoebae. Third, testate amoebae have not been comprehensively described in Hawai‘i apart from cursory observations at the turn of the 20th century (Richters 1908). Fourth, microbial diversity in Hawaiian peatlands is unknown, but surveys of microbial diversity in Hawai‘i’s few lakes and a submarine volcano suggest that Hawai‘i is a hot spot of microbial biodiversity and endemism (Donachie *et al.* 2004). Furthermore, bacterial biomass and diversity is higher in Hawaiian forest soils than would be expected of isolated, tropical islands with relatively low plant diversity when compared with continental ecosystems (Nüsslein and Tiedje 1998). And, finally, paleoenvironmental reconstructions based on the testate amoebae approach can complement a rich body of paleoecological research of the vegetation and climatic history of the Hawaiian Islands from peat and lake sediment archives (Selling 1948, Athens *et al.* 1992, Athens and Ward 1993, Athens 1997, Burney *et al*. 1995, Hotchkiss 1998, 2004, Hotchkiss and Juvik 1999, Uchikawa *et al*. 2010, Pau *et al*. 2012, Crausbay *et al*. 2012, 2014a, b, Beilman *et al*. 2019).

In this thesis, I use testate amoebae as bioindicators of spatial and temporal environmental variability in montane peatlands in Hawai‘i Island. I focus on the wet forest – montane peatland ecosystem complex on Kohala Volcano, where peatlands are numerous, and a series of smaller, younger peatlands on Mauna Loa Volcano. In Chapter 1, I describe fine-scale environmental heterogeneity and testate amoebae diversity in montane peatlands through taxonomic and functional trait frameworks, and I evaluate community-environment relationships that are useful for biomonitoring applications. In Chapter 2, I evaluate the relationship between

testate amoebae community distribution and peatland hydrology in Hawai‘i. This assessment involves modeling environmental data from species data using a transfer function. I develop a novel testate amoebae transfer function that incorporates species data from an unrelated peatland functional group, the Cladocera, or “water fleas”. I apply this transfer function to two Hawaiian peat core records—a *Sphagnum* peatland spanning 300 years (Chapter 2) and a non-*Sphagnum* peatland spanning 4,000 years (Chapter 3)—to reconstruct peatland hydrology. This work unearths the history of Hawaiian peatlands using a framework that can complement a robust portfolio of independent lines of evidence of Hawaiian vegetation and climate change.

References

Amesbury, M. J., Swindles, G. T., Bobrov, A., Charman, D. J., Holden, J., Lamentowicz, M., Mallon, G., Mazei, Y., Mitchell, E. A., Payne, R. J., and T. P. Roland. 2016. Development of a new pan-European testate amoeba transfer function for reconstructing peatland palaeohydrology. Quaternary Science Reviews 152:132-151.

Athens, J. S., Ward, J. V., and S. Wickler. 1992. Late Holocene lowland vegetation, O‘ahu, Hawai‘i. New Zealand Journal of Archaeology 14:9-34.

Athens, J. S., and J. V. Ward. 1993. Environmental change and prehistoric Polynesian settlement in Hawai‘i. Asian Perspectives 32:205-223.

Athens, J. S. 1997. Hawaiian native lowland vegetation in prehistory. *Historical Ecology in the Pacific Islands. Prehistoric Environmental and Landscape Change* (ed. by P.V. Kirch and T.L. Hunt), pp. 248–270, Yale University Press, New Haven and London.

Beilman, D., Massa, C., Nichols, J., Elison Timm, O., Kallstrom, R., and S. Dunbar-Co. 2019. Dynamic Holocene vegetation and North Pacific Hydroclimate recorded in a mountain peatland, Moloka‘i, Hawai‘i. Frontiers in Earth Science 7:188.

Bobrov, A. A., Charman, D. J., and B. G. Warner. 1999. Ecology of testate amoebae (Protozoa: Rhizopoda) on peatlands in western Russia with special attention to niche separation in closely related taxa. Protist 150:125-136.

Bonn, A., Allott, T., Evans, M., Joosten, H., and R. Stoneman (eds.). 2016. Peatland restoration and ecosystem services: science, policy and practice. Cambridge University Press.

Booth, R. K., Notaro, M., Jackson, S. T., and J. E. Kutzbach. 2006. Widespread drought episodes in the western Great Lakes region during the past 2000 years: geographic extent and potential mechanisms. Earth and Planetary Science Letters 242:415-427.

Booth, R. K. 2008. Testate amoebae as proxies for mean annual water-table depth in Sphagnum-dominated peatlands of North America. Journal of Quaternary Science 23:43-57.

Booth, R. K., Brewer, S., Blaauw, M., Minckley, T. A., and S. T. Jackson. 2012. Decomposing the mid-Holocene Tsuga decline in eastern North America. Ecology 93:1841-1852.

Burney, D. A., DeCandido, R. V., Burney, L. P., Kostel-Hughes, F. N., Stafford, T. W., Jr., and H. F. James. 1995. A Holocene record of climate change, fire ecology, and human activity from montane Flat Top Bog, Maui. Journal of Paleolimnology 13**:**209-217.

Buytaert, W., Célleri, R., De Bièvre, B., Cisneros, F., Wyseure, G., Deckers, J., and R. Hofstede. 2006. Human impact on the hydrology of the Andean páramos. Earth Science Reviews 79:53-72.

Buytaert, W., Cuesta-Camacho, F., and C. Tobón, C. 2011. Potential impacts of climate change on the environmental services of humid tropical alpine regions. Global Ecology and Biogeography 20:19-33.

Canfield, J. E. 1986. The role of edaphic factors and plant water relations in plant distribution in the bog/wet forest complex of Alaka'i Swamp, Kaua'i, Hawai'i. Doctoral dissertation, University of Hawai'i-Manoa.

Chambers, F. M., Mauquoy, D., Brain, S. A., Blaauw, M., and J. R. Daniell. 2007. Globally synchronous climate change 2800 years ago: proxy data from peat in South America. Earth and Planetary Science Letters 253:439-444.

Charman, D. J. 1997. Modelling hydrological relationships of testate amoebae (Protozoa: Rhizopoda) on New Zealand peatlands. Journal of the Royal Society of New Zealand 27:465-483.

Crausbay, S. D., and S. C. Hotchkiss. 2012. Pollen-vegetation relationships at a cloud forest's upper limit and accuracy of vegetation inference. Review of Paleobotany and Palynology 184:1-13.

Crausbay, S. D., Genderjahn, S., Hotchkiss, S., Sachse, D., Kahmen, A., and S. Arndt. 2014a. Vegetation dynamics at the upper reaches of a tropical montane forest are driven by disturbance over the past 7300 years. Arctic, Antarctic, and Alpine Research 46:787-799.

Crausbay, S.D., A. Frazier, T. Giambelluca, R. Longman, and S.C. Hotchkiss. 2014b. Moisture status during a strong El Niño explains a tropical montane cloud forest's upper limit. Oecologia 175:273–284.

Donachie, S. P., Hou, S., Lee, K. S., Riley, C. W., Pikina, A., Belisle, C., Kempe, S., Gregory, T. S., Bossuyt, A., Boerema, J., and J. Liu. 2004. The Hawaiian Archipelago: a microbial diversity hotspot. Microbial Ecology 48:509-520.

Hooijer, A., Page, S., Canadell, J. G., Silvius, M., Kwadijk, J., Wosten, H., and J. Jauhiainen. 2010. Current and future CO2 emissions from drained peatlands in Southeast Asia. Biogeosciences 7:1505-1514.

Hotchkiss, S. C. 1998. Quaternary vegetation and climate of Hawai'i. Doctoral dissertation, University of Minnesota, Twin Cities.

Hotchkiss, S. C. and J. O. Juvik. 1999. A Late-Quaternary pollen record from Ka'au Crater, O'ahu, Hawai'i. Quaternary Research 52:115-128.

Hotchkiss, S. C. 2004. Quaternary history of the U.S. tropics. *The Quaternary Period* (ed. by A. Gillespie, S. Porter, and B. Atwater), pp. 441-457, Elsevier, New York.

IPCC Special Report (2019). Climate Change and Land. website: https://www.ipcc.ch/report/srccl/

Jassey, V. E., Chiapusio, G., Binet, P., Buttler, A., Laggoun-Défarge, F., Delarue, F., Bernard, N., Mitchell, E. A., Toussaint, M. L., Francez, A. J., and D. Gilbert. 2013. Above-and belowground linkages in Sphagnum peatland: climate warming affects plant-microbial interactions. Global Change Biology 19:811-823.

Joosten, H. and J. Couwenberg. 2008. Peatlands and carbon. Assessment on peatlands, biodiversity and climate change. Global Environment Centre, Kuala Lumpur and Wetlands International Wageningen 99-117.

Kosakyan, A., Gomaa, F., Lara, E., and D. J. Lahr. 2016. Current and future perspectives on the systematics, taxonomy and nomenclature of testate amoebae. European journal of protistology 55:105-117.

Krashevska, V., Bonkowski, M., Maraun, M., and S. Scheu. 2007. Testate amoebae (protista) of an elevational gradient in the tropical mountain rain forest of Ecuador. Pedobiologia 51:319-331.

Krashevska, V., Bonkowski, M., Maraun, M., Ruess, L., Kandeler, E., and S. Scheu. 2008. Microorganisms as driving factors for the community structure of testate amoebae along an altitudinal transect in tropical mountain rain forests. Soil Biology and Biochemistry 40:2427-2433.

Krashevska, V., Sandmann, D., Maraun, M., and S. Scheu. 2012. Consequences of exclusion of precipitation on microorganisms and microbial consumers in montane tropical rainforests. Oecologia 170:1067-1076.

Krashevska, V., Sandmann, D., Maraun, M., and S. Scheu. 2014. Moderate changes in nutrient input alter tropical microbial and protist communities and belowground linkages. The ISME journal 8:1126.

Liu, B., Booth, R. K., Escobar, J., Wei, Z., Bird, B. W., Pardo, A., Curtis, J. H., and J. Ouyang. 2019. Ecology and paleoenvironmental application of testate amoebae in peatlands of the high-elevation Colombian páramo. Quaternary Research 92:14-32.

Loope, L. L. and T. W. Giambelluca. 1998. Vulnerability of island tropical montane cloud forests to climate change, with special reference to East Maui, Hawaii. *Potential Impacts of Climate Change on Tropical Forest Ecosystems*, pp. 363-377. Springer, Dordrecht.

Medeiros, A. C., Loope, L. L., and B. H. Gagne. 1991. Degradation of Vegetation in Two Montane Bogs. Technical Report, Cooperative National Park Resources Study Unit, 1982-1988.

Mitchell, E. A., Charman, D. J., and B. G. Warner. 2008. Testate amoebae analysis in ecological and paleoecological studies of wetlands: past, present and future. Biodiversity and Conservation 17:2115-2137.

Munang, R., Andrews, J., Alverson, K., and D. Mebratu. 2014. Harnessing ecosystem-based adaptation to address the social dimensions of climate change. Environment: Science and Policy for Sustainable Development 56:18-24.

Nüsslein, K. and J. M. Tiedje. 1998. Characterization of the dominant and rare members of a young Hawaiian soil bacterial community with small-subunit ribosomal DNA amplified from DNA fractionated on the basis of its guanine and cytosine composition. Applied and Environmental Microbiology 64:1283-1289.

Page, S. E., Rieley, J. O. and C. J. Banks. 2011. Global and regional importance of the tropical peatland carbon pool. Global Change Biology 17:798-818.

Pau, S., MacDonald, G. M., and T. W. Gillespie. 2012. A dynamic history of climate change and human impact on the environment from Keālia Pond, Maui, Hawaiian Islands. Annals of the Association of American Geographers 102:748-762.

Qin, Y., Mitchell, E. A., Lamentowicz, M., Payne, R. J., Lara, E., Gu, Y., Huang, X., and H. Wang. 2013. Ecology of testate amoebae in peatlands of central China and development of a transfer function for paleohydrological reconstruction. Journal of Paleolimnology 50:319-330.

Richters, F. 1908. Beitrag zur Kenntnis der Moosfauna Australiens und der Inseln des Pazifischen Ozeans. Zoologische Jahrbücher 26:196-213.

Salvador, F., Monerris, J., and L. Rochefort. 2014. Peatlands of the Peruvian Puna ecoregion: types, characteristics and disturbance. Mires and Peat 15:1-17.

Selling, O. H. 1948. Studies in Hawaiian Pollen Statistics. Part III. On the Late Quaternary History of the Hawaiian Vegetation. Bernice P. Bishop Museum Special Publication 39.

Sjögersten, S., Van der Wal, R., Loonen, M. J., and S. J. Woodin. 2011. Recovery of ecosystem carbon fluxes and storage from herbivory. Biogeochemistry 106:357-370.

Swindles, G. T., Reczuga, M., Lamentowicz, M., Raby, C. L., Turner, T. E., Charman, D. J., Gallego-Sala, A., Valderrama, E., Williams, C., Draper, F., and E. N. H. Coronado. 2014. Ecology of testate amoebae in an Amazonian peatland and development of a transfer function for palaeohydrological reconstruction. Microbial ecology 68:284-298.

Uchikawa, J., Popp, B. N., Schoonmaker, J. E., Timmermann, A., and S. J. Lorenz. 2010. Geochemical and climate modeling evidence for Holocene aridification in Hawaii: dynamic response to a weakening equatorial cold tongue. Quaternary Science Reviews 29:3057-3066.

Van Bellen, S., Mauquoy, D., Payne, R. J., Roland, T. P., Daley, T. J., Hughes, P. D., Loader, N. J., Street-Perrott, F. A., Rice, E. M., and V. A. Pancotto. 2014. Testate amoebae as a proxy for reconstructing Holocene water table dynamics in southern Patagonian peat bogs. Journal of Quaternary Science 29:463-474.

Van der Wal, R., Bonn, A., Monteith, D., Reed, M., Blackstock, K., Hanley, N., Thompson, D., Evans, M., Alonso, I., Allott, T., and H. Armitage. 2011. Mountains, Moorlands and Heaths. Chapter 5, 105-159.

Vogl, R. J. and J. Henrickson. 1971. Vegetation of an alpine bog on East Maui, Hawaii. Pacific Science 25.

Zheng, X., Amesbury, M. J., Hope, G., Martin, L. F., and S. D. Mooney. 2019. Testate amoebae as a hydrological proxy for reconstructing water-table depth in the mires of south-eastern Australia. Ecological Indicator*s* 96:701-710.

-Chapter 1-

Patterns of diversity in the microbial grazers (testate amoebae) in Hawaiian montane peatlands

Kevin D. Barrett[1], Sara C. Hotchkiss[1,2]

University of Wisconsin-Madison, Botany[1]

University of Wisconsin-Madison, Center for Climatic Research[2]

Abstract

Our aims were to survey the taxonomic and functional trait diversity of testate amoebae (TA) in Hawaiian peatlands and the distribution of TA functional traits along peatland environmental gradients. We sampled peatlands within the wet forest – montane peatland complex on Kohala Mountain and peatland pockets on windward Mauna Loa. Multiple Factor Analysis of environmental and vegetation data and hierarchical agglomerative cluster analysis identified five separate peatland habitats: *Sphagnum* hummocks, sedge-*Sphagnum* tussocks, *Sphagnm* hollows, *Juncus*, and a bryophyte-*Rhynchospora* association. TA communities were more taxonomically diverse in emergent *Juncus* habitats than in *Sphagnum* hummocks, resembling patterns of TA diversity along the hummock-hollow microtopographic gradient in high-latitude peatlands. Many TA taxa in Hawai‘i commonly occur in northern high-latitude peatlands, however some taxa common to nothern peatlands were rare or absent in Hawai‘i. A TA functional group with filose pseudopods and compressed tests that is affiliated with early soil colonization was correlated with the distribution of early-successional Hawaiian bryophytes (*i.e. Racomitrium lanuginosum* (Hedw.) Brid.), likely due to environmental filtering. Generalized additive models were used to assess how key TA functional traits were distributed along peatland environmental gradients. Test compression and a trend towards round test shapes positively correlated with water table depth ($r^2 = 0.16$, $p < 0.001$ and $r^2 = 0.24$, $p < 0.04$; respectively), and test biovolume and aperture diameter positively correlated with pH ($r^2 = 0.22$, $p < 0.001$ and $r^2 = 0.24$, $p < 0.001$; respectively). TA taxonomic richness increased, lobose amoebae relative abundance increased, test compression decreased, and ovoid test shapes increased with increasing mean annual rainfall up to ~2700 mm/yr; at sites with mean annual rainfall >2700 mm/yr variations in taxonomic richness and functional traits did not correlate with increasing rainfall.

Introduction

Hawai‘i is home to the most isolated tropical highlands in the world. Vertical elevation gradients span over 4000 m, with climates ranging from tropical in the lowlands to alpine and snow-covered volcanic peaks. Between 1000 and 2300 m, high-elevation (montane) peatlands have developed in depressions and relatively flat hillsides and mountain summits where rainfall is abundant and an accumulation of clay impedes water drainage (Fosberg 1961). Due to waterlogged soils and relative acidity compared with montane forest soils, the montane peatland biota is highly specialized (Canfield 1986) and typically limited in range to the peatland boundary (Gagné & Cuddihy 1999).

The similarities between Hawai‘i’s montane peatlands and peatlands in temperate and boreal regions have long been recognized (Skottsberg 1940). One particularly striking example is the presence of *Sphagnum* moss as the dominant understory component in the wet forest – montane peatland complex on Kohala in Hawai‘i Island. The moss is a single population of *S. palustre* L., a carpet moss of mid- to high- latitude peatlands and paludified forests. In Hawai‘i, *S. palustre* is considered indigenous to Kohala (Karlin *et al.* 2012), although intentional and unintentional human action have led to aggressive expansion of the population to the windward flank of Mauna Kea and the island of O‘ahu (Hoe 1971).

The Hawaiian montane peatlands are therefore an interesting model system to study patterns of peatland spatial variability in relation to peatlands at higher latitudes. Paleoecological and genetic evidence point to a colonization event of *S. palustre* to the islands around 20,000 years ago, but the population has expanded at an accelerated rate in the past two centuries (Karlin *et al.* 2012). There is as much phenotypic diversity in the population of *S. palustre* in Kohala as is found across populations of the species throughout its range (Karlin *et al.* 2012);

thus the moss has created *Sphagum* hummock-hollow topography in Kohala that is more reminiscent of temperate and boreal bogs than of a tropical forest.

One aspect of peatland ecology that has yet to be explored in Hawai‘i is the diversity of peatland microbes. In this paper, we focused on a group of microbial grazers that are abundant and diverse in peatlands, the testate amoebae (TA), which are free-living, single-celled protozoa that produce their own protective shells ("tests"). We aimed to describe patterns of TA diversity across Hawaiian peatlands differing in vegetation, rainfall, and environmental history. We analyzed those patterns in the context of Hawaiian peatland ecology to gain perspective on the range of Hawaiian peatland variability and its relationship to peatlands outside the tropics.

The TA are a useful functional group for assessing peatland dyamics for several reasons. (1) They are abundant and morphologically distinguishable to the species level in most cases, allowing for detailed species-specific comparisons. (2) They are top predators of the microbial food web, and their community composition is correlated with the composition of the microbes they consume (Krashevska *et al*. 2014, Jassey *et al*. 2013a). (3) The shells that TA produce preserve well in peatland sediments, making them ideal for biomonitoring and paleoenvironmental investigations (Mitchell *et al*. 2008). (4) Many of the TA are cosmopolitan, which allows for direct species comparisons across multiple sites (*i.e.* low vs. high latitudes). (5) the TA have been used for classifying peatlands in the northern hemisphere for decades (*e.g.* Heal 1964), and there is a rich body of literature on peatland-microbial community interactions that is useful for comparison with the patterns of diversity in Hawai‘i.

In addition to classical taxonomic approaches, diversity can be interpreted within the framework of functional trait space. This framework involves defining the morphological and behavioral diversity within communities to understand how those traits relate to environmental

gradients (Violle *et al*. 2007). The functional diversity framework was originally applied to studies of plants, fish, and macro-invertebrates but has recently been applied to studies of microorganisms (Fournier *et al*. 2012, Fournier *et al*. 2016, Koenig *et al*. 2017). The study of functional traits can complement the taxonomic approach by incorporating information that is relevant to competitive interactions and environmental filtering.

We used taxonomic and functional trait approaches to characterize the diversity of TA in the montane peatlands of Kohala Mountain, Hawai‘i Island. These habitats include *Sphagnum* – dominated peatlands, sedge/shrublands, and wet rush and sedge meadows, all within the Kohala wet forest – montane peatland complex. We also investigated patterns of TA diversity in the sedgelands of windward Mauna Loa over 50 km southeast of Kohala Mountain. These small peatland pockets have no history of *Sphagnum* occurrence and overlie much younger substrate than Kohala peatlands. In northern peatlands, soil moisture and, to a lesser degree, pH, routinely emerge as the dominant environmental gradients that structure testate amoebae species and functional trait distribution (Mitchell *et al*. 2008, Fournier *et al*. 2012). We expected to observe comparable species-environment relationships in Hawaiian montane peatlands. We also expected differences in species composition and functional traits to emerge among testate amoebae communities in peatlands with and without *Sphagnum*.

Methods

Study site

The ten peatland sites (hereafter “macrosites”) sit between 1100 and 1800 m.a.s.l. on windward Kohala Mountain (20° 05’ N, 155° 42’ W; nine macrosites) and windward Mauna Loa (19° 37’ N, 155° 21’ W; one macrosite), Hawai‘i (Figure 1). Kohala is the oldest of Hawai‘i

Island's five shield volcanoes. The most recent basalt and ash on Kohala were deposited 120 to 460 kya (Sherrod *et al*. 2007). Conversely, the basalts underlying the Mauna Loa peatlands are much younger, and were formed 1.5 to 3.0 kya (Trusdell and Lockwood 2017). Both regions experience year-round tradewinds, although they occur more frequently in summer (85-95% of the time) than winter (50-80% of the time) (Sanderson 1993). Mean annual rainfall at the macrosites in Kohala ranges between 2500 and >4500 mm/yr, while the macrosites on Mauna Loa average ~2300 mm/yr (Giambelluca *et al*. 2013). The summit and windward slopes of Kohala also receive frequent cloud cover and fog-driven moisture that can contribute large amounts of additional moisture to the system (Scholl *et al*. 2004, Giambelluca *et al*. 2011). The upland vegetation of both regions is wet forest that is composed of a mixture of *Metrosideros polymorpha* Gaudich. and *Cheirodendron trigynum* A. Heller, and a mid-story composed primarily of tree ferns (*Cibotium* Kaulf. and *Sadleria* Kaulf.). *Acacia koa* Gray is also an important component of the canopy at the Mauna Loa sites.

I collected 107 samples from the surfaces of the ten macrosites in 2015, 2016, and 2018 for analysis of testate amoebae assemblage composition. Sampling locations (hereafter "microsites") were selected to capture the full range of environmental heterogeneity within each peatland macrosite. I collected roughly 10 cm^3 of the peatland surface at each microsite to a depth of 3-5 cm. When *Sphagnum* was collected in the sample, I removed the upper 1-2 cm of each stem including the capitulum prior to bagging because testate amoebae are often vertically zoned in the uppermost portion of *Sphagnum* stems (Charman & Warner 1997, Booth 2002). I carved a bore hole at each microsite to reach the peatland water table. Water table depth (WTD) was measured in centimeters relative to the peatland surface after 30 minutes to allow water tables to equilibrate. Positive values correspond to WTD below the surface and negative values

correspond to standing water. I estimated local vegetation percent cover visually at each microsite within a 30 cm x 30 cm plot surrounding each bore hole. Taxonomy of peatland vegetation followed Wagner *et al*. (1999) updated by Wagner *et al*. (2005). I measured conductivity (EC) and pH directly from the exposed water table using a Hannah 9813-6-series dual probe, and I measured bulk density (BD) and loss-on-ignition (LOI) of each surface peat sample in the laboratory.

TA microfossils were isolated from peat following standard practices outlined in Booth *et al*. (2010). Boiled samples were filtered through 300- and 15-µm sieves and the fraction between the sieves was retained and stored in glycerine. Subsamples were mounted on microscope slides and examined under 100-400X magnification. A minimum of 100 TA individuals were counted for each sample and counts were converted to relative abundance in each assemblage. Taxonomy of testate amoebae followed Charman, Hendon, & Woodland (2000), modified by Booth (2008), and identification was aided with guides by Siemensma (2019)

Functional traits

I selected six TA functional traits to analyze: phylogeny, biovolume, test shape, test compression, aperture position, and aperture diameter.

(1) Pseudopod morphology (continuous, L/F index: (number of lobose individuals - filose individuals)/(lobose + filose individuals)) refers to the broad morphological grouping of testate amoebae pseudopods as lobose versus filose. Many TA with filose pseudopods are small, produce their own self-secreted tests, and feed on bacteria and fungi, while many TA with lobose pseudopods are large, have a wide variety of food preferences, and construct their tests from material in the environment. An index of lobose to filose

amoebae from +1 (all lobose, stabilized community) to -1 (all filose, developing community) may be related to soil development and maturity, *e.g.* increasing L/F index is predicted to reflect increasing humus and food availability, as well as availability of test building materials (Bonnet 1964, Wanner *et al.* 2008).

(2) Biovolume (continuous: μm^3) is the volume of TA tests derived from the geometric equations in Fournier *et al*. (2012). Biovolume is expected to be positively correlated with greater soil moisture and/or larger soil pore size (Decloitre 1950, Fournier *et al.* 2012)

(3) Test shape (semi-continuous: 1 – 4, hemisphere to ovoid) may be constrained by soil moisture content as a result of hemispheric TA having greater difficulty with mobility in thin water films (Bonnet 1964).

(4) Test compression (semi-continuous: 1 – 4, least compressed to most compressed) is an adaptation to thin water films. Wet soils are likely to contain less compressed, round TA taxa (Bonnet 1964).

(5) Aperture position (semi-continuous: 1 – 3, axial to plagiostomic) that is more hidden on the test (plagiostomic) is likely to be better defended against desiccation (Bonnet 1964).

(6) Aperture diameter (continuous: μm^3) limits the size of prey than can be ingested by TA and is used as a measure of trophic position (Fournier *et al*. 2012, Payne *et al*. 2016).

Multiple factor analysis (MFA), a method in the principal components analysis (PCA) family that calculates correlations between the structures of different data matrices (Escofier and Pagés 1994), was used to compare the environment and vegetation datasets to evaluate common structures and identify habitat types. The environment data matrix includes continuous measures

of WTD, pH, BD, EC, and LOI that were standardized by subtracting the mean and dividing by standard deviation. The vegetation data matrix contains proportional cover data that were Hellinger-transformed to reduce the problem of double-zeroes for the principal components analysis (PCA) involved in MFA.

Similar microsites were grouped using a hierarchical agglomerative cluster analysis of microsite scores extracted from the first two dimensions of the MFA, because these dimensions represented the variation in vegetation cover that was most meaningful for our analysis of peatland heterogeneity. Cluster analysis was performed using Ward's method on Euclidean distances between microsites to identify vegetation-based habitat categories. The dendrogram was cut at five groups to group microsites into five habitat categories. Descriptions for the habitat categories were made according to each group's common vegetation composition, physical characters, and microtopographic features.

Numerical analyses

Testate amoebae diversity across habitat

Testate amoebae diversity was evaluated by calculating species richness, Shannon diversity (Shannon and Weaver 1998), L/F index, and four functional trait indices—functional richness, evenness, divergence, and dispersion—to detect any differences in community function. Functional richness (FRich) is a measure of the volume of functional trait space that species in a community occupy as calculated by convex-hull volumes (Cornwell *et al*. 2006). Functional evenness (FEve) is a measure of how evenly species abundance is distributed in functional trait space. Functional divergence (FDiv) indicates the amount of spread along the axis of functional traits, with high values indicative of greater differentiation of niche space

among species (Mason *et al*. 2005). Functional dispersion (FDis) is a multivariate index that considers the absolute volume of the trait space (*i.e.* FRic) as well as the relative distribution of species within that space (*i.e.* FEve and FDiv) (Laliberté and Legendre 2010). FDis is derived from the mean distance of each species in the community to the centroid of all species in the community in a principal coordinates analysis (PCoA) of the measured functional traits (Laliberté and Legendre 2010). Analysis was performed by the function "*dbFD*" in the *R* package "FD" (Laliberté *et al*. 2014) and FD was weighted by species relative abundance. The differences between communities in each habitat were evaluated post-hoc by Tukey's Honest Significant Difference (TukeyHSD), and *p* values were corrected for multiple comparisons.

Functional traits and community-weighted means

The functional composition of testate amoebae communities was interpreted through community-weighted means (CMW) of species traits. CMW is computed by the equation:

$$\text{CMW} = \sum_{i=1}^{S} p_i x_i$$

where p_i and x_i are the relative abundance and functional trait values, respectively, of species *i* and CMW is the weighted mean of the given functional trait within the community (Garnier *et al.* 2008). CMW is a measure of the dominant traits in a community, and has been used to define the functional identity of testate amoebae communities (Fournier *et al*. 2012, Payne *et al*. 2016). The CMW for each trait was standardized by subtracting the mean and dividing by the standard deviation.

Community-environment relationships

Relationships between environmental variables and community composition were evaluated by using generalized additive models (GAM). These models allow for non-linear relationships among species and functional trait distributions along environmental gradients. Each GAM framework modeled taxonomic (*i.e.* richness, Shannon diversity) or functional trait data (CMWs) as a function of WTD, pH, EC, LOI, BD, and mean annual rainfall (MAR). All GAM fitting followed the same process. The initial model included all terms and the model was allowed to estimate a smooth spline for the relationship between the independent variable and dependent variable. The degree of smoothness was estimated by reduced maximum likelihood, which adds a penalty to over-fitting. Terms that did not have significant smooth splines (α = 0.05) were not plotted. Significant terms were then modeled individually with the dependent variables to extract the measure of correlation and significance of the splines. Models were built using the *gam()* function in the 'mgcv' R package set with Gaussian distributions for the dependent variable (Wood 2011).

Results

A total of 53 testate amoebae taxa were found in the Hawaiian surface samples prior to removal of rare taxa in fewer than 3% of samples (n=9) (Figure 3). Members of the order Euglyphida, represented by five genera and 11 morpho-species, are present in 98% of all communities and make up 32.4% of the total abundance. The order Arcellenida is represented by sixteen genera and 33 morpho-species, is present in all communities, and makes up 66.4% of the total abundance. The remaining 1.2% of the total abundance belongs to the recently established order Amphitremida (Gomaa *et al.* 2013), represented by the single taxon *Amphitrema stenostoma* Nüsslin, which is present in 26% of all communities.

The most abundant and common taxa were *Difflugia pulex* Penard 'minor' type (12.9% relative abundance, 70.1% relative occurrence), *Assulina muscorum* Greeff (10.8%, 85.0%), *Heleopera sylvatica* Penard (10.7%, 81.3%) and *Cryptodifflugia oviformis* Penard (8.0%, 81.0%). *Euglypha* Dujardin is present in 93% of communities, *Heleopera* Leidy in 92%, and *Centropyxis* Stein in 88% of communities.

Habitat classification

The first MFA dimension explains 16% of total variance and shows a gradient from microsites dominated by *Sphagnum* to microsites dominated by sedges and rushes (Figure 2a). The most negative microsite on the first dimension is the tallest *Sphagnum* hummock (58 cm above water table) and the most positive microsite on the first dimension is a pool (WTD = -15 cm) surrounded by *Juncus planifolius* R. Br. The two microsites also represent the gradient length of pH (3.3 and 5.7, respectively). The second dimension explains 9.2% of variance and reflects the gradient of bulk density of the soil, surface wetness, and non-*Sphagnum* vegetation cover. For example, the rush *J. planifolius* is negatively correlated with the second dimension and the tussock-forming sedge *Rhynchospora rugosa* var. *lavarum* Gaudich. is positively correlated with the second dimension. I cut the dendrogram of microsite scores from the MFA at five groups and assigned the grouped microsites to a vegetaion-microenvironment type based on shared vegetation composition, microenvironment, and microtopgraphic characteristics. Those types were (1) dry-acidic *Sphagnum* hummocks, (2) *Sphagnum* hollows, (3) mixed sedge-*Sphagnum* tussocks, (4) *Juncus*, and (5) bryophyte-*Rhynchospora*. The decision to cut the tree at five groups over a more conservative grouping of four, based on cluster height (Figure 2c), was made in oder to preserve the separation of *Sphagnum* hollows and sedge-*Sphagnum* tussock

microsites because 1) one of our aims was to study the diversity of TA in relation to vegetation composition and 2) joining two groups made one supergoup with half of all microsites in this study.

Some peatland macrosites support a single vegetation-microenvironment type, while other macrosites support many different types. For example, Pu‘u O‘o only has bryophyte-*Rhynchospora* microsites whereas Alakahi supports four of the five vegetation-microenvironment types (Figure 2c).

Testate amoebae community composition in peatland habitats

Sphagnum hummocks were dominated by a relatively small number of TA taxa compared to the other habitats. The most commonly occurring and abundant TA taxa in *Sphagnum* hummocks were *Heleopera sylvatica* Penard, *Cyclopyxis arcelloides* Penard type, and *Cryptodifflugia oviformis* (Figure 2). These taxa were also common in the sedge-*Sphagnum* tussocks, but were not as abundant as in *Sphagnum* hummocks. Sedge-*Sphagnum* tussocks had greater abundances of *Difflugia pulex* “minor” type, *Physochila griseola* Wailes & Penard, *Amphitrema stenostoma*, and *Nebela* Leidy species than *Sphagnum* hummocks. *Sphagnum* hollows had some of the highest abundances of *Difflugia pulex* “minor” type and had frequent occurrence of *Difflugia* species, in general, among vegetation-microenvironment types. *Juncus* microsites had the highest abundances of *Centropyxis cassis* Wallich type and the only occurrence of *Centropyxis aculeata* Ehrenberg type among vegetation-microenvironment types. *Juncus* also had the highest abundances of the genus *Arcella* Ehrenberg among vegetation-microenvironment types and the only occurrence of *Arcella hemisphaerica* Perty. *Quadruella*

symmetrica Wallich type was also only found in *Juncus* microsites. Bryophyte-*Rhynchospora* microsites had the highest abundances of *Assulina muscorum*, *Euglypha tuberculata* type, *Euglypha strigosa* type, and *Euglypha rotunda* type among vegetation-microenvironment types. *Corythion dubium* Taranek was common in bryophyte-*Rhynchospora* microsites, but not abundant. In general, *Difflugia* and *Nebela* are not common in bryophyte-*Rhynchospora* microsites, except for two communities from the macrosite Pu‘u o Umi C (PUC) where *Difflugia pulex* “minor” type was very abundant (Figure 2).

Testate amoebae taxonomic richness was lowest in the dry-acidic *Sphagnum* hummocks (# species = 11.6) and highest in *Juncus* microsites (# species = 19.3, Figure 4). Similarly, Shannon diversity (SDI) was lowest in dry-acidic *Sphagnum* hummocks (SDI = 1.7) and highest in *Juncus* microsites (SDI = 2.4). Bryophyte-*Rhynchospora* microscites had the second lowest taxonomic richness and Shannon diversity values (# species = 13.0, SDI = 1.9, Figure 4). *Sphagnum* hollows had lower functional richness than *Juncus* microsites. *Sphagnum* hollows had lower functional dispersion than *Juncus* microsites, bryophyte-*Rhynchospora* microsites, and dry-acidic *Sphagnum* hummocks (Figure 4).

TA communities with the highest CMWs for test volume and aperture diameter were from *Juncus* microsites. TA communities with the lowest CMWs for test volume were from dry-acidic *Sphagnum* hummocks. There were no significant differences in the CMWs of aperture diameter among the three *Sphagnum* habitats and the bryophyte-*Rhynchospora* microsites (Figure 4). CMWs of test shape indicate that bryophyte-*Rhynchospora* microsites and *Sphagnum* hummocks have TA with more cylindrical or rounded tests than the TA in *Sphagnum* hollows and the sedge-*Sphagnum* tussock microsites. *Sphagnum* hummocks had more TA with axial or ventral apertures than *Juncus* and bryophyte-*Rhynchospora* microsites, which had more TA with

terminal and/or cryptic apertures (Figure 4). The clearest differences among CMWs of TA functional traits emerged for the Lobose/Filose Index (L/F Index) and the degree of test compression. TA taxa were consistently more compressed and more often had filose pseudopods in the bryophyte-*Rhynchospora* microsites than in any other vegetation-microenvironment type (Figure 4).

Community-environment relationships

Bulk density of the peat weakly correlated to taxonomic richness (smooth spline summary statistics: $r^2 = 0.1$, $p = 0.01$) and Shannon diversity ($r^2 = 0.15$, $p = 0.04$), and had a hump-shaped relationship in which the greatest richness and Shannon diversity occurred at intermediate bulk density (Figure 5). pH was weakly correlated with Shannon diversity ($r^2 = 0.1$, $p < 0.01$) and the relationship was similarly described by a hump-shape in which Shannon diversity was lowest at intermediate pH and increased towards low and high pH (Figure 5). Neither taxonomic richness nor Shannon diversity were correlated with WTD. On the other hand, functional diversity increased linearly with an increase in WTD, ($r^2 = 0.14$, $p < 0.001$; Figure 5).

CMW of test biovolume and aperture diameter were positively correlated with pH ($r^2 = 0.22$, $p < 0.001$ and $r^2 = 0.24$, $p < 0.001$; respectively). The increase in test biovolume was linearly related to the increase in pH along the full pH gradient, while the increase in aperture diameter was linearly related to a pH increase at units > 4.0 (Figure 5). Communities with TA having terminal or hidden apertures increased linearly with an increase in soil bulk density ($r^2 = 0.1$, $p = 0.02$). Round test shapes increased with an increase in WTD ($r^2 = 0.24$, $p = 0.04$), and this relationship was linear for WTD > 0 cm. The degree of test compression increased nearly

linearly with an increase in WTD ($r^2 = 0.16$, $p < 0.001$), although there was no increase in test compression at WTD > 35 cm. Decreasing mean annual rainfall was also correlated with an increase in test compression ($r^2 = 0.36$, $p < 0.001$). The index of filose to lobose amoebae was related to changes in depth to water table, bulk density, and rainfall, but relationships were non-linear and difficult to parse. In general, wetter sites with greater rainfall had a higher proportion of lobose amoebae in their communities than drier sites that receive less rainfall (Figure 5).

Discussion

Testate amoebae occurrence in Hawaiian peatlands

This is the first detailed investigation of testate amoebae diversity in Hawai‘i and the first assessment of occurrence in the last century (Richters 1908). The genera *Difflugia*, *Heleopera,* and *Euglypha* are particularly well-represented in the peatlands I sampled (Figure 3). The diversity and species occurrence of testate amoebae in Hawaiian montane peatlands share similarities with peatlands in temperate and boreal latitudes (Amesbury *et al*. 2018; Figure 3), and with other high-elevation tropical peatlands (Liu *et al.* 2019). The Hawaiian TA communities, however, also show some striking contrasts to TA communities from higher-latitude peatlands. For example, *Difflugia pulex* reaches higher abundance in Hawaiian peatlands than in many temperate and boreal peatlands (Charman *et al.* 2007, Booth *et al*. 2008, Van Bellen *et al*. 2014).

Some common Northern Hemisphere taxa are notably missing or rare in Hawai‘i. *Archerella flavum* (Archer) Loeblich & Tappan, *Hyalosphenia papilio* Leidy, and *H. elegans* Leidy are important components of northern peatland testate amoebae communities (Amesbury *et al*. 2018), but are absent or very rare in the peatlands studied here. *Archerella flavum* and

Hyalosphenia papilio are examples of mixotrophic testate amoebae (*i.e.* combining autotrophy and heterotrophy) that have endosymbiotic partnerships with photosynthetic zoochlorellae living within their tests. Mixotrophic strategies can provide a competitive edge in food-limited systems (Jassey *et al*. 2013b). *A. flavum* and *H. papilio* appear to be infrequent outside of North America and Europe (Qin *et al*. 2013, Swindles *et al*. 2014, Fournier *et al*. 2016) and may be restricted to the more oligotrophic *Sphagnum* bogs of those regions. In Hawai‘i, the only mixotrophic species reaching noteworthy abundance is *Amphitrema stenostoma,* and it is restricted primarily to *Sphagnum* habitat (Figure 3). This may change as trophic dynamics in Kohala forest soils respond to ongoing *Sphagnum* growth.

No unique or potentially endemic TA species were identified, despite the high degree of endemism in the flora of Hawaiian peatlands (Sakai *et al.* 2002). Free-living protists are often highlighted as exemplars of cosmopolitanism, in which “everything is everywhere, but the environment selects” (De Wit and Bouvier 2006), however, some species of TA appear to be dispersal-limited (Wilkinson 2001, Smith and Wilkinson 2007). The testate amoeba *Apodera* (*Nebela*) *vas* Certes is a well-known case of a species apparently restricted to the Southern Hemisphere and a handful of tropical locations in the Northern Hemisphere, including Hawai‘i Island (Smith and Wilkinson 2007, Richters 1908). However, I did not find *Apodera* (*Nebela*) *vas* at any of the peatland macrosites studied. This absence is perplexing given that 1) *A. vas* is easily detectable, due to its conspicuous test shape of large size (typically > 150 µm, Smith and Wilkinson 2007); 2) Kohala and windward Mauna Loa have suitable habitat (cool and moist mossy substrate); and 3) the remaining three testate amoebae taxa recorded by Richters (1908) were frequently encountered in this study. Richters (1908) did not describe the sampling location (aside from consisting of moss), but it is possible that *A. vas* is limited to the Hawaiian lowlands

as elevation has been shown to be an important constraint on large testate amoebae in insular tropical peatlands (Fournier *et al.* 2016). Given the isolation and heterogenous topography of Hawai‘i, comprehensive studies of testate amoeabae occurrence on the other islands, coupled with genetic analysis, will lead to further insight into the role of environmental filtering and dispersal limitation on microbial distributions.

Habitat and Diversity

When analyzing testate amoebae diversity, classifying habitat by environment and vegetation was more meaningful than by peatland site, because of the high environmental heterogeneity of most of the peatlands sampled (Figure 2b,c). *Sphagnum palustre* is hummock-forming in Hawai‘i, so peatlands with *Sphagnum* have broader hydrologic and chemical gradients than peatlands without *Sphagnum*.

Testate amoebae diversity was highest in the minerotrophic *Juncus* habitat, lowest in dry-acidic *Sphagnum* hummocks, and intermediate in wet *Sphagnum* hollows. This pattern resembles that of some northern peatlands, where testate amoebae diversity is highest in fens, lowest in *Sphagnum* hummocks, and intermediate in bog pools (Heal 1964, Lamentowicz *et al.* 2010). Low diversity of testate amoebae in *Sphagnum* microsites may also be a function of low bryophyte diversity. In a study along the fen-bog gradient in the Swiss Alps, Lamentowicz *et al.* (2010) observed a correlation between testate amoebae diversity and bryophyte diversity. It is likely that a lack of bryophyte diversity in the monotypic *S. palustre* carpet (Schomaker 2017) likely inhibits microbial diversity in these peatlands.

Phylogenetic grouping

TA play an important role in primary succession of young ecosystems because they are among the first eukaryotes to arrive on newly exposed land surfaces (Smith 1985, Hodkinson *et al*. 2002). Filose TA are often found in high abundance in new soils prior to an increase of the larger TA with lobose pseudopods. This pattern may be attributed to dispersal/colonization processes, life strategies, food availability, or availability of test-building materials (*e.g.* sediment particles). In Hawai‘i, the average L/F index was high and positive for all habitats (more lobose), except for the bryophyte-*Rhynchospora* association (more filose, +0.43 to +0.76 vs. -0.25) (Figure 4). The bryophyte-*Rhynchospora* association had high abundances of the filose amoebae *Assulina muscorum, Euglypha rotunda* type*, Euglypha strigosa* type, and *Corythion dubium* and low or zero abundances of the lobose genera *Difflugia* and *Nebela*, which were common at other habitats. The peatlands on windward Mauna Loa only supported the bryophyte-*Rhynchospora* microsites and, therefore, had the lowest community L/F index measures of all peatlands in this study. The underlying volcanic substrate of the macrosites sampled on Mauna Loa is much younger than Kohala (1.5-3.0 ky vs. 230-460 ky, Trusdell and Lockwood 2017), and pedogenesis may influence testate amoebae community composition, for example by determining soil carbon stocks and N-mineralization rates (Kitayama *et al*. 1997). But pedogenesis does not explain the low L/F index of bryophyte-*Rhynchospora* microsites on the older Kohala flows. There were also no clear relationships between environmental gradients and the L/F index of TA communities (Figure 5). This suggests that the composition of the bryophyte-*Rhynchospora* microsites may constrain the composition of testate amoebae. The principal non-*Sphagnum* moss species in the peatlands was *Racomitrium lanuginosum* Hedwig., which is a widespread carpet moss in Hawaiian montane peatlands and one of the earliest plants to colonize montane lava flows (Clarkson 1998). *R. lanuginosum* has associations with epiphytic

cyanobacteria (Pérez *et al.* 2017), a potential food source of TA species in the genera *Euglypha* and *Assulina* (Gilbert 1998). Water-holding capacity of the moss may also be a factor. Elumeeva *et al.* (2011) compared water-retention rates of 22 moss species in northern Sweden, including *R. lanuginosum* and several species of *Sphagnum*. They found that *R. lanuginosum* had one of the lowest water-content capacities (680% of colony dry weight) and *Sphagnum fuscum* (Schimp.) Klinggr., a hummock-forming species, had one of the highest (2,373% of colony dry weight). *R. lanuginosum* colonies also lost water twice as quickly as *S. fuscum* colonies (Elumeeva *et al.* 2011). High water retention and holding capacity in *Sphagnum* should favor hygrophilous lobose amoebae while low water retention and quick desiccation in *R. lanuginosum* should favor small, more compressed, xerophilous amoebae. My observations support this statement as microsites with *Sphagnum* had greater diversity and abundances of *Difflugia* species than microsites with non-*Sphagnum* bryophytes, which had greater abundances of *Assulina* and *Euglypha* species (Figure 3).

Community-environment relationships

Testate amoebae taxonomic diversity and richness did not clearly relate to WTD or pH (Figure 5). Instead, variance in taxonomic diversity was more strongly associated with differences in microsite vegetation and microtopography (Figure 4). Functional diversity increased linearly with increasing WTD (Figure 5), suggesting that TA species may be occupying narrower niches in drier microsites through competitive exclusion. Higher functional diversity in drier microsites suggests that the collective niche of all TA is broader than the collective niche in wetter microsites. In contrast to observations from other studies, test size and aperture diameter were unrelated to WTD in Hawai‘i (Laggoun-Défarge *et al*. 2008, Van Bellen

et al. 2017). These functional traits were instead positively correlated with pH, suggesting that these traits are controlled by food availability in less acidic sites. Test compression was positively correlated with WTD, which is consistent with previous observations (Van Bellen *et al.* 2017). Amoebae in the Mauna Loa peatlands had the most compressed tests. These peatlands have the lowest mean annual rainfall of all the sites in this study (<2500 mm/yr). At this location, cloud-water interception is less abundant and frequent and precipitation is more seasonal than at Kohala (Giambelluca *et al*. 2013). An increased frequency of low-humidity conditions is likely to favor tests that are more compressed and better adapted to thin water films, but a broader sampling network of peatlands at varying climates is required to assess those regional patterns of diversity.

Environmental variability in Hawaiian peatlands

Floristically, the Kohala montane peatlands differ from the peatlands on Maui, Molokaʻi, and Kauaʻi due to the presence of *Sphagnum palustre*. Outside of Kohala, the principal peat-forming species is the endemic sedge *Oreobolus furcatus* H. Mann (Selling 1948, Vogl & Henrickson 1971, Canfield 1986). *Oreobolus* forms dense tussocks that grow to heights > 50 cm, interspersed with hollows (Vogl & Henrickson 1971). *Oreobolus* can be found on Kohala northeast of the summit on peatlands deep within the wet forest but in low abundance and intermingled with patches of *Sphagnum*. *Oreobolus* may have been more abundant in Kohala prior to the recent expansion of *Sphagnum*. For example, Rock (1913) writes of a visit to a "bog" near the Kohala summit in 1910 that resembled the montane peatlands on Maui and Kauaʻi, which likely refers to an *Oreobolus* bog. Seven *Oreobolus* tussocks were sampled in this study for TA community composition (PUB4, 6, PUC3, 5, 7, 12; Figure 3). TA composition in

Oreobolus was very similar to the TA composition of *Sphagnum* hummocks, with high abundances of *Heleopera sylvatica* and *Cyclopyxis arcelloides* type.

A floristic feature common to the montane peatlands on the Island of Hawai‘i (both on Kohala and Mauna Loa) and the montane peatlands on other Hawaiian islands is the bryophyte-*Rhynchospora* association. *Rhynchospora rugosa* var. *lavarum* tussocks that harbor mosses such as *Racomitrium lanuginosum* and *Campylopus* Brid. and lichens such as *Cladonia* P. Brown, are recurring features of Maui and Kaua‘i peatlands (Selling 1948, Vogl & Henrickson 1971, Canfield 1986). On Hawai‘i Island, this plant community was associated with a distinct TA functional group: amoebae with filose pseudopods, narrow apertures, and compressed tests. This community may be the result of a limitation on food availability or a physical constraint on large TA. High rainfall appeared to reduce this constraint because TA communities in bryophyte-*Rhynchospora* microsites on the wettest peatlands had much higher abundances of lobose amoebae, especially *Difflugia pulex,* than the communities on peatlands with the least rainfall. Rainfall amount may therefore be important for structuring TA communities of *Rhynchospora* peatlands on Maui and Kaua‘i.

Conclusions

This first survey of testate amoebae on the Island of Hawai‘i in over a century has shown that the TA of Hawaiian montane peatlands have similar patterns of taxonomic diversity with TA in temperate and boreal peatlands. Hummock-forming *Sphagnum palustre* produced a vertical and chemical gradient in Kohala peatlands that is analogous to the fen – bog gradient in northern peatlands. Peatland composition of non-*Sphagnum* bryophytes, including taxa such as *Racomitrium lanuginosum*, constrained testate amoebae community composition and functional

diversity. Early-colonizing Hawaiian bryophytes co-occurred with early-colonizing TA species. In peatlands where rainfall is greatest, this relationship between early colonizers weakened. Functional diversity, amoeba test shape, and test compression were related to peatland water table depth, while test biovolume and aperture diameter were related to pH. Hence, TA functional traits and community composition appear to be robust indicators of peatland environmental heterogeneity in Hawai‘i.

References

Amesbury, M. J., Booth, R. K., Roland, T. P., Bunbury, J., Clifford, M. J., Charman, D. J., Elliot, S., Finkelstein, S., Garneau, M., Hughes, P. D., and A. Lamarre. 2018. Towards a Holarctic synthesis of peatland testate amoeba ecology: Development of a new continental-scale palaeohydrological transfer function for North America and comparison to European data. Quaternary Science Reviews 201:483-500.

Bonnet, L. 1964. Le peuplement thécamoebien des sols. Revue D'Écologie et de Biologie du Sol 1:123-408.

Bonnet, L. 1976. Le euplement thécamoebien édaphique de la Côte-d'Ivoire. Sols de la région de Lamto. Protistologica 12:539-554.

Booth, R. K. 2001. Ecology of testate amoebae (Protozoa) in two Lake Superior coastal wetlands: implications for paleoecology and environmental monitoring. Wetlands 21:564-576.

Booth, R. K. 2002. Testate amoebae as paleoindicators of surface-moisture changes on Michigan peatlands: modern ecology and hydrological calibration. Journal of Paleolimnology 28:329-348.

Booth, R. K. 2008. Testate amoebae as proxies for mean annual water-table depth in Sphagnum-dominated peatlands of North America. Journal of Quaternary Science 23:43-57.

Booth, R. K., Lamentowicz, M., and D. J. Charman. 2010. Preparation and analysis of testate amoebae in peatland palaeoenvironmental studies. Mires & Peat 7:1-7.

Canfield, J. E. 1986. The role of edaphic factors and plant water relations in plant distribution in the bog/wet forest complex of Alaka'i Swamp, Kaua'i, Hawai'i. Doctoral dissertation, University of Hawai'i-Mānoa.

Charman, D. J., and B. G. Warner. 1997. The ecology of testate amoebae (Protozoa: Rhizopoda) in oceanic peatlands in Newfoundland, Canada: modelling hydrological relationships for palaeoenvironmental reconstruction. Ecoscience 4:555-562.

Charman, D. J., Hendon, D. and W. A. Woodland. 2000. The identification of testate amoebae (Protozoa: Rhizopoda) in peats. Technical Guide No. 9. Quaternary Research Association, London, 147.

Charman, D. J., Blundell, A., and ACCROTELM members. 2007. A new European testate amoebae transfer function for palaeohydrological reconstruction on ombrotrophic peatlands. Journal of Quaternary Science 22:209–221.

Clarkson, B. D. 1998. Vegetation succession (1967-89) on five recent montane lava flows, Mauna Loa, Hawaii. New Zealand Journal of Ecology 22:1-9.

Cornwell, W. K., Schwilk, D. W., and D. D. Ackerly. 2006. A trait-based test for habitat filtering: convex hull volume. Ecology 87:1465-1471.

Crews, T. E., Kitayama, K., Fownes, J. H., Riley, R. H., Herbert, D. A., Mueller-Dombois, D., and P. M. Vitousek. 1995. Changes in soil phosphorus fractions and ecosystem dynamics across a long chronosequence in Hawaii. Ecology 76:1407-1424.

De Wit, R. and T. Bouvier. 2006. 'Everything is everywhere, but, the environment selects'; what did Baas Becking and Beijerinck really say?. Environmental microbiology 8:755-758.

Decloitre, L. 1950. Etudes sur les Rhizopodes. La Feuille des Naturalistes. Bulletin de la Societe des Naturalistes Parisiens TV, Paris, 41-46.

Elumeeva, T. G., Soudzilovskaia, N. A., During, H. J., and J. H. Cornelissen. 2011. The importance of colony structure versus shoot morphology for the water balance of 22 subarctic bryophyte species. Journal of Vegetation Science 22:152-164.

Escofier, B. and Pagés, J. 1994. Multiple factor analysis (AFMULT package). Computational statistics & data analysis 18:121-140.

Finlay, B. J. 2002. Global dispersal of free-living microbial eukaryote species. Science 296:1061-1063.

Fosberg, F. R. 1948. Derivation of the flora of the Hawaiian islands. *Insects of Hawaii* (ed. by E. C. Zimmerman), pp. 107–119.

Fosberg, F. R. (Ed.). 1961. Guide to Excursion III: Tenth Pacific Science Congress. Published jointly by Tenth Pacific Science Congress and University of Hawaii.

Fournier, B., Malysheva, E., Mazei, Y., Moretti, M., and E. A. Mitchell. 2012. Toward the use of testate amoeba functional traits as indicator of floodplain restoration success. European Journal of Soil Biology 49:85-91.

Fournier, B., Coffey, E. E., van der Knaap, W. O., Fernández, L. D., Bobrov, A., and E. A. Mitchell. 2016. A legacy of human-induced ecosystem changes: spatial processes drive the taxonomic and functional diversities of testate amoebae in Sphagnum peatlands of the Galápagos. Journal of Biogeography 43:533-543.

Gagné, W. C. and L. W. Cuddihy. 1999. Vegetation. *Manual of the flowering plants of Hawaii* (ed. by W. L. Wagner, D. R. Herbst, and S. H. Sohmer), University of Hawaii Press.

Garnier, E., Cortez, J., Billès, G., Navas, M. L., Roumet, C., Debussche, M., Laurent, G., Blanchard, A., Aubry, D., Bellmann, A., and C. Neill. 2004. Plant functional markers capture ecosystem properties during secondary succession. Ecology 85:2630-2637.

Giambelluca, T. W., DeLay, J. K., Nullet, M. A., Scholl, M., and S. B. Gingerich. 2011. Interpreting canopy water balance and fog screen observations: separating cloud water from wind-blown rainfall at two contrasting forest sites in Hawai'i. Tropical Montane Cloud Forests: Science for Conservation and Management 342.

Giambelluca, T. W., Chen, Q., Frazier, A. G., Price, J. P., Chen, Y. L., Chu, P. S., Eischeid, J. K., and D. M. Delparte. 2013. Online rainfall atlas of Hawai'i. Bulletin of the American Meteorological Society 94:313-316.

Gilbert, D. 1998. Les communautés microbiennes à la surface des tourbières à sphaignes: structure, fonctionnement et impact des apports de fertilisants. Doctoral dissertation, Clermont-Ferrand.

Gilbert, D. and E. A. Mitchell. 2006. Microbial diversity in Sphagnum peatlands. Developments in Earth Surface Processes 9:287-318.

Hawai'i GIS Portal. (geoportal.hawaii.gov). Maps are derived from *Vegetation Maps of the Upland Plant Communities on the Islands of Hawai'i, Maui, Moloka'i, and Lana'i June* (J. D. Jacobi), 1989.

Heal, O. W. 1964. Observations on the seasonal and spatial distribution of Testacea (Protozoa: Rhizopoda) in Sphagnum. The Journal of Animal Ecology 33:395-412.

Hodkinson, I. D., Webb, N. R., and S. J. Coulson, S. J. 2002. Primary community assembly on land–the missing stages: why are the heterotrophic organisms always there first? Journal of Ecology 90:569-577.

Hoe, W. J. 1971. Additional New and Noteworthy Records for Hawaiian Mosses. The Bryologist 74:501-502.

Jassey, V. E., Chiapusio, G., Binet, P., Buttler, A., Laggoun-Défarge, F., Delarue, F., Bernard, N., Mitchell, E. A., Toussaint, M. L., Francez, A. J., and D. Gilbert. 2013a. Above and belowground linkages in *Sphagnum* peatland: climate warming affects plant-microbial interactions. Global Change Biology 19:811-823.

Jassey, V. E., Meyer, C., Dupuy, C., Bernard, N., Mitchell, E. A., Toussaint, M. L., Metian, M., Chatelain, A. P., and D. Gilbert. 2013b. To what extent do food preferences explain the trophic position of heterotrophic and mixotrophic microbial consumers in a *Sphagnum* peatland? Microbial Ecology 66:571-580.

Karlin, E. F., Hotchkiss, S. C., Boles, S. B., Stenøien, H. K., Hassel, K., Flatberg, K. I., and A. J. Shaw. 2012. High genetic diversity in a remote island population system: sans sex. New Phytologist 193:1088-1097.

Kitayama, K., Schuur, E. A., Drake, D. R., and D. Mueller-Dombois. 1997. Fate of a wet montane forest during soil ageing in Hawai‘i. Journal of Ecology 85:669-679.

Koenig, I., Schwendener, F., Mulot, M., and E. A. Mitchell. 2017. Response of *Sphagnum* Testate Amoebae to Drainage, Subsequent Re-wetting and Associated Changes in the Moss Carpet. Acta Protozoologica, 56:191-210.

Krashevska, V., Sandmann, D., Maraun, M., and S. Scheu. 2014. Moderate changes in nutrient input alter tropical microbial and protist communities and belowground linkages. The ISME journal 8:1126-1134.

Laliberté, E. and P. Legendre. 2010. A distance-based framework for measuring functional diversity from multiple traits. Ecology 91:299-305.

Laliberté, E., Legendre, P., and B. Shipley. 2014. FD: measuring functional diversity from multiple traits, and other tools for functional ecology. R package version 1.0-12.

Laggoun-Défarge, F., Mitchell, E., Gilbert, D., Disnar, J.R., Comont, L., Warner, B.G. and A. Buttler. 2008. Cut-over peatland regeneration assessment using organic matter and microbial indicators (bacteria and testate amoebae). Journal of Applied Ecology 45:716-727.

Lamentowicz, M., Lamentowicz, Ł., van der Knaap, W. O., Gąbka, M., and E. A. Mitchell. 2010. Contrasting species—environment relationships in communities of testate amoebae, bryophytes and vascular plants along the Fen–Bog gradient. Microbial Ecology 59:499-510.

Liu, B., Booth, R. K., Escobar, J., Wei, Z., Bird, B. W., Pardo, A., Curtis, J. H., and J. Ouyang. 2019. Ecology and paleoenvironmental application of testate amoebae in peatlands of the high-elevation Colombian páramo. Quaternary Research 92:14-32.

Mason, N. W., Mouillot, D., Lee, W. G., and J. B. Wilson. 2005. Functional richness, functional evenness and functional divergence: the primary components of functional diversity. Oikos, 111:112-118.

Mitchell, E. A., Charman, D. J., and B. G. Warner. 2008. Testate amoebae analysis in ecological and paleoecological studies of wetlands: past, present and future. Biodiversity and Conservation 17:2115-2137.

Payne, R. J., Creevy, A., Malysheva, E., Ratcliffe, J., Andersen, R., Tsyganov, A. N., Rowson, J. G., Marcisz, K., Zielińska, M., Lamentowicz, M., and E. D. Lapshina. 2016. Tree encroachment may lead to functionally-significant changes in peatland testate amoeba communities. Soil Biology and Biochemistry 98:18–21.

Pérez, C. A., Thomas, F. M., Silva, W. A., Aguilera, R., and J. J. Armesto. 2017. Biological nitrogen fixation in a post-volcanic chronosequence from south-central Chile. Biogeochemistry, 132:23-36.

Qin, Y., Mitchell, E. A., Lamentowicz, M., Payne, R. J., Lara, E., Gu, Y., Huang, X., and H. Wang. 2013. Ecology of testate amoebae in peatlands of central China and development of a transfer function for paleohydrological reconstruction. Journal of Paleolimnology 50:319-330.

Richters, F. 1908. Beitrag zur Kenntnis der Moosfauna Australiens und der Inseln des Pazifischen Ozeans. Zoologische Jahrbücher 26:196-213.

Rock, J. F. 1913. The Indigenous Trees of the Hawaiian Islands. Published privately, Honolulu.

Sakai, A. K., Wagner, W. L., and L. A. Mehrhoff. 2002. Patterns of endangerment in the Hawaiian flora. Systematic biology 51:276-302.

Sanderson, M. (Ed.). (1993). *Prevailing trade winds: climate and weather in Hawaii*. University of Hawaii Press.

Scholl, M., Gingerich S, Loope, L., Giambulluca, T.M., and M. Nullet. 2004. Quantifying the importance of fog drip to ecosystem hydrology and water resources in windward and leeward tropical montane cloud forests on East Maui. Venture Capital Project Final Report.

Schomaker, A.L. 2017. The moss that ate Kohala: Plant diversity loss across a *Sphagnum palustre* gradient in Hawaiian montane wet forest. M.S. Thesis, Department of Botany, University of Wisconsin-Madison.

Selling, O. H. 1948. Studies in Hawaiian Pollen Statistics. Part III. On the Late Quaternary History of the Hawaiian Vegetation. Bernice P. Bishop Museum Special Publication 39.

Shannon, C. E., & Weaver, W. 1998. *The mathematical theory of communication*. University of Illinois press.

Sherrod, D. R., J. M. Sinton, S. E. Watkins, and K. M. Brunt. 2007. Geologic map of the State of Hawai‘i.

Siemensma, F. J. (2019). Microworld, world of amoeboid organisms. World-wide electronic publication, Kortenhoef, the Netherlands.

Skottsberg, C. 1940. The flora of the Hawaiian Islands and the history of the Pacific basin. Proceedings 6th Pacific Science Congress 4:685-707.

Smith, H. G. 1985. The colonization of volcanic tephra on Deception Island by protozoa: long-term trends. British Antarctic Survey Bulletin 66:19-33.

Smith, H. G. and D. M. Wilkinson. 2007. Not all free-living microorganisms have cosmopolitan distributions–the case of Nebela (Apodera) vas Certes (Protozoa: Amoebozoa: Arcellinida). Journal of Biogeography 34:1822-1831.

Swindles, G. T., Reczuga, M., Lamentowicz, M., Raby, C. L., Turner, T. E., Charman, D. J., Gallego-Sala, A., Valderrama, E., Williams, C., Draper, F., and E. N. H. Coronado. 2014. Ecology of testate amoebae in an Amazonian peatland and development of a transfer function for palaeohydrological reconstruction. Microbial ecology 68:284-298.

Trusdell, F. A., & Lockwood, J. P. (2017). *Geologic map of the northeast flank of Mauna Loa volcano, Island of Hawai'i, Hawaii* (No. 2932-A). US Geological Survey.

Van Bellen, S., Mauquoy, D., Payne, R. J., Roland, T. P., Daley, T. J., Hughes, P. D., Loader, N. J., Street-Perrott, F. A., Rice, E. M., and V. A. Pancotto. 2014. Testate amoebae as a proxy for reconstructing Holocene water table dynamics in southern Patagonian peat bogs. Journal of Quaternary Science 29:463-474.

Van Bellen, S., Mauquoy, D., Payne, R. J., Roland, T. P., Hughes, P. D., Daley, T. J., Loader, N. J., Street-Perrott, F. A., Rice, E. M., and V. A. Pancotto. 2017. An alternative approach to transfer functions? Testing the performance of a functional trait-based model for testate amoebae. Palaeogeography, palaeoclimatology, palaeoecology 468:173-183.

Violle, C., Navas, M. L., Vile, D., Kazakou, E., Fortunel, C., Hummel, I., and E. Garnier. 2007. Let the concept of trait be functional! Oikos 116:882-892.

Vogl, R. J. and J. Henrickson. 1971. Vegetation of an alpine bog on East Maui, Hawaii. Pacific Science 25.

Wagner, W. L., Herbst, D. R., and S. H. Sohmer. 1990. Manual of the flowering plants of Hawaii. University of Hawaii Press.

Wagner, W. L., Herbst, D. R., and D. H. Lorence. 2005. Flora of the Hawaiian Islands website. http://botany.si.edu/pacificislandbiodiversity/hawaiianflora/index.htm

Wanner, M., Elmer, M., Kazda, M., & Xylander, W. E. (2008). Community assembly of terrestrial testate amoebae: how is the very first beginning characterized?. *Microbial ecology*, *56*(1), 43-54.

Wilkinson, D. M. (2001). What is the upper size limit for cosmopolitan distribution in free-living microorganisms?. *Journal of Biogeography*, *28*(3), 285-291.

Wilkinson, D. M., & Mitchell, E. A. (2010). Testate amoebae and nutrient cycling with particular reference to soils. *Geomicrobiology Journal*, *27*(6-7), 520-533.

Wood, S.N. 2011. Fast stable restricted maximum likelihood and marginal likelihood estimation of semiparametric generalized linear models. Journal of the Royal Statistical Society 73:3-36.

Figure legends

Figure 1: Site map of Hawaiian peatlands. Nine peatland macrosites were sampled in Kohala montane forest. Several small peatland pockets were sampled on windward Mauna Loa along Pu‘u O‘o trail and grouped as a single macrosite. Green polygons show the extent of wet forest cover in the two sampled areas. Dark green polygons in Kohala map insert are locations of other peatlands within the wet forest – montane bog complex. Black lines are 100-ft (30.3 m) elevation contours. Mean annual rainfall contours on map inset are from Giambelluca *et al*. (2013). Elevation contours and land cover data are from Hawai‘i GIS Portal (geoportal.hawaii.gov).

Figure 2: A) Multiple factor analysis of microsite environment and vegetation data sets. **A)** The first two dimensions of the MFA, explaining 16% and 9.2% of the total variance, respectively. WTD = water table depth (cm), BD = bulk density of the top 3 cm of peat (g/cm^3). **B)** Heirarchical agglomerative cluster analysis of microsite scores of the first two dimensions of the MFA using Ward’s method. Color blocks indicate five vegetation-microenvironment types labeled according to vegetation composition, microenvironment, and mictroopgraphy **C)** Frequency of microsites belonging to the five vegetation-microenvironment types in each peatland macrosite.

Figure 3: Top 30 most abundant testate amoebae taxa plotted as relative abundance (%) from the 107 peatland sampling locations (microsites) on the Island of Hawai‘i. Microsites are grouped by the five vegetation-microenvironment types determined by MFA and cluster analysis. Taxa are arranged in columns according to ranked relative abundance at each vegetation-microenvironment type.

Figure 4: Comparisons of testate amoebae taxonomic and functional diversity, community-weighted means of functional traits (CMWs), and phylogenetic diversity among the five vegetation-microenvironment types. Functional diversity is measured as functional dispersion (Lailiberté *et al.* 2014). Letters signify differences between groups that are significant ($p < 0.05$, TukeyHSD with p-correction for multiple comparisons).

Figure 5: Generalized additive models of **A)** testate amoebae taxonomic and functional diversity measures on environmental variables. Mean annual rainfall (mm/yr) estimates derived from Giambelluca *et al.* (2013). Black circles are the partial residuals of the observations, smoothed lines are splines, and shaded area shows one standard error of the spline. Black tick marks on x-axis represent the values of the microsite environmental measurements.

Figure 6: Generalized additive models of community-weaighted means of functional traits on environmental variables. Mean annual rainfall (mm/yr) estimates derived from Giambelluca *et al.* (2013). Figure format follows Figure 5.

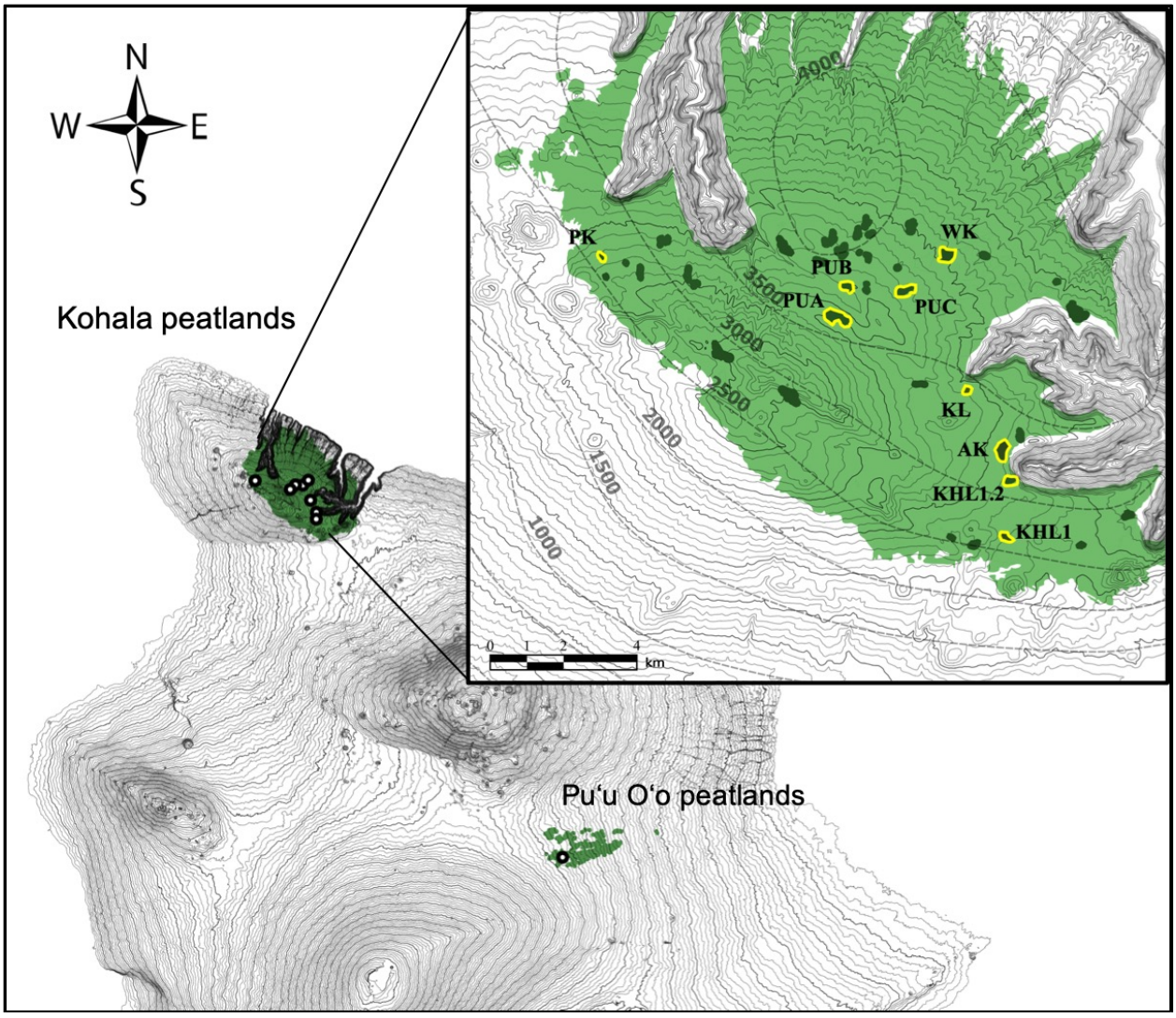

Figure 1: Site map of Hawaiian peatlands. Nine peatland macrosites were sampled in Kohala montane forest. Several small peatland pockets were sampled on windward Mauna Loa along Pu‘u O‘o trail and grouped as a single macrosite. Green polygons show the extent of wet forest cover in the two sampled areas. Dark green polygons in Kohala map insert are locations of other peatlands within the wet forest – montane bog complex. Black lines are 100-ft (30.3 m) elevation contours. Mean annual rainfall contours on map inset are from Giambelluca *et al*. (2013). Elevation contours and land cover data are from Hawai‘i GIS Portal (geoportal.hawaii.gov).

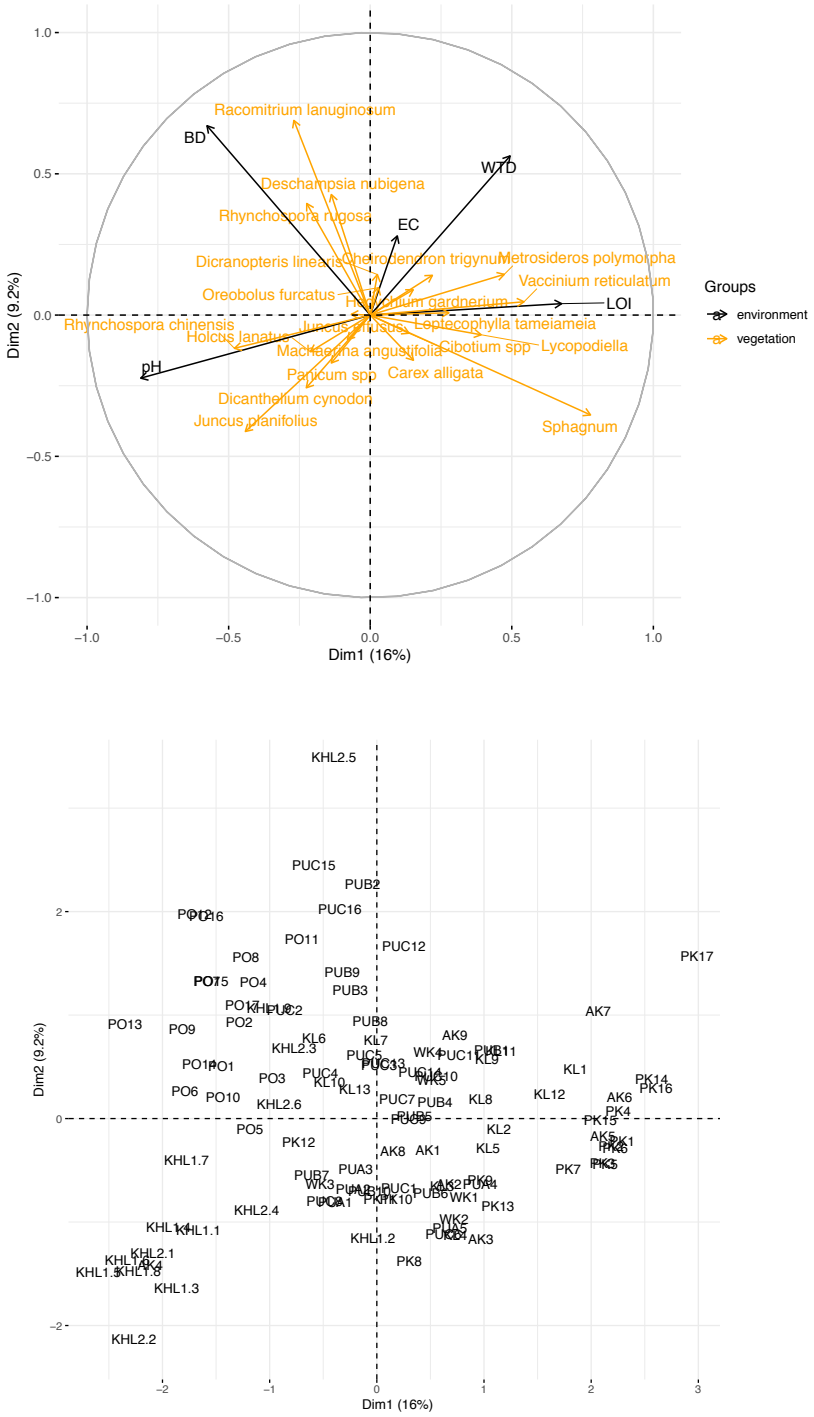

Figure 2: Multiple factor analysis of microsite environment and vegetation data sets. **A)** The first two dimensions of the MFA, explaining 16% and 9.2% of the total variance, respectively. WTD = water table depth (cm), BD = bulk density of the top 3 cm of peat (g/cm^3), LOI = loss-on-ignition (% organic matter). Bottom plot shows microsite scores of the MFA.

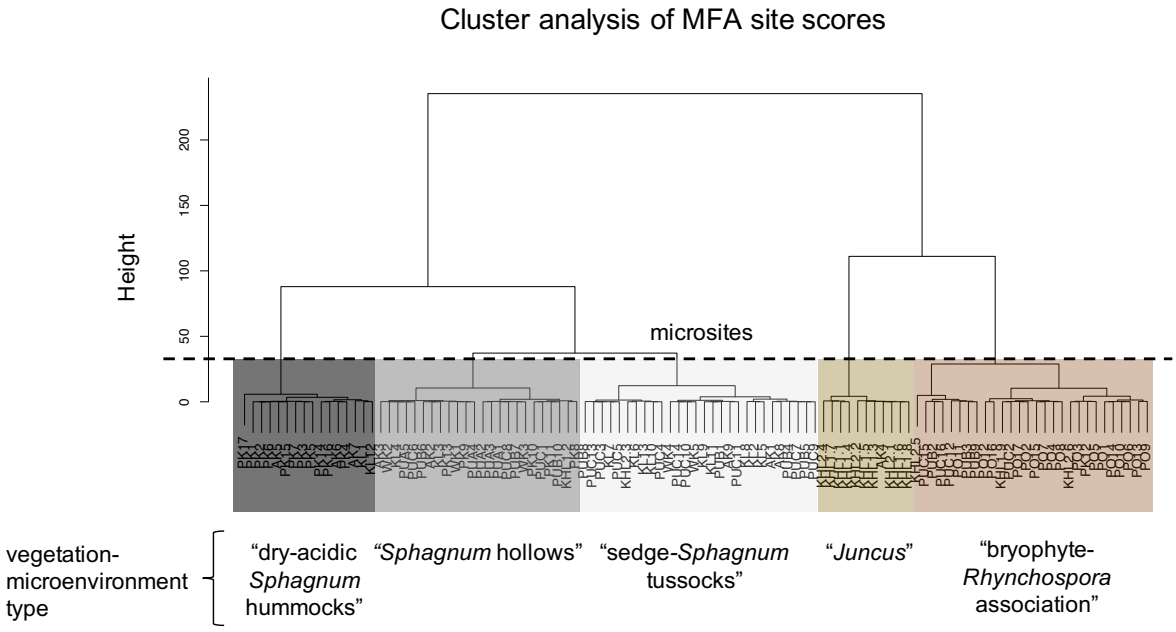

Figure 2: B) Heirarchical agglomerative cluster analysis of microsite scores of the first two dimensions of the MFA using Ward's method. Color blocks indicate five vegetation-microenvironment types labeled according to vegetation composition, microenvironment, and mictroopgraphy

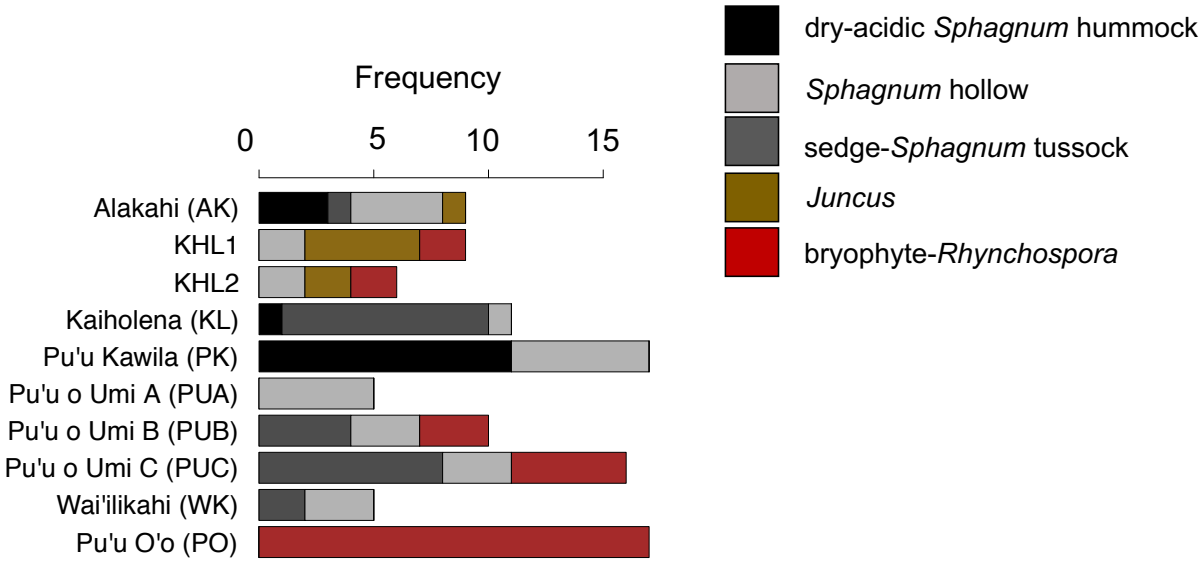

Figure 2: C) Frequency of microsites belonging to the five vegetation-microenvironment types in each peatland macrosite.

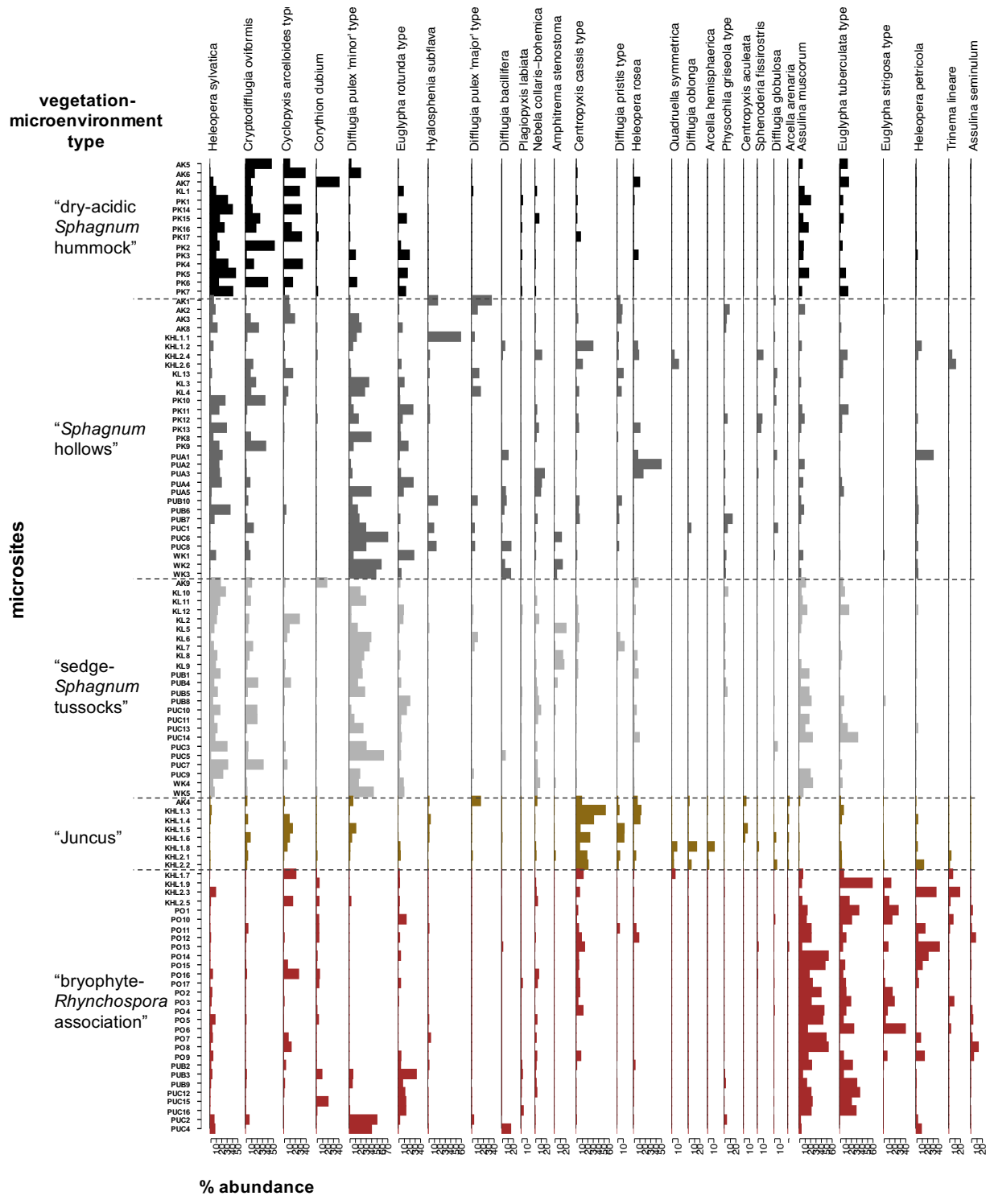

Figure 3: Top 30 most abundant testate amoebae taxa plotted as relative abundance (%) from the 107 peatland sampling locations (microsites) on the Island of Hawai'i. Microsites are grouped by the five vegetation-microenvironment types determined by MFA and cluster analysis. Taxa are arranged in columns according to ranked relative abundance at each vegetation-microenvironment type.

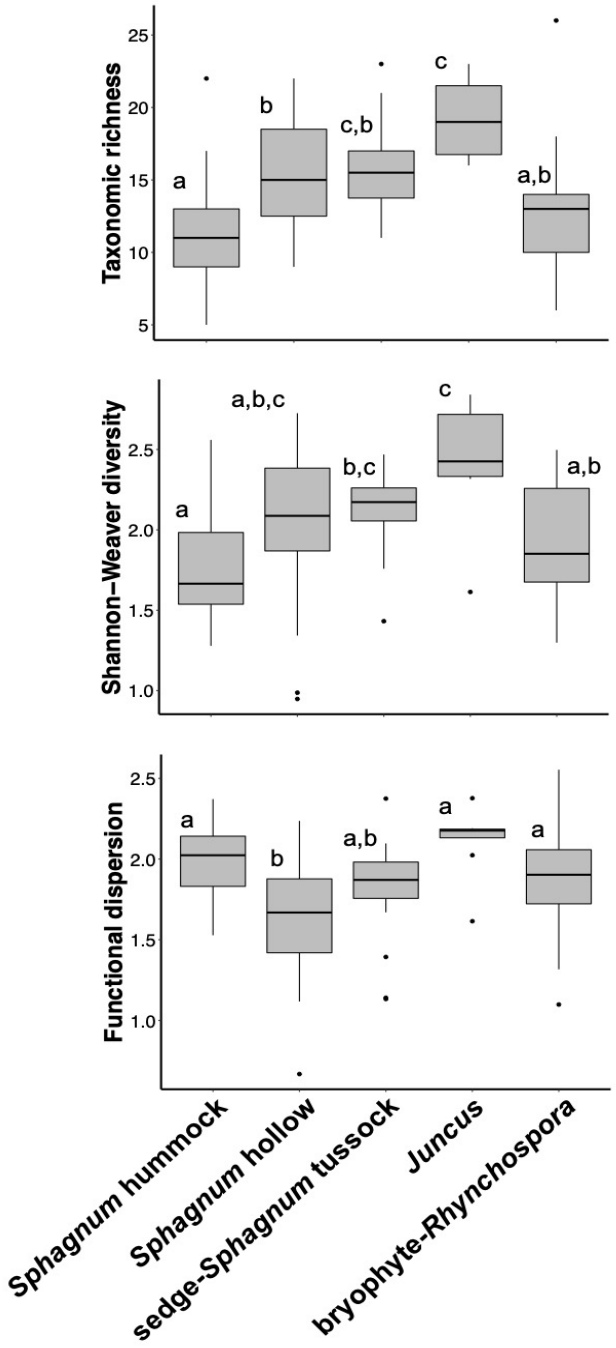

Figure 4: Comparisons of testate amoebae taxonomic and functional diversity, community-weighted means of functional traits (CMWs), and phylogenetic diversity among the five vegetation-microenvironment types. Functional diversity is measured as functional dispersion (Lailiberté *et al.* 2014). Letters signify differences between groups that are significant ($p < 0.05$, TukeyHSD with p-correction for multiple comparisons).

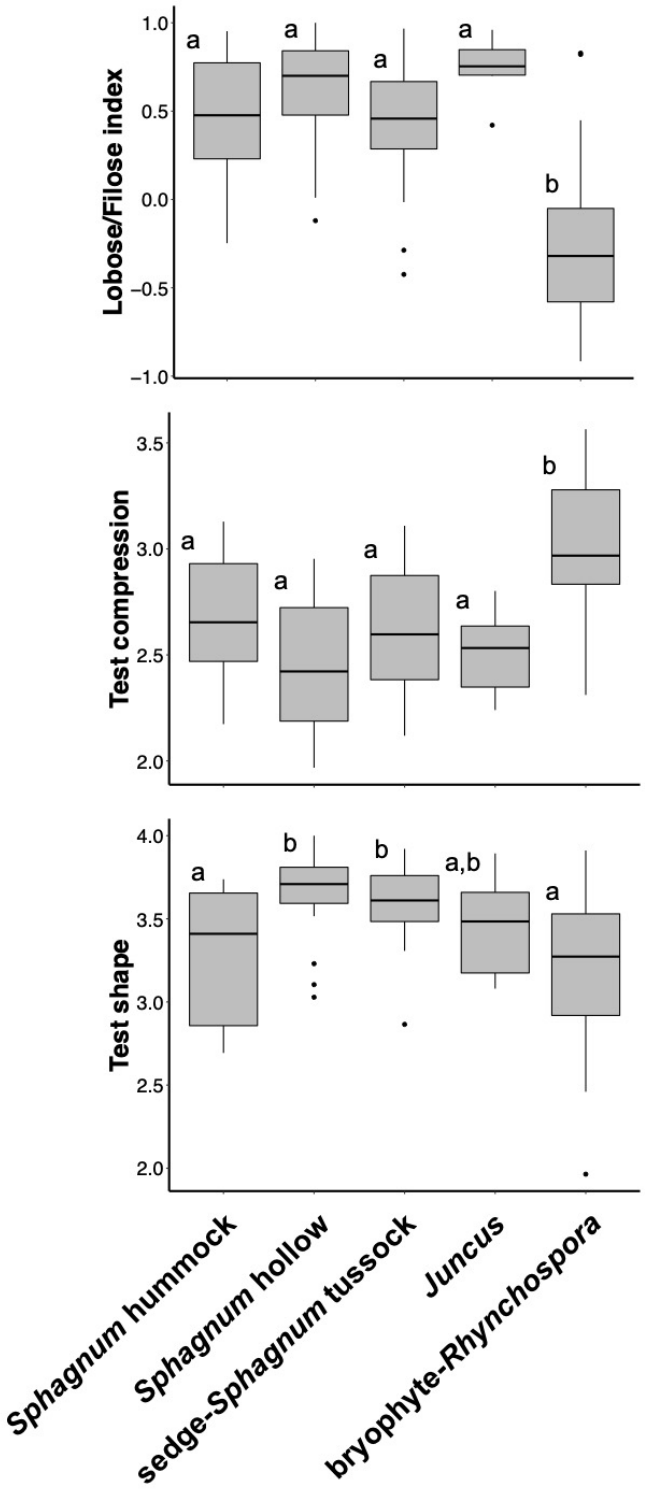

Figure 4: Continued.

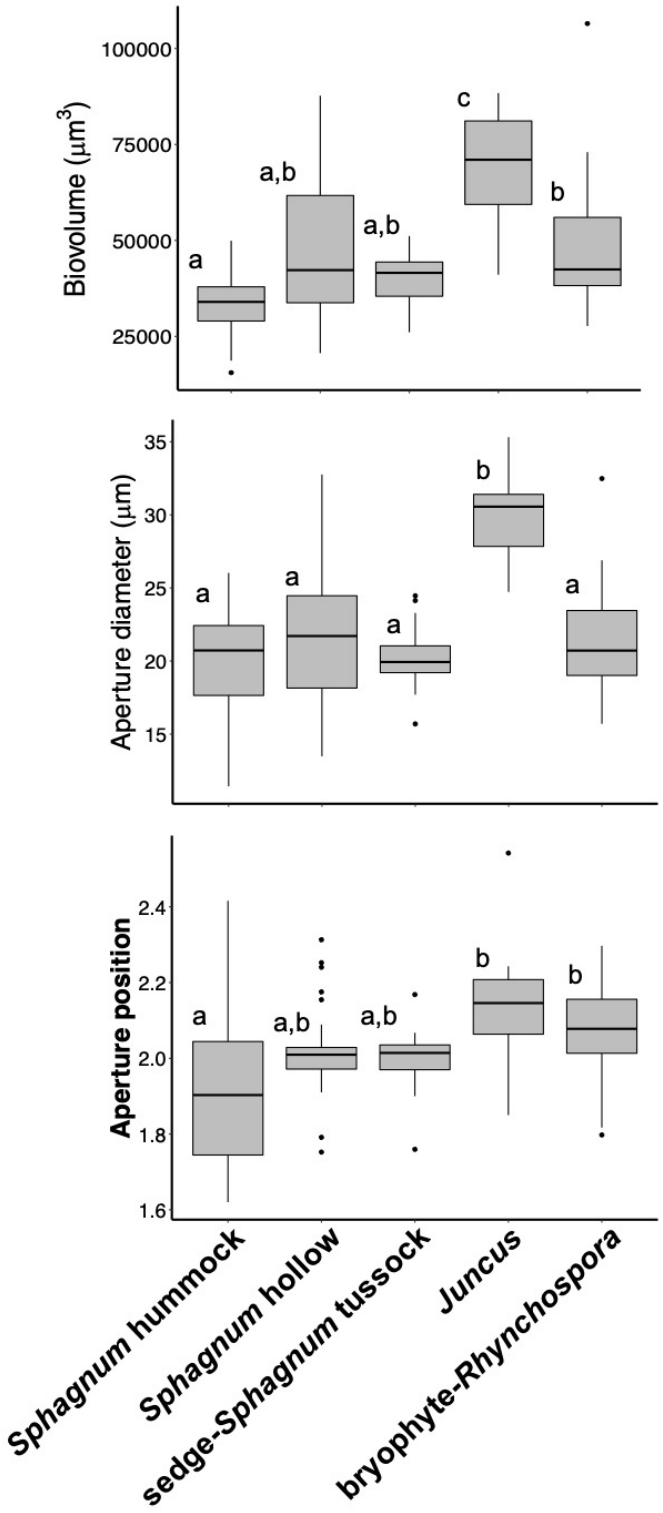

Figure 4: Continued.

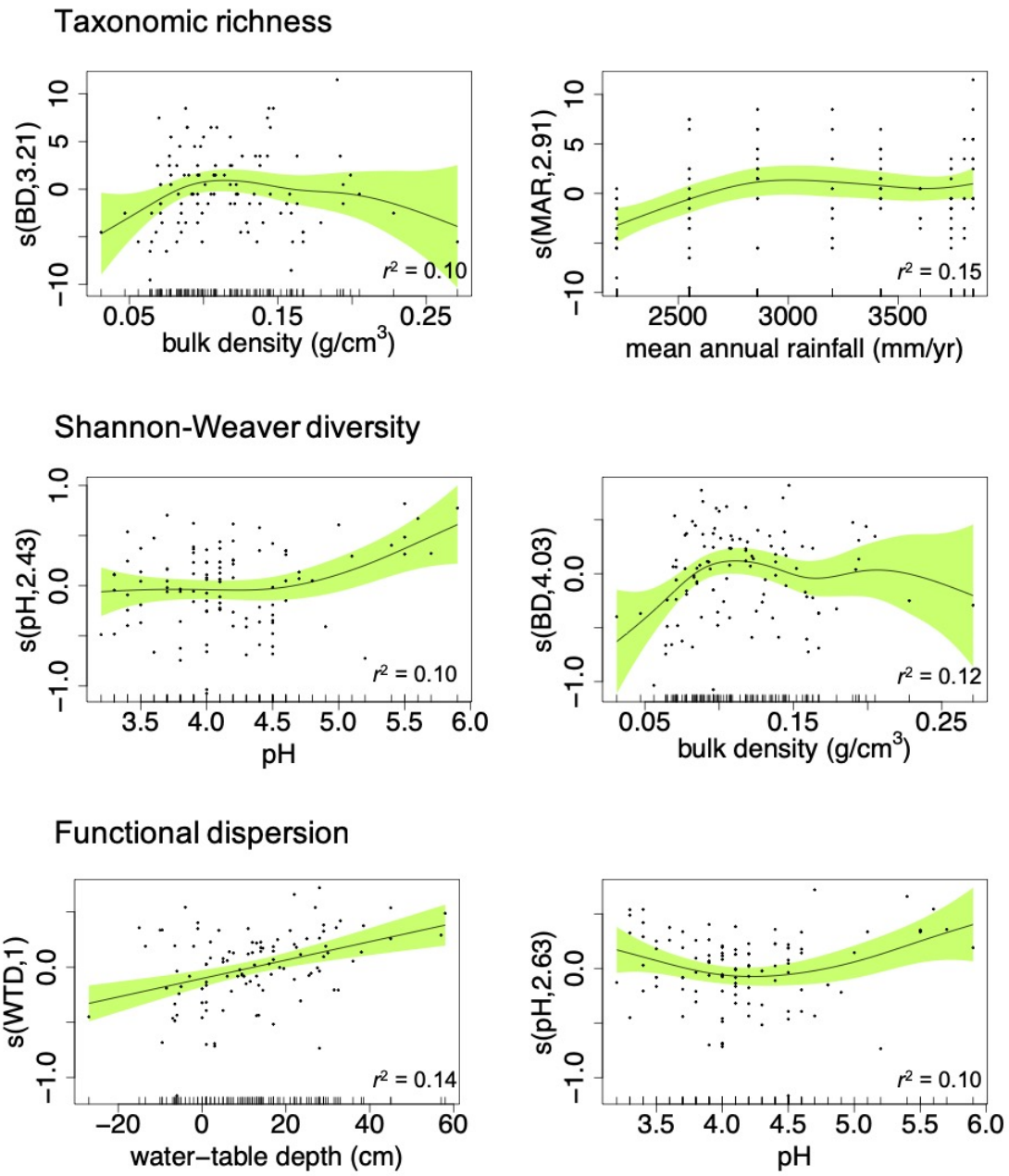

Figure 5: Generalized additive models of testate amoebae taxonomic and functional diversity measures. Mean annual rainfall (mm/yr) estimates are from Giambelluca *et al.* (2013). Black circles are the partial residuals of the observations, smoothed lines are splines, and shaded area shows one standard error of the spline. Black tick marks on x-axis represent the values of the environmental measurements.

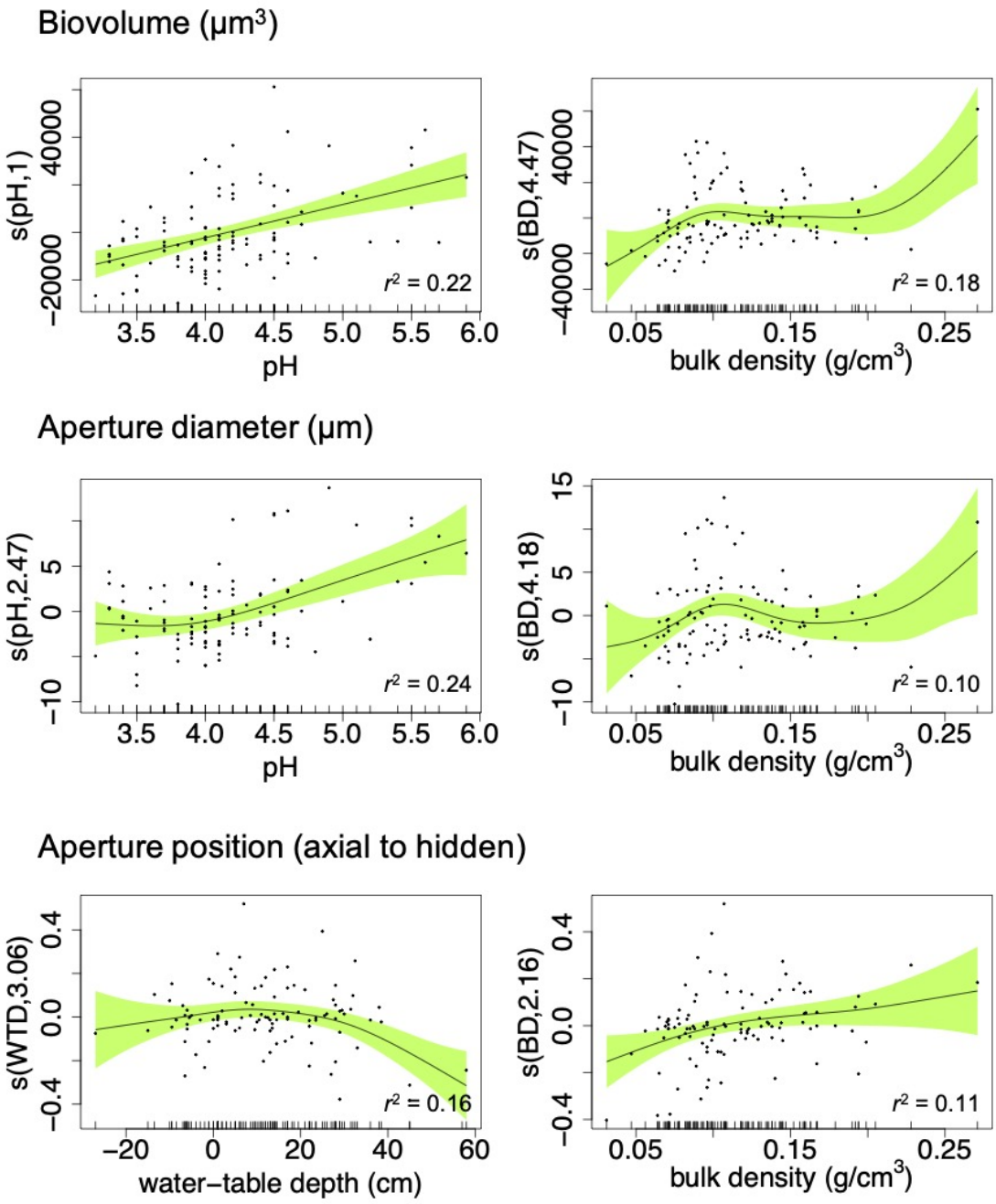

Figure 6: Generalized additive models of community-weighted means of functional traits on environmental variables. Figure format follows Figure 5.

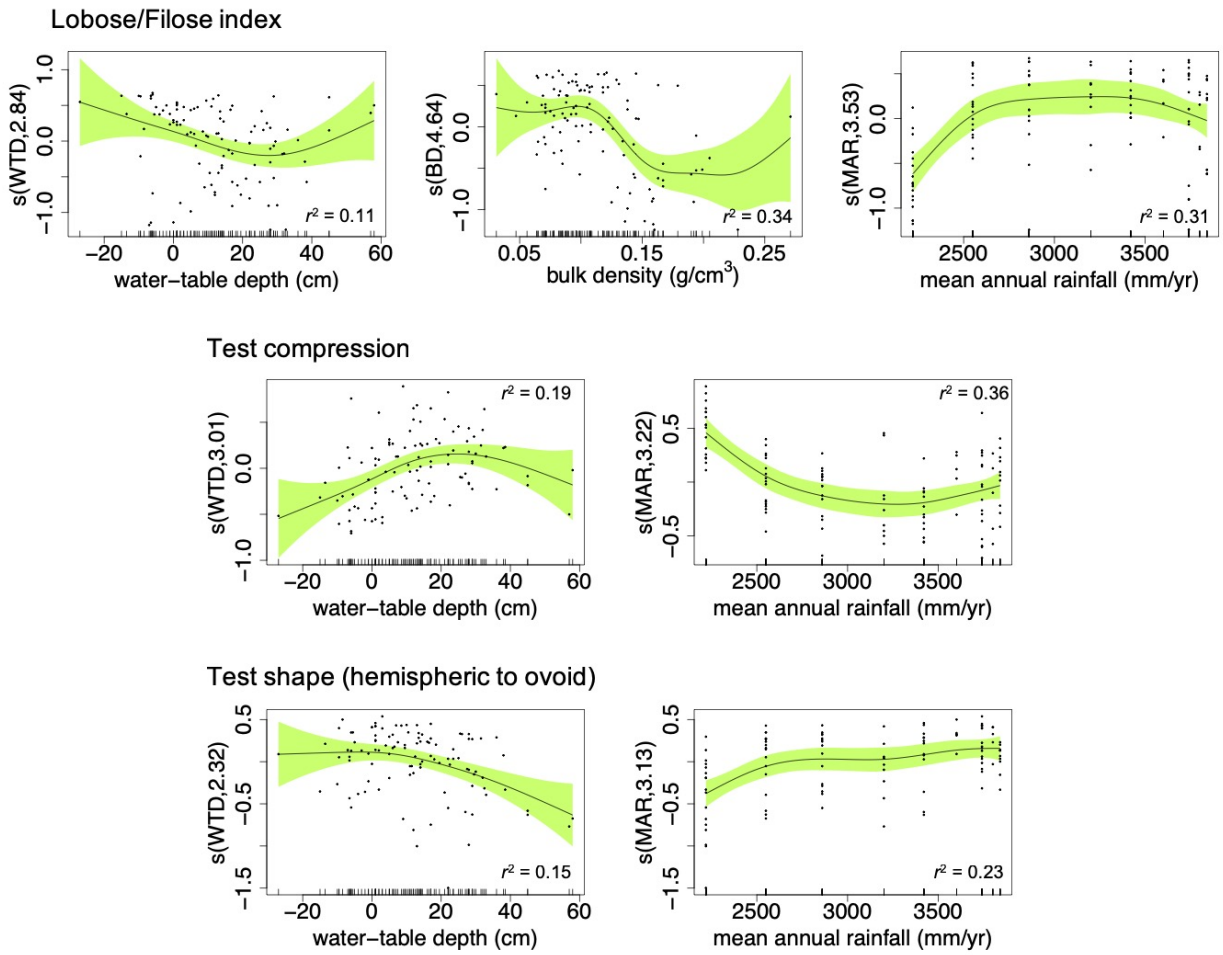

Figure 6: Continued.

-Chapter 2-

Testate amoebae and Cladocera as paleoenvironmental indicators in Hawaiian peatlands

Kevin D. Barrett[1], Patricia Sanford[2], Sara C. Hotchkiss[1,2]

University of Wisconsin-Madison, Botany[1]

University of Wisconsin-Madison, Center for Climatic Research[2]

Abstract

Peatlands in tropical highlands are vital repositories of biodiversity, water resources, and terrestrial carbon, but the ecological and climatic history of these ecosystems remains poorly understood. We investigated the ecology and paleoecology of testate amoebae and Cladocera (water fleas) in a wet forest-montane peatland complex in North Kohala, Hawai‘i Island to evaluate their potential as indicators of peatland environmental change. Surface peat was collected from a variety of ecohydrological habitats (from water pools to hummocks) and analyzed for modern testate amoebae and Cladocera species relative abundance. We identified 54 taxa from 21 genera of testate amoebae, 4 taxa and genera of Cladocera, and the common peat rotifer *Habrotrocha angusticollis* Murray. Constrained and unconstrained ordination supports the hypothesis that surface moisture, measured as depth to water table, is an important control on the distribution of testate amoebae and Cladocera. Transfer functions relying on weighted-averaging and modern-analog techniques were developed to predict water table depths from species relative abundance data, and these perform well under leave-one-site-out cross-validation: RMSEP = 9.8-10.3 cm, R^2 = 0.56-0.63. Including Cladocera abundance data in the models improved RMSEP by 1-8% and R^2 by 2-12%. A weighted average partial-least-squares transfer function was applied to microfossil assemblages from a 0.5 m-long peat core with a ^{210}Pb decay chronology anchored by ten measurements of excess ^{210}Pb activity. The microfossils were well-preserved in the peat core and assemblages were dominated by taxa that are adapted to variable hydrologic conditions. The reconstruction indicates a drying trend from the base of the profile (c. 1700 CE) to 1850±40 CE followed by a wetting trend to 1930±5 CE, then a return to drier conditions. The results signal that testate amoebae and Cladocera may be useful proxies of Hawaiian peatland paleohydrology.

Introduction

Tropical highlands are widespread in both continental (*e.g.* Northern Andes, Central America, Uganda) and island locations (*e.g.* Madagascar, Indonesia, Caribbean and high volcanic Pacific islands). Montane wet and "cloud" forests in these regions harbor unique, discontinuous, and often endemic biological communities as well as indispensable fresh water resources for downstream regions (Vazquez-Garcia 1995, Merlin & Juvik 1995, Bruijnzeel & Scatena. 2011). However, ecosystems in tropical highlands are vulnerable to changes in rainfall, cloudiness, and relative humidity, which are compounded by threats of habitat degradation and replacement of endemic native biota by exotic species (Loope & Giambelluca 1998).

In Hawai‘i, montane wet forests blend into cloud forests and are important refuge for ecological resources. Wet forest-montane peatland mosaics develop on the wettest volcanic slopes and are home to specialized and often endemic plant species (Sakai *et al*. 2002). These complexes also store large amounts of water due to the buffering capacity of peat soils and relatively low topographic relief, which regulates streamflow and the recharge of deep groundwater (Price & Waddington 2000). Water retention and regulation in the Hawaiian highlands is critical for supporting irrigation and human consumption, but the long-term ecohydrological dynamics of these ecosystems are not comprehensively understood.

Climatological trends in recent decades raise concerns for future stability. For decades, precipitation has declined across the state (Frazier & Giambelluca 2017), precipitation extremes have increased (Chen & Chu 2014), consecutive days without rain have increased (Chu *et al.* 2010), relative humidity has decreased (Diaz *et al.* 2011), and streamflow has decreased (Oki 2004). Given these trends, conservation of ecological resources and watershed sustainability increasingly depend on understanding the spatial complexity of wet forest-montane peatland

ecosystems and the ecohydrological variability that these systems have experienced on a variety of timescales.

We explored the application of testate amoebae and Cladocera remains in peat sediments for developing long records of hydrological variability from peatlands in the wet forest-montane peatland complex of Kohala Mountain on Hawai‘i Island. This research built upon our survey of testate amoebae in Hawaiian peatlands that identified water table depth and pH controls on testate amoebae taxonomic and functional diversity (Chapter 1).

Testate amoebae are a polyphyletic group of single-celled protists that are defined by having a protective shell ("test"). Testate amoebae inhabit the water films of humid soils in forests, wetlands, and the benthic zones of lakes, but they reach particularly high abundances and diversity in peatlands (Mitchell *et al.* 2008). Studies of testate amoebae ecology in oligotrophic peatlands have confirmed the importance of surface moisture, typically measured as water table depth (WTD), in structuring community composition (Schönborn 1963, Meisterfield 1977, Charman & Warner 1992, Tolonen *et al.* 1992). Because the tests are well-preserved in peat sediments, past WTD can be quantitatively estimated using transfer functions that relate WTD to assemblages of testate amoebae subfossils (Warner & Charman 1994). The Cladocera (Crustacea: Branchiopoda) are microscopic crustaceans abundant as both planktonic and littoral species in freshwater bodies and are a commonly used paleolimnological tool (Frey & Pamini 1986). Littoral Cladocera can be abundant in the pools of peatlands (Duigan 1992) and "crawling" Cladocera can inhabit bryophytes and leaf litter of tropical cloud forests (Frey 1980).

The development of species-environment transfer functions is improved by a deep understanding of the ecology of species in the local environment (Imbrie & Kipp 1971), particularly for organisms that have different relative environmental optima. The vast majority of

testate amoebae transfer functions have been developed in mid- to high-latitude peatlands, primarily in ombrotrophic *Sphagnum* bogs (Booth 2008, Qin *et al*. 2013, Van Bellen *et al*. 2014, Amesbury *et al*. 2016). However new transfer functions for tropical regions have been developed, including the Peruvian Amazon lowlands (Swindles *et al*. 2014), coastal Panama lowlands (Swindles *et al*. 2018a), and the high-elevation Columbian páramo (Liu *et al*. 2019), and these studies signal the potential for testate amoebae paleohydrology in tropical peatlands. Hydrologic variation in tropical highlands can be extreme due to abundant orographic precipitation and fog-derived moisture that can inundate peatland surfaces for considerable lengths of time (Canfield 1986, Chimner 2004).

The Cladocera may be useful indicators of saturated conditions in addition to testate amoebae and if so they would improve hydrological transfer function performance in tropical peatlands. While downcore cladoceran microfossils have been included in paleo-investigations as qualitative indicators of past wet conditions (Mitchell *et al*. 2001, Swindles *et al*. 2012, Słowiński *et al*. 2016, Booth *et al*. 2004), inclusion of quantitative cladoceran abundance data in peatland hydrological transfer functions has not been explored.

In this paper we aim to achieve the following goals:

1. Describe testate amoebae and Cladocera communities inhabiting the soils of montane tropical peatlands in Kohala, Hawai‘i
2. Test the hypothesis that hydrology, measured as depth to water table, is the principal control on microfaunal community composition in these tropical montane peatlands
3. Develop quantitative transfer functions relating microfaunal assemblage data to depth to water table and cross-check transfer function models with and without cladoceran data

4. Apply a final transfer function to fossil assemblages in a peat core to test the potential for paleohydrological reconstructions in Hawaiian peatlands.

Materials and methods

Study site

The Kohala forest-montane peatland complex crowns the summit region of Kohala Mountain, the oldest of Hawai‘i's five shield volcanoes. The mountain intercepts the prevailing trade winds that deliver clouds and abundant rainfall to its windward and summit slopes. Surface and ground water from Kohala Mountain is the primary source of drinking water for north Hawai‘i and necessary for agriculture and ranchlands in the region. The state recognizes the conservation value of Kohala forest and has designated approximately 4000 ha to the Natural Area Reserve System (NARS), which is tasked with preserving and managing large tracts of important Hawaiian habitat. A mosaic of wet forest and montane peatland pockets occurs on the shallowly sloping windward flank of Kohala Mountain. Peatlands developed in level areas that are often underlain with an impervious layer of ash and clay that impedes rates of water drainage (Fosberg 1961). The surrounding volcanic substrate is heavily cracked and porous, and rainfall quickly percolates through the surface. Many of these peatlands are therefore effectively ombrogenous. However, heavy and prolonged rain events can inundate the volcanic soils, resulting in overland surface water flow (Canfield 1986).

We selected nine peatlands for sampling testate amoebae and Cladocera on the windward side of Kohala (Figure 1). The peatlands sit between 1100 and 1400 m elevation within Kohala forest and have a mean annual rainfall ranging from 2500 mm/yr to >4000 mm/yr (Giambelluca *et al*. 2013). In this region, cloud water interception (fog drip) can contribute substantially to the

hydrological cycle and total moisture inputs can exceed 5000 mm/yr (Scholl *et al*. 2004, Giambelluca *et al*. 2011). The ground cover of Kohala forest is distinguished from other Hawaiian wet forests by a thick carpet of the moss *Sphagnum palustre* L. We selected peatlands that span the rainfall gradient of the wet forest and variations in surface vegetation (Table 1). Woody vegetation composition is nearly consistent among the peatlands and is dominated by *Metrosideros polymorpha* Gaudich., *Vaccinium reticulatum* Smith, *Leptecophylla tameiameiae* Schltdl., and *Cheirodendron trigynum* Gaudich., although stem density, tree and shrub height, and canopy cover do vary markedly. Ground cover vegetation composition, on the other hand, varies widely among peatlands and may be dominated by ground-dwelling bryophytes, such as *Sphagnum palustre* or *Racomitrium lanuginosum* Hedwig., or endemic and nonnative sedges, grasses, and rushes (*e.g. Deschampsia nubigena* Hillebr., *Oreobolus furcatus* H. Mann, *Carex alligata* Boott, *Rhynchospora chinensis* ssp. *spiciformis* Hillebr., and *Juncus planifolius* R. Br.).

Field Sampling

Ninety surface samples were collected from the nine peatlands in 2015, 2016, and 2018 for analysis of testate amoebae and Cladocera assemblage composition. Sampling locations (microsites) were selected to capture the full range of topographic, hydrologic, and vegetative habitats within each of the nine peatlands. Roughly 10 cm^3 of the surface of the peatland was collected at each microsite to a depth of 3-5 cm. When *Sphagnum* was collected in the sample, the upper 1-2 cm of each stem including the capitulum was removed prior to bagging because previous studies have observed vertical zonation of testate amoebae in the uppermost portion of *Sphagnum* stems (Charman & Warner 1997, Booth 2002). Moreover, testate amoebae living on the lower portion of the living stem are thought to be representative of the death assemblage that

is incorporated into the fossil record (Booth 2002). We dug a bore hole at each microsite to reach the peatland water table. WTD was measured in centimeters relative to the peatland surface, 30 minutes after digging to allow water tables to equilibrate. Positive values correspond to WTD below the surface and negative values correspond to standing water. We estimated local vegetation cover visually at each microsite within a 30 cm x 30 cm plot surrounding each bore hole. Taxonomy of peatland vegetation followed Wagner *et al*. (1990) with updates from the Smithsonian website (Wagner *et al*. 2005). Conductivity and pH were measured directly from the exposed water table using a Hannah 9813-6-series dual probe, and bulk density and loss-on-ignition of each surface sample were measured in the laboratory after drying peat samples at 90°C for 12 hours to determine dry weight and burning at 550°C for 4 hours to determine organic matter loss.

Testate amoebae and Cladocera sample preparation

Microfossils were isolated from peat following standard practices outlined in Booth *et al*. (2010). One cm^3 of each sample was disaggregated in boiling water for 10 min. The boiled samples were filtered through 300- and 15-μm sieves and each sieve fraction was retained and stored in glycerine. Subsamples were mounted on microscope slides and examined under 100-400X magnification. Testate amoebae and cladoceran remains were tallied together on the same slides, along with the common peatland rotifer *Habrotrocha angusticollis* Murray that is frequently included in testate amoebae transfer functions (Charman 1997, Booth 2002, Qin *et al*. 2013). Each subsample of testate amoebae and rotifers had a minimum of 100 individuals counted, which has been shown to produce reliable environmental reconstructions from testate

amoebae assemblage data (Payne & Mitchell 2009). Cladoceran individuals were counted in addition to the 100 minimum and then included in the calculations of relative abundance.

The preparation outlined above differed from standard preparation of cladocerans for paleolimnological studies in two important ways. First, 10% KOH was not used for deflocculation (Frey & Pamini 1986), because the boiling method sufficiently disaggregated organic matter for viewing cladoceran remains. Second, sieving out the >300 μm fraction of the sample likely excluded larger cladoceran remains and some taxa may have been missed (Frey & Pamini 1986). However, this method was necessary for identification of testate amoebae and was likely to capture the smaller remains, such as post abdomens, from large Cladocera. Identifiable remains (*i.e.* head shields, carapaces, post abdomens, and post abdominal claws) were recorded, and the most abundant category of remains for each taxon was used to calculate minimum number of individuals (Frey & Pamini 1986).

Testate amoebae and Cladocera identification

Taxonomy of testate amoebae followed Charman, Hendon, & Woodland (2000), modified by Booth (2008), and identification was aided with guides by Siemensma (2019). We applied the morphospecies approach for classifying testate amoebae taxa, which involves grouping like species into 'types' (Table 2). *Difflugia pulex* Penard type and *Hyalosphenia subflava* Cash & Hopkinson were split by size class into *D. pulex* 'minor' type (< 45 μm) and *D. pulex* 'major' type (> 45 μm) and *H. subflava* ‘minor’ (< 65 μm) and *H. subflava* ‘major’ (> 65 μm) because the size classes had different WTD optima. Cladoceran taxonomy followed Dodson & Frey (1991).

Multivariate analysis

Patterns in community composition were first explored using non-metric multidimensional scaling (NMDS). In contrast to other commonly applied ordination techniques, NMDS does not make assumptions about species distributions along environmental gradients (McCune & Grace, 2002). Rare taxa, defined as present in fewer than 3% of samples, were removed prior to ordination. A single microsite sample collected from a deep water pool (WTD = -27 cm) was removed because water tables that high are rarely reported in similar studies.

The ordination on 89 samples was carried out using the R 'vegan' package (Oksanen *et al.* 2016). Community data were square-root transformed to reduce the influence of common taxa (Overpeck *et al*. 1985) and ordinated using the *metaMDS*() function and Sørenson distance metric. Linear relationships between community data and environmental variables were explored using the *envfit*() function. The hypothesis that hydrology is the dominant environmental control on testate amoebae species distribution was tested with canonical correspondence analysis (CCA). Environmental variables were selected for constrained ordination based on forward selection criteria. A series of partial CCAs were run to estimate how variance in the community data is partitioned on each variable. The significance of each individual component was evaluated with permutation tests (999 permutations). The explanatory power of WTD on species distribution was tested by comparing the eigenvalue of the axis constrained by depth to water table with the eigenvalue of the first unconstrained axis in the CCA (λ_1/λ_2, Juggins 2013). A λ_1/λ_2 value greater than 1.0 indicates that variable is the main determinant of species distribution in the data set (Ter Braak 1986, Juggins 2013). In our previous survey (Chapter 1), we found that peatland vegetation composition, especially between *Sphagnum* and non-*Sphagnum* sampling locations, influenced taxonomic diversity and testate amoebae functional traits. We explored the

influence of vegetation on WTD control by dividing the calibration dataset between *Sphagnum* and non-*Sphagnum* sampling locations and analyzed relationships between taxon assemblages and individual environmental variables in each subgroup.

Transfer functions, calibration, and paleohydrological reconstruction

Microfossil assemblage data were square-root transformed prior to transfer function analysis to reduce the influence of commonly occurring taxa (Overpeck *et al*. 1985) relative to taxa with more narrow environmental distributions, which tended to be less common in assemblages. We developed transfer functions using weighted averaging with inverse deshrinking (Wa.Inv), the same weighted averaging model with tolerance downweighting (Wa.Tol.Inv), weighted averaging with partial least-squares regression (Wa-PLS), and the modern analog technique (MAT, method: average WTD of k = 7 nearest neighbors based on squared chord distance and inverse weighting by distance) using the 'palaeoSig' package in R (Telford 2015). We used jack-knifing ('leave-one-out', LOO), and bootstrapping cross-validation methods to calculate the root mean square error of prediction (RMSEP) and correlation (R^2) between predicted and observed WTD for each of the models. We also used an additional validation method that removes all samples from each peatland macrosite prior to making predictions from that peatland's microsite assemblage data, or 'leave-one-site-out' (LOSO) cross-validation (Payne *et al*. 2012). The effect on bias due to uneven sampling of the WTD gradient was investigated by dividing the environmental gradient into ten equal lengths and calculating RMSEP using the *segmentwise.rmse*() function in the 'palaeoSig' R package(Telford 2015). Finally, we compared results between transfer functions that include and exclude

Cladocera abundance data to evaluate whether Cladocera counts can improve transfer function performance.

Application to short peatland core

We then applied the best-performing transfer function to a ~0.5 m peat monolith retrieved in the year 2000 from Wai‘ilikahi (WK), a *Sphagnum* peatland that was sampled in this study. A minimum of 100 testate amoebae and rotifer individuals plus Cladocera remains were counted in contiguous 1-cm stratigraphic samples. We interpreted stratigraphy of the profile using stratigraphically constrained cluster analysis on Euclidean distances between assemblages. Determination of zonation was guided by the broken stick model. The monolith has a series of ten excess ^{210}Pb measurements and age estimates were calculated for depth using the CRS model and linear interpolation (Table 2). This age model enables comparisons of reconstructed hydrology with instrumental and derived Hawaiian climate measures to explore the relative potential for paleohydrological reconstructions.

Results

Ordination, variable selection, and species-environment relationships

A total of 44 testate amoebae taxa, 1 peatland rotifer taxon, and 3 cladoceran taxa were found after the removal of ten rare taxa. The ten taxa removed include the testate amoebae *Argynnia dentistoma* var. *laevis* Cash & Hopkinson, *Centropyxis platystoma* Penard type, *Difflugia lucida* Penard, *Difflugia pyriformis* Perty, *Euglypha acanthophora* Ehrenberg, *Euglypha cristata* Leidy, *Euglypha filifera* Penard, *Gibbocarina gracilis* Penard, *Hyalosphenia papilio* Leidy, and the cladoceran *Oxyurella tunuicaudis* Sars. The most common testate

amoebae taxa were *Difflugia pulex* Penard 'minor' type, *Heleopera sylvatica* Penard, *Cryptodifflugia oviformis* Penard, and *Assulina muscorum* Greeff. The three Cladocera were *Alona rustica* Scott, *Chydorus* cf. *eurynotus* Sars, and cf. *Alonella* spp. *A. rustica* was by far the most abundant of the Cladocera, at more than 90% of all cladocerans observed.

A 3-dimensional NMDS of the 89 contemporary testate amoebae assemblages was chosen (Figure 2a) because adding additional dimensions had little effect on final stress (final stress for k=3 dimensions: 14.2 after 40 runs). Community assemblage scores for each peatland macrosite generally overlap, except for KHL1 and KHL2, the two rush peatlands, which cluster apart from the other macrosites. The pattern of testate amoebae taxa distribution along Axis 1 resembles the pattern of taxa distribution in ombrotrophic peatlands at higher latitudes. *Centropyxis aculeata* Ehrenberg type, *Arcella* Penard, and *Difflugia* Leclerc species are positioned on one end of the first axis, along with all Cladocera taxa, and *Corythion* dubium, *Trigonopyxis arcula* Penard, *T. minuta* Schönborn & Peschke, *Assulina muscorum*, and *Assulina seminulum* Ehrenberg are positioned on the opposite end of the first axis (Figure 2b).

When environmental variables are overlain on the ordination, WTD has the strongest correlation with variation in taxon assemblages and is significantly correlateed with the first axis (r^2=0.52, P<0.001) along with loss-on-ignition (r^2=0.12, P<0.01), while pH (r^2=0.26, P<0.001) and bulk density (r^2=0.16, P<0.001) are significantly correlated with the second axis, but not particularly strongly (Figure 3b). Vectors representing fine-resolution vegetation cover around the microsite sampling locations are associated with the second axis (Figure 3c). *Rhynchospora*, *Juncus*, *Dicanthelium*, and *Racomitrium* vectors are correlated with taxon assemblages that have low Axis 2 scores and *Sphagnum*, *Metrosideros*, *Vaccinium*, and *Leptecophylla* vectors are correlated with high Axis 2 scores.

The variables WTD, pH, conductivivity, bulk density, and loss-on-ignition together explain 21.2% of the variance in the CCA of taxon assemblages (Table 3). WTD accounts for the greatest variance in the CCA (9.4%, $p < 0.001$) followed by pH (6.8%, $p < 0.001$) (Table 3). Variance partitioning from a series of partial CCAs indicates that only up to 1.2% of the variance explained by WTD is confounded by any of the other environmental variables explaining significant fractions of the variance in the taxon assemblage data set (Table 3). The ratio of eigenvalues of the first axis constrained on WTD alone to the first unconstrained axis (λ_1/λ_2) is 0.98. WTD explains a much greater fraction of the variance in taxon assemblages collected from non-*Sphagnum* habitats (n=33) than in habitats with *Sphagnum* present (n=56; 15.2%, $p <0.001$ vs. 9.7%, $p < 0.001$, respectively). The ratio of the eigenvalue of the axis constrained by an environmental variable in a CCA with the eigenvalue of the first unconstrained axis in a CCA (λ_1/λ_2) is a measure of the explanatory power of that variable (Juggins 2013). A λ_1/λ_2 value greater than 1.0 indicates that variable is the main determinant of species distribution in the dataset (Ter Braak 1986, Juggins 2013). λ_1/λ_2 for WTD is greater than 1.0 in the non-*Sphagnum* data set and less than 1.0 in the *Sphagnum* data set (1.02 vs. 0.89, respectively).

Transfer function

Among the transfer functions, the best-performing model was the second component of a weighted average with partial-least-squares regression (Wa-PLS) model (Table 4). This model has the lowest RMSEP, highest r^2, and the lowest maximum bias (Table 4). Including Cladocera data in taxon assemblages modestly improved the performance of each of the transfer function methods that we tested (Wa.Inv, Wa.Tol.Inv, Wa-PLS, and MAT). Prediction errors were reduced by 1-8% and r^2 increased by 2-12% (Table 4), depending on the model, with the modern

analog technique improving the most. The Wa-PLS model also performed well testing for spatial autocorrelation in the calibration dataset (Figure 4). Our final $RMSEP_{LOSO}$ of 9.75 cm is well below the standard deviation of the depth to water table gradient (sd_{WTD} = 15.63 cm) in this study and within the range of other developed transfer functions (Payne *et al*. 2012), indicating the model has suitable predictive power. However, segment-wise analysis warns that predictive capacity does not extend to the driest segment of the environmental gradient (WTD >50 cm) which suffers from under sampling and very high RMSEP values (Figure 5) even though these samples are dominated by species whose relative abundance peaks in drier microsites compared to other species.

Subfossils in a peat core

Within the peat monolith, the most abundant subfossil testate amoebae taxa were *Sphenoderia fissirostris* Penard, *Cryptodifflugia oviformis*, *Difflugia pulex* "minor" type, and *Hyalosphenia subflava* "major" and 'minor' (Figure 6). The cladocerans *Alona rustica* and cf. *Alonella* spp. were also present, but in low abundances. Fossil tests were well-preserved, and taxon richness was similar to the modern data set. Four biostratigraphic zones were determined to be significant in the record based on the broken-stick model. *Zone 4* from the base (47 cm) to 33 cm consists of high *Hyalosphenia subflava* "minor" relative abundance and increasing relative abundance of *Trigonopyxis arcula* Penard. Reconstructed water-table depths suggest a drying trend but with a high degree of variability. *Zone 3* extends from 33 to 17 cm depth and has high relative abundance of *Hyalosphenia subflava* "major", *Difflugia pulex* "major" type, and *Cryptodifflugia oviformis*. Cladocera abundance reaches its peak and reconstructed water tables reach their shallowest depth during this interval. *Zone 2* from 17 to 4 cm depth is marked

by an abrupt shift to dominance of the dry taxon *Pseudodifflugia fulva* (Archer) Penard type, *Cyclopyxis arcelloides* Penard type, and *Assulina muscorum*. *Nebela* Leidy species and *Amphitrema stenostoma* Nüsslin also increase in relative abundance. Reconstructed water tables are relatively deep and stable throughout this zone. The onset of *Zone 1* from 4 cm to the core surface is marked by an increase of *Sphenoderia fissirostris*, which reaches peak relative abundance of > 50% at the core top, and an increase in reconstructed water table height.

Discussion

The relative positions of testate amoebae taxa at the extremes of the hydrological gradient in ordination, as well as relative water table depth optima, closely resemble the findings of studies of testate amoebae at higher latitudes (Charman 1997, Charman & Warner 1997, Booth 2008, Amesbury *et al*. 2016). *Trigonopyxis arcula*, *Assulina seminulum* Ehrenberg, and *Corythion dubium* Taranek are unambiguous indicators of dry conditions, while *Centropyxis aculeata* Penard type, *Arcella hemisphaerica* Perty, and *Difflugia bacillifera* Penard are indicators of standing water. However, *Hyalosphenia subflava* occupies moderately to very dry environments in other published datasets (Booth 2008, Amesbury *et al*. 2016), but has a more complex relationship with wetness in Hawaiian peatlands. Shorter test length *H. subflava* "minor" (50-65 µm) inhabit environments of intermediate wetness and longer *H. subflava* "major" (70-85 µm) inhabit very wet environments, including pools. Swindles *et al*. (2018a) observed *H. subflava* "minor" (< 60 µm) and *H. subflava* "major" (> 60 µm) in a Panamanian peatland with nearly identical hydrological optima to the taxa here. Different test lengths of *H. subflava* appear to be common in tropical peatlands and may suggest the existence of a species complex (Swindles *et al*. 2014, 2018a, 2018b). All members of the Cladocera group are also

positioned on the extreme wet end of the hydrological gradient and are reliable indicators of saturated conditions. Elsewhere these species are commonly found in the littoral region of lakes and pools within bogs (Santos-Wisniewski *et al*. 2008, Hannigan & Kelly-Quinn 2014).

Constrained ordination and variance partitioning support the hypothesis that depth to water table is strongly and significantly ($p < 0.001$) related to testate amoebae and Cladocera distribution. However, a large proportion of the variance remains unexplained by the variables measured. Factors such as the influence of fog-driven moisture, edaphic features, and cation concentrations, particularly between *Sphagnum* and non-*Sphagnum* sampling locations, may affect species distributions. The finding here that the relationship between testate amoebae and hydrology was considerably stronger for non-*Sphagnum* habitats is interesting, given that strong hydrological controls are generally identified in temperate and boreal *Sphagnum* peatlands. Some peatlands lacking *Sphagnum*, or where *Sphagnum* is locally present, demonstrate that hydrology is not always the primary influence on species distribution (Booth 2001, Booth *et al*. 2008, Payne 2011). Variations in pH and nutrients may be more important in some of those systems (Mitchell *et al*. 2008). The pH of Hawaiian peatlands is somewhat low, even at microsites without *Sphagnum* (mean±SD = 4.4±0.6 units, across all microsites that have no *Sphagnum*). Low pH is a common feature of Hawaiian wet forest soils in general (Kitayama and Mueller-Dombois 1994) and other tropical montane forests soils (Krashevska *et al*. 2007), so hydrology may be the greatest source of natural variation in these systems.

The importance of depth to water table in our study as an environmental factor is also indicated by λ_1/λ_2 values of 0.98 for all assemblages and 1.02 for assemblages in non-*Sphagnum* habitats (Juggins 2013). The λ_1/λ_2 in *Sphagnum*, however, is 0.89 and suggests that testate amoebae may be strongly influenced by secondary variables in these habitats, such as

conductivity (Table 2). Lack of *sphagna* diversity in Kohala may also contribute because only a single species of *Sphagnum*, *S. palustre*, forms the hummocks and hollows of Kohala whereas many species of *sphagna* would be found in temperate peatlands. The lack of *sphagna* diversity may inhibit comparable patterns of testate amoebae diversity (Lamentowicz *et al*. 2010) and thereby reduce the information content in these assemblages. This species of *Sphagnum* also forms particularly tall hummocks in Hawai‘i which reflect dry conditions from a depth to water table perspective but may be insulated from "dryness" on the scale that is important to testate amoebae (*e.g.* water film thickness). Nevertheless, high λ_1/λ_2 in non-*Sphagnum* microsites is promising for paleohydrology in Hawai‘i because *Sphagnum* is not an important component of the Kohala flora prior to recent centuries (Karlin *et al*. 2012) or to the peatland flora of the other major islands.

Differences in temporal grain among samples and our timeline of sample collection over a four-year period may also be a source of uncertainty in our species-environment analysis. Hawaiian climate is sensitive to fluctuations in El Niño variability, and interannual rainfall can vary considerably. Testate amoebae and Cladocera are certainly sensitive to seasonal and interannual moisture fluctuations changes, but we did not identify obvious differences in assemblages based on sampling year. This is likely an artefact of focusing sampling during summer months which experience reduced interannual rainfall variation relative to winter months (Chu & Chen 2005). The samples collected also integrate living and dead tests, and probably reflect a few years of integration. Measurements of long-term water table variability can improve transfer function development and interpretation (Woodland *et al*. 1998, Swindles *et al*. 2015, Swindles *et al*. 2018a) so we installed water level loggers in two peatlands beginning in

2015 to begin tracking daily peatland water table fluctuations. These data will be analyzed in future papers.

Transfer function statistics

Our results demonstrate that hydrology is an important determinant of testate amoebae and Cladocera distribution in Hawaiian peatlands, although other factors such as pH contribute. Due to the spatial structure of the dataset, it is preferable to use LOSO over LOO cross-validation, because the latter overlooks spatial dependences among samples within a site and so produces overly-optimistic evaluations of transfer functions from clustered datasets (Payne *et al*. 2012). We found the second component of a Wa-PLS model performed best under LOSO cross-validation (Figure 4). Because our dataset suffers from under-sampling at the extreme dry end of the water table gradient (WTD > 50 cm), the transfer function is not currently capable of predicting accurate WTD from the "driest" assemblages (Figure 5). These assemblages are pulled from *Sphagnum* hummocks where other variables, such as humidity, may be more related to the factors directly affecting testate amoebae. We need to analyze additional testate amoebae communities from dry habitats, from both *Sphagnum* and non-*Sphagnum* microsites, to better estimate WTD from species data at this end of the gradient.

Cladocera

Cladocera data did improve each of the transfer function models that we tested, albeit modestly. These taxa are reliable indicators of wet conditions and, depending on taxonomic diversity, may inform other environmental signals such as acidity and food availability. Including cladoceran counts in testate amoebae calibration datasets has the potential to improve

other hydrological transfer functions, particularly from peatlands prone to flooding. Because a high density of cladoceran remains and multiple taxa can be isolated from peat using the standard testate amoebae preparation, analysts do not need to substantially modify their current methods to incorporate these data.

Fossil core

Testate amoebae and Cladocera microfossils are well-preserved in a Hawaiian peat sediment core. *H. subflava* appears to be a dominant testate amoebae taxon in fossil assemblages from lowland tropical peatlands (Swindles *et al*. 2014, Biagioni *et al.* 2015), as well as the montane tropical peatland here, but was not encountered in a high-elevation Columbian páramo peat core (Liu *et al*. 2019). One explanation for the high abundance of *H. subflava* ("major" and "minor") in the Hawaiian peat core is that peatland surface moisture conditions in the past were highly variable at seasonal to inter-annual timescales (Sullivan and Booth 2011). The subsequent reduction of *H. subflava* "major" and "minor" abundances correlates with *Sphagnum* peat appearance in the core. Testate amoebae communities may then have been altered by the expansion of *Sphagnum* at the site. *Sphagnum* expansion and peat growth apparently accelerated in recent centuries (Karlin *et al*. 2012), and likely replaced tussock-forming sedges, grasses, and a diversity of ground-dwelling bryophytes. *Sphagnum* may have altered surface hydrology by stabilizing the water table due to its extreme moisture-holding potential.

While care should be taken to avoid over-interpreting the timing of these inferred hydrological shifts without finer age control, there is utility in comparing broad trends with available instrumental records. Dinapoli & Morrison (2017) combined spatiotemporal drought uncertainty estimates in Kohala (Frazier & Giambelluca 2017) with a model of rainfall history

(Diaz *et al*. 2016) and identified the period 1800-1850 CE as prone to more frequent drought, and the timing corresponds with a lowering of water tables in our reconstruction. Wet conditions and high water tables in the beginning of the 20th century have support from the instrumental record, which shows that Hawai‘i had an anomalously high rainfall period from 1906-1923 CE (Chu & Chen 2005).

Lake and peatland records in Hawai‘i have already revealed substantial shifts in climate and vegetation in the past few thousand years, and these variations have been linked to variability in the El Niño-Southern Oscillation. For example, paleorecords identify greater aridity, drought, and forest canopy dieback events between 2.3 and 1.5 kya (Crausbay *et al*. 2014, Pau *et al*. 2012, Burney *et al*. 1995), a period that coincides with heightened El Niño frequency (Conroy *et al*. 2008). El Niño activity in the Pacific is believed to have declined during the Medieval Climate Anomaly (1.3 to 0.7 ka, Graham *et al*. 2007), and there is evidence that drought conditions were less frequent in Hawai‘i (Crausbay *et al*. 2014, Pau *et al*. 2012). El Niño activity increased after the MCA (Cobb *et al*. 2003), however this time period coincides with extensive land use change on the Hawaiian Islands and proxies derived from vegetation are difficult to untangle from anthropogenic disturbance (Crausbay *et al*. 2014, Pau *et al.* 2012). Testate amoebae-inferred records hence have the potential to shed light on hydrological dynamics during this period, especially on Hawai‘i Island, which currently lacks high-resolution Holocene records of climate and vegetation change.

Conclusions

Hawai‘i is experiencing a century-long drying trend that has deepened in recent decades. If current trends continue, there will be added pressure on water resources. Tropical montane

forests and peatlands are an integral component of the hydrological system in Hawai‘i by intercepting orographic moisture, buffering surface water runoff, recharging below ground aquifers, and providing freshwater to the islands. Peatlands are also important archives of hydrological variability in these critical ecosystems. We found that testate amoebae and Cladocera are reliable indicators of hydrology in Hawaiian peatlands and so can be used as paleohydrological proxies. We found that WTD control on testate amoebae and Cladocera was stronger in non-*Sphagnum* microsites than in *Sphagnum*, counter to observations in temperate and boreal peatlands. A transfer function to estimate water table depth from species assemblage data performs reasonably well under cross-validation ($RMSEP_{LOSO}$=9.75 cm, R^2_{LOSO}=0.62). The inclusion of Cladocera data modestly improved transfer function performance, improving RMSEP up to 8% and R^2 up to 12%.

Fossil assemblages in a 0.5-m peat profile are well-preserved. A water-table-depth reconstruction suggests a drying trend from the base of the profile (at least 1700 CE) to 1850±40 CE followed by a wetting trend to 1930±5 CE, then a return to drier conditions, and these trends have support from modeled and instrumental records. This work lays the foundation for testate amoebae and Cladocera paleoecology in Hawaiian peatlands and suggests that fossil remains of testate amoebae and Cladocera are useful complements in multi-proxy studies of hydrological and climatic change in Hawai‘i.

References

Amesbury, M. J., Swindles, G. T., Bobrov, A., Charman, D. J., Holden, J., Lamentowicz, M., Mallon, G., Mazei, Y., Mitchell, E. A., Payne, R. J., and T. P. Roland. 2016. Development of a new pan-European testate amoeba transfer function for reconstructing peatland palaeohydrology. Quaternary Science Reviews 152:132-151.

Biagioni, S., Krashevska, V., Achnopha, Y., Saad, A., Sabiham, S. and H. Behling, H. 2015. 8000 years of vegetation dynamics and environmental changes of a unique inland peat ecosystem of the Jambi Province in Central Sumatra, Indonesia. Palaeogeography, Palaeoclimatology, Palaeoecology 440:813-829.

Booth, R. K. 2001. Ecology of testate amoebae (Protozoa) in two Lake Superior coastal wetlands: implications for paleoecology and environmental monitoring. Wetlands 21:564-576.

Booth, R. K. 2002. Testate amoebae as paleoindicators of surface-moisture changes on Michigan peatlands: modern ecology and hydrological calibration. Journal of Paleolimnology 28:329-348.

Booth, R. K. 2008. Testate amoebae as proxies for mean annual water-table depth in Sphagnum-dominated peatlands of North America. Journal of Quaternary Science 23:43-57.

Booth, R. K., Jackson, S. T., and C. E. Gray. 2004. Paleoecology and high-resolution paleohydrology of a kettle peatland in upper Michigan. Quaternary Research 61:1-13.

Booth, R. K., Sullivan, M. E., and V. A. Sousa. 2008. Ecology of testate amoebae in a North Carolina pocosin and their potential use as environmental and paleoenvironmental indicators. Ecoscience 15:277-289.

Booth, R. K., Lamentowicz, M., and D. J. Charman. 2010. Preparation and analysis of testate amoebae in peatland palaeoenvironmental studies. Mires & Peat 7:1-7.

Bruijnzeel, L. A. and F. N. Scatena. 2011. Hydrometeorology of tropical montane cloud forests. Hydrological Processes 25:319-509.

Canfield, J. E. 1986. The role of edaphic factors and plant water relations in plant distribution in the bog/wet forest complex of Alaka'i Swamp, Kaua'i, Hawai'i. Doctoral dissertation, University of Hawai'i-Mānoa.

Charman, D. J. 1997. Modelling hydrological relationships of testate amoebae (Protozoa: Rhizopoda) on New Zealand peatlands. Journal of the Royal Society of New Zealand 27:465-483.

Charman, D. J. and B. G. Warner. 1992. Relationship between testate amoebae (Protozoa: Rhizopoda) and microenvironmental parameters on a forested peatland in northeastern Ontario. Canadian Journal of Zoology 70:2474-2482.

Charman, D. J., and B. G. Warner. 1997. The ecology of testate amoebae (Protozoa: Rhizopoda) in oceanic peatlands in Newfoundland, Canada: modelling hydrological relationships for palaeoenvironmental reconstruction. Ecoscience 4:555-562.

Charman, D. J., Hendon, D. and W. A. Woodland. 2000. The identification of testate amoebae (Protozoa: Rhizopoda) in peats. Technical Guide No. 9. Quaternary Research Association, London, 147.

Charman, D. J., Blundell, A., and ACCROTELM members. 2007. A new European testate amoebae transfer function for palaeohydrological reconstruction on ombrotrophic peatlands. Journal of Quaternary Science 22:209-221.

Chen, Y. R. and P. S. Chu, P. S. 2014. Trends in precipitation extremes and return levels in the Hawaiian Islands under a changing climate. International Journal of Climatology 34:3913-3925.

Chu, P. S and H. Chen. 2005. Interannual and interdecadal rainfall variations in the Hawaiian Islands. Journal of Climate 18:4796-4813.

Chu, P. S., Chen, Y. R., and T. A. Schroeder. 2010. Changes in precipitation extremes in the Hawaiian Islands in a warming climate. Journal of Climate 23: 4881-4900.

Chimner, R. A. 2004. Soil respiration rates of tropical peatlands in Micronesia and Hawai‘i. Wetlands 24:51.

Chimner, R. A. and Karberg, J. M. 2008. Long-term carbon accumulation in two tropical mountain peatlands, Andes Mountains, Ecuador. Mires & Peat 3.

Cobb, K. M., Charles, C. D., Cheng, H., and R. L. Edwards. 2003. El Niño/Southern Oscillation and tropical Pacific climate during the last millennium. Nature 424:271-276.

Conroy, J. L., Overpeck, J. T., Cole, J. E., Shanahan, T. M., and M. Steinitz-Kannan. 2008. Holocene changes in eastern tropical Pacific climate inferred from a Galápagos lake sediment record. Quaternary Science Reviews 27:1166-1180.

Crausbay, S., Genderjahn, S., Hotchkiss, S., Sachse, D., Kahmen, A., and S. K. Arndt. 2014. Vegetation dynamics at the upper reaches of a tropical montane forest are driven by disturbance over the past 7300 years. Arctic, Antarctic, and Alpine Research 46:787-799.

Diaz, H. F., Giambelluca, T. W., and J. K. Eischeid. 2011. Changes in the vertical profiles of mean temperature and humidity in the Hawaiian Islands. Global and Planetary Change 77:21-25.

Diaz, H. F., Wahl, E. R., Zorita, E., Giambelluca, T. W., and J. K. Eischeid. 2016. A five-century reconstruction of Hawaiian Islands winter rainfall. Journal of Climate 29:5661-5674.

DiNapoli, R. J., and A. E. Morrison. 2017. A spatiotemporal model of risk and uncertainty for Hawaiian dryland agriculture and its implications for ahupua'a community formation. Journal of Archaeological Science: Reports 15:109-119.

Dodson, S. I., and D. G. Frey. 1991. Cladocera and other Branchiopoda. *Ecology and classification of North American freshwater invertebrates* (ed. by J. H. Thorp and A. P. Covich), Academic press.

Duigan, C. A. 1992. The ecology and distribution of the littoral freshwater Chydoridae (Branchiopoda, Anomopoda) of Ireland, with taxonomic comments on some species. Hydrobiologia 241:1-70.

Fosberg, F. R. (Ed.). 1961. Guide to Excursion III: Tenth Pacific Science Congress. Published jointly by Tenth Pacific Science Congress and University of Hawaii.

Frazier, A. G., and T. W. Giambelluca. 2017. Spatial trend analysis of Hawaiian rainfall from 1920 to 2012. International Journal of Climatology 37:2522-2531.

Frey, D. G. 1980. The non-swimming chydorid Cladocera of wet forests, with descriptions of a new genus and two new species. Internationale Revue der gesamten Hydrobiologie und Hydrographie 65:613-641.

Frey, B. S. and P. Pamini. 1986) Cladocera analysis. *Handbook of palaeoecology and palaeohydrology* (ed. by B. E. Berglund), pp. 667-692, Wiley, New York.

Giambelluca, T. W., DeLay, J. K., Nullet, M. A., Scholl, M., and S. B. Gingerich. 2011. Interpreting canopy water balance and fog screen observations: separating cloud water from wind-blown rainfall at two contrasting forest sites in Hawai'i. Tropical Montane Cloud Forests: Science for Conservation and Management 342.

Giambelluca, T. W., Chen, Q., Frazier, A. G., Price, J. P., Chen, Y. L., Chu, P. S., Eischeid, J. K., and D. M. Delparte. 2013. Online rainfall atlas of Hawai'i. Bulletin of the American Meteorological Society 94:313-316.

Graham, N.E., Hughes, M.K., Ammann, C.M., Cobb, K.M., Hoerling, M.P., Kennett, D.J., Kennett, J.P., Rein, B., Stott, L., Wigand, P.E., and T. Xu. 2007 Tropical Pacific – mid-latitude teleconnections in medieval times, Climatic Change 83:241-285 .

Hannigan, E. and M. Kelly-Quinn. 2014. Aquatic invertebrate communities of ombrotrophic bogs in Ireland with special reference to microcrustaceans. Biology and Environment: Proceedings of the Royal Irish Academy 114:249-263.

Imbrie, J., & Kipp, N.G. (1971). A new micropaleontological method for quantitative paleoclimatology: application to a late Pleistocene Caribbean core, in: Turekian, K. (Ed.), The Late Cenozoic Glacial Ages. Yale University Press, New Haven, 71-181.

Juggins, S. 2013. Quantitative reconstructions in palaeolimnology: new paradigm or sick science? Quaternary Science Reviews 64:20-32.

Karlin, E. F., Hotchkiss, S. C., Boles, S. B., Stenøien, H. K., Hassel, K., Flatberg, K. I., and A. J. Shaw. 2012. High genetic diversity in a remote island population system: sans sex. New Phytologist 193:1088-1097.

Kitayama, K. and D. Mueller-Dombois. 1994. An altitudinal transect analysis of the windward vegetation on Haleakala, a Hawaiian island mountain:(1) climate and soils. Phytocoenologia 24:111-133.

Krashevska, V., Bonkowski, M., Maraun, M., and S. Scheu, S. 2007. Testate amoebae (protista) of an elevational gradient in the tropical mountain rain forest of Ecuador. Pedobiologia 51:319-331.

Lamentowicz, M., Lamentowicz, Ł., van der Knaap, W. O., Gąbka, M., and E. A. Mitchell. 2010. Contrasting species—environment relationships in communities of testate amoebae, bryophytes and vascular plants along the Fen–Bog gradient. Microbial Ecology 59:499-510.

Liu, B., Booth, R. K., Escobar, J., Wei, Z., Bird, B. W., Pardo, A., Curtis, J. H., and J. Ouyang. 2019. Ecology and paleoenvironmental application of testate amoebae in peatlands of the high-elevation Colombian páramo. Quaternary Research 92:14-32.

Loope, L. L., and T. W. Giambelluca. 1998. Vulnerability of island tropical montane cloud forests to climate change, with special reference to East Maui, Hawaii. *Potential Impacts of Climate Change on Tropical Forest Ecosystems*, Springer, Dordrecht, 363-377.

McCune B. J., and B. Grace. 2002 Analysis of ecological communities. MjM Software Design, Gleneden Beach, Oregon.

Meisterfeld, R. 1977. Die horizontale und vertikale verteilung der testaceen (Rhizopoda, Testacea) in Sphagnum. Arch. Hydrobiol 79:319-356.

Merlin, M. D., & Juvik, J. O. (1995) Montane cloud forest in the tropical Pacific: some aspects of their floristics, biogeography, ecology, and conservation. *Tropical montane cloud forests* (ed. by Hamilton, L. S., Juvik, J. O., Scatena, F. N), pp. 234-253, Springer, New York, NY,.

Mitchell, E. A., van der Knaap, W. O., van Leeuwen, J. F., Buttler, A., Warner, B. G., and J. M. Gobat. 2001. The palaeoecological history of the Praz-Rodet bog (Swiss Jura) based on pollen, plant macrofossils and testate amoebae (Protozoa). The Holocene 11:65-80.

Mitchell, E. A., Charman, D. J., and B. G. Warner. 2008. Testate amoebae analysis in ecological and paleoecological studies of wetlands: past, present and future. Biodiversity and Conservation 17:2115-2137.

Oki, D. S. 2004. Trends in streamflow characteristics at longterm gaging stations, Hawaii. Scientific Investigations Report 2004-5080. US Geological Survey, Reston, Virginia, USA.

Oksanen, J., Blanchet, F. G., Friendly, M., Kindt, R., Legendre, P., McGlinn, D. Peter R., Minchin, P. R., O'Hara, R. B., Simpson, G. L., Solymos, M. P., Stevens, H. H., Szoecs, E., and H. Wagner. (2019). vegan: Community Ecology Package. R package version 2.5-5.

Overpeck, J. T., Webb, T., and I. C. Prentice. 1985. Quantitative interpretation of fossil pollen spectra: dissimilarity coefficients and the method of modern analogs. Quaternary Research 23:87-108.

Pau, S., MacDonald, G. M., and T. W. Gillespie. 2012. A dynamic history of climate change and human impact on the environment from Keālia Pond, Maui, Hawaiian Islands. Annals of the Association of American Geographers 102:748-762.

Payne, R. J. 2011. Can testate amoeba-based palaeohydrology be extended to fens? Journal of Quaternary Science 26:15-27.

Payne, R. J. and E. A. Mitchell. 2009. How many is enough? Determining optimal count totals for ecological and palaeoecological studies of testate amoebae. Journal of Paleolimnology 42:483-495.

Payne, R. J., Telford, R. J., Blackford, J. J., Blundell, A., Booth, R. K., Charman, D. J., Lamentowicz, Ł., Lamentowicz, M., Mitchell, E. A., Potts, G., and G. T. Swindles. 2012. Testing peatland testate amoeba transfer functions: appropriate methods for clustered training-sets. The Holocene 22:819-825.

Price J. S. and J. M. Waddington. 2000. Advances in Canadian wetland hydrology an biogeochemistry. Hydrological Processes 14:1579-1589.

Qin, Y., Mitchell, E. A., Lamentowicz, M., Payne, R. J., Lara, E., Gu, Y., Huang, X., and H. Wang. 2013. Ecology of testate amoebae in peatlands of central China and development of a transfer function for paleohydrological reconstruction. Journal of Paleolimnology 50:319-330.

Sakai, A. K., Wagner, W. L., and L. A. Mehrhoff. 2002. Patterns of endangerment in the Hawaiian flora. Systematic biology 51:276-302.

Santos-Wisniewski, M. J., Rocha, O., Guntzel, A. M., and T. Matsumura-Tundis. 2008. Species richness and geographic distribution of the genera Chydorus and Pseudochydorus (Cladocera, Chydoridae) in São Paulo State. Biota Neotropica 8:61-63.

Scholl, M., Gingerich S, Loope, L., Giambulluca, T.M., and M. Nullet. 2004. Quantifying the importance of fog drip to ecosystem hydrology and water resources in windward and leeward tropical montane cloud forests on East Maui. Venture Capital Project Final Report.

Schönborn, W. 1963. Die Stratigraphie lebender Testaceen im Sphagnetum der Hochmoore. Limnologica 1:315-321.

Siemensma, F. J. (2019). Microworld, world of amoeboid organisms. World-wide electronic publication, Kortenhoef, the Netherlands.

Słowiński, M., Marcisz, K., Płóciennik, M., Obremska, M., Pawłowski, D., Okupny, D., Słowińska, S., Borówka, R., Kittel, P., Forysiak, J., and D. J. Michczyńska. 2016. Drought as a stress driver of ecological changes in peatland-A palaeoecological study of peatland development between 3500 BCE and 200 BCE in central Poland. Palaeogeography, palaeoclimatology, palaeoecology 461:272-291.

Sullivan, M. E. and R. K. Booth, R. K. 2011. The potential influence of short-term environmental variability on the composition of testate amoeba communities in Sphagnum peatlands. Microbial Ecology 62:80-93.

Swindles, G. T., Morris, P. J., Baird, A. J., Blaauw, M., and G. Plunkett. 2012. Ecohydrological feedbacks confound peat-based climate reconstructions. Geophysical Research Letters 39.

Swindles, G. T., Reczuga, M., Lamentowicz, M., Raby, C. L., Turner, T. E., Charman, D. J., Gallego-Sala, A., Valderrama, E., Williams, C., Draper, F., and E. N. H. Coronado. 2014. Ecology of testate amoebae in an Amazonian peatland and development of a transfer function for palaeohydrological reconstruction. Microbial ecology 68:284-298.

Swindles, G. T., Holden, J., Raby, C. L., Turner, T. E., Blundell, A., Charman, D. J., Menberu, M. W., and B. Kløve. 2015. Testing peatland water-table depth transfer functions using high-resolution hydrological monitoring data. Quaternary Science Reviews 120:107-117.

Swindles, G. T., Baird, A. J., Kilbride, E., Low, R., and O. Lopez. (2018a). Testing the relationship between testate amoeba community composition and environmental variables in a coastal tropical peatland. Ecological Indicators 91:636-644.

Swindles, G. T., Morris, P. J., Whitney, B., Galloway, J. M., Gałka, M., Gallego-Sala, A., Macumber, A. L., Mullan, D., Smith, M. W., Amesbury, M. J., and T. P. Roland. (2018b). Ecosystem state shifts during long-term development of an Amazonian peatland. Global change biology 24:738-757.

Sullivan, M. E. and R. K. Booth. 2011. The potential influence of short-term environmental variability on the composition of testate amoeba communities in Sphagnum peatlands. Microbial Ecology 62:80-93.

Telford, R. J. 2015. palaeoSig: significance tests of quantitative palaeoenvironmental reconstructions, R package version 1.1-3.

Ter Braak, C. J. 1986. Canonical correspondence analysis: a new eigenvector technique for multivariate direct gradient analysis. Ecology 67:1167-1179.

Tolonen, K., Warner, B. G., and H. Vasander. 1992. Ecology of Testaceans (Protozoa: Rhizopoda) in mires in southern Finland: Autecology. Archiv für Protistenkunde 142:119–138.

Van Bellen, S., Mauquoy, D., Payne, R. J., Roland, T. P., Daley, T. J., Hughes, P. D., Loader, N. J., Street-Perrott, F. A., Rice, E. M., and V. A. Pancotto. 2014. Testate amoebae as a proxy for reconstructing Holocene water table dynamics in southern Patagonian peat bogs. Journal of Quaternary Science 29:463-474.

Vázquez-Garcia, J. A. 1995. Cloud forest archipelagos: preservation of fragmented montane ecosystems in tropical America. *Tropical montane cloud forests*, pp. 315-332, Springer, New York, NY.

Wagner, W. L., Herbst, D. R., and S. H. Sohmer. 1990. Manual of the flowering plants of Hawaii. University of Hawaii Press.

Wagner, W. L., Herbst, D. R., and D. H. Lorence. 2005. Flora of the Hawaiian Islands website. http://botany.si.edu/pacificislandbiodiversity/hawaiianflora/index.htm

Warner, B. G. and Charman, D. J. 1994. Holocene changes on a peatland in northwestern Ontario interpreted from testate amoebae (Protozoa) analysis. Boreas 23:270-279.

Woodland, W. A., Charman, D. J., and P. C. Sims. 1998. Quantitative estimates of water tables and soil moisture in Holocene peatlands from testate amoebae. The Holocene 8:261-273.

Table 1: Site details and metadata for the nine peatlands, including descriptions of dominant vegetation cover. MAR = mean annual rainfall, ET = annual evapotranspiration, WTD = water-table depth. *MAR and ET estimates are derived from Giambelluca *et al.* (2013).

Site Name Code	*MAR (mm/ yr)	*ET (mm/ yr)	WTD Range (cm)	pH Range	n	Peatland description	Dominant plant taxa
Pu‘u Kawila (PK)	2550	840	-9-58	3.2-4.8	17	*Sphagnum* peatland in cinder cone depression	*Sphagnum palustre*, *Lycopodiella cernua*, *Deschampsia nubigena*, *Metrosideros polymorpha*
Pu‘u o Umi A (PUA)	3600	640	-8-15	3.7-4.6	5	*Sphagnum* peatland, sedges in valley	*Rhynchospora*, *Sphagnum palustre*, *Panicum*, *Holcus lanatus*
Pu‘u o Umi B (PUB)	3840	750	-5-39	3.6-4.4	10	Open sedge peatland, *Sphagnum* hummocks	*Sphagnum palustre*, *Racomitrium*, *Oreobolus furcatus*, *Rhynchospora*
Pu‘u o Umi C (PUC)	3740	720	-9-33	3.5-4.7	16	Open sedge peatland, *Sphagnum* hummocks	*Sphagnum palustre*, *Racomitrium*, *Oreobolus furcatus*, *Rhynchospora*
Wai‘ilikahi (WK)	3800	700	0-26	4.0-4.2	5	Open *Sphagnum* peatland	*Sphagnum palustre*, *Rhynchospora*, *Dicranopteris linearis*
Kaiholena (KL)	3420	700	-6-45	3.3-4.5	13	Forested *Sphagnum* peatland	*Sphagnum palustre*, *Deschampsia nubigena*, *Metrosideros polymorpha*, *Cibotium*
Alakahi (AK)	3200	630	-13-57	3.4-5.9	9	Forested *Sphagnum* peatland	*Sphagnum palustre*, *Deschampsia nubigena*, *Metrosideros polymorpha*, *Leptecophylla tameiameia*, *Dicranopteris linearis*
KHL1	2760	760	-15-28	4.2-5.7	9	Sedge and rush peatland	*Juncus planifolius*, *Machaerina angustifolia*, *Rhynchospora*, *Racomitrium*
KHL2	2960	760	-1-29	4.1-5.5	6	Sedge and rush peatland	*Juncus planifolius*, *Rhynchospora*, *Carex alligata*, *Racomitrium*

Table 2: Unsupported activities of ^{210}Pb and ^{137}Cs and ^{210}Pb ages calculated by CRS modeling for the core WK. Parentheses show ^{210}Pb measurement error and age error propagated through CRS model.

Depth interval (cm)	^{210}Pb Age (±error) (CE)	Unsupported ^{210}Pb (±error) (Bq/kg)	^{137}Cs (Bq/kg)
0	2000 (1)	1180	-
0-5	1998 (1)	1112 (60)	42
5-10	1992 (1)	915 (134)	47
10-14	1988 (1)	815 (132)	58
14-18	1984 (1)	723 (28)	107
18-21	1976 (1)	563 (28)	297
21-24	1961 (2)	355 (21)	778
24-27	1939 (5)	177 (16)	678
27-30	1905 (20)	62 (12)	280
30-32	1879 (90)	28 (13)	132
32-37	-	-	42
37-42	-	-	12
42-47	-	-	8

Table 3: Explained variance and variance partitioning of the variables depth to water table, pH, and conductivity, based on a CCA of surface taxon assemblages. Results are for the full, *Sphagnum*-only, and non-*Sphagnum*-only datasets. Parentheses () indicate the percentage of total explained variance that is shared with a confounding variable. Significance: ***($p < 0.001$), **($p < .01$), ns (not significant).

	Dataset		
	Full	*Sphagnum*	Non-*Sphagnum*
Variable name	n = 89	n = 56	n = 33
Depth to water table	9.4^{***} (1.6)	9.7^{***} (2.9)	15.2^{***} (0.8)
pH	6.9^{***} (2.8)	6.5^{***} (3.1)	10.8^{***} (0.8)
Conductivity	2.1^{ns} (0.2)	4.3^{**} (0.1)	3.7^{ns} (0.7)
λ_1/λ_2 of CCA constrained on depth to water table	0.98	0.87	1.02

Table 4: Transfer function performance statistics for the testate amoebae plus Cladocera calibration data set given three cross-validation techniques: LOO = leave-one-out, BOOT = bootstrapping at 999 cycles, LOSO = leave-one-site-out. Parentheses ( ) show the improvement of $RMSEP_{LOSO}$ and r^2_{LOSO} of testate amoebae plus Cladocera transfer function over testate amoebae without Cladocera transfer function

Method	RMSEP LOO	r^2 LOO	Avg.Bias LOO	Max.Bias LOO	RMSEP BOOT	r^2 BOOT	RMSEP LOSO	r^2 LOSO
Wa.Inv	9.99	0.59	0.10	36.49	10.22	0.59	10.27 (-0.13)	0.56 (+0.01)
Wa.Tol.Inv	10.12	0.58	0.32	35.95	10.54	0.59	10.12 (-0.40)	0.58 (+0.04)
Wa-PLS (*Comp. II*)	9.37	0.64	0.44	28.53	9.97	0.65	9.75 (-0.54)	0.62 (+0.05)
MAT (*k=7*)	9.65	0.63	-1.10	35.38	10.35	0.65	9.85 (-0.80)	0.63 (+0.08)

Figure legends

Figure 1: Site map of Kohala wet forest-peatland complex indicating locations of the nine peatland locations in this study (highlighted in yellow). Light green shows the extent of wet forest vegetation cover, and dark green polygons indicate montane peatland vegetation cover. Solid grey contours are 100 ft (30.3 m) elevation contours and dashed grey contours are the interpolated mean annual rainfall contours (mm/yr). Vegetation and elevation GIS layers downloaded from HI Statewide GIS Program (geoportal.hawaii.gov). Rainfall contours are from Giambelluca *et al*. (2013).

Figure 2: Surface sample testate amoebae and Cladocera relative abundances (%) arranged according to depth to water table at each sampling location.

Figure 3: First two axes of a 3-dimensional NMDS of surface sample assemblages using Sørenson dissimilarity metric. A) Sample scores for the nine peatlands (codes link to table of descriptions of the nine peatlands). B) Species scores for testate amoebae taxa (black text) and Cladocera taxa (blue text) with environmental vectors overlain. WTD = depth to water table, BD = bulk density, LOI = loss-on-ignition, EC = conductivity. C) Vectors representing fine-resolution vegetation cover (orange) and environmental variables (black).

Figure 4: Leave-one-site-out cross-validation of a weighted average partial least-squares regression transfer function (2^{nd} component). Plots on the right show the results of predicting water-table depth from biological assemblage data at each peatland from a calibration dataset that excludes that peatland. Plot on the left shows all samples from leave-one-site-out cross-validation. Dashed line is a 1:1 realtionship. Solid black line is the linear trend of the data points.

Figure 5: Sampling bias evaluated by dividing the water table depth gradient into 10 equal segments and calculating RMSEP for each segment. Gray bars represent the frequency of samples in the gradient segment, green lines represent the RMSEP for the segment, red dashed line is the $RMSEP_{LOO}$ for the entire gradient length, and the black dashed line is the average of the RMSEP values of each segment along the gradient, also called the segment-wise RMSEP.

Figure 6: Stratigraphic diagram of testate amoebae and Cladocera assemblages in fossil core WK plotted against depth with ^{210}Pb age of the peat. Taxa present in fewer than three samples are excluded from the plot. Zonation is based on stratigraphically constrained cluster analysis (CONISS) and is derived from Euclidean distances.

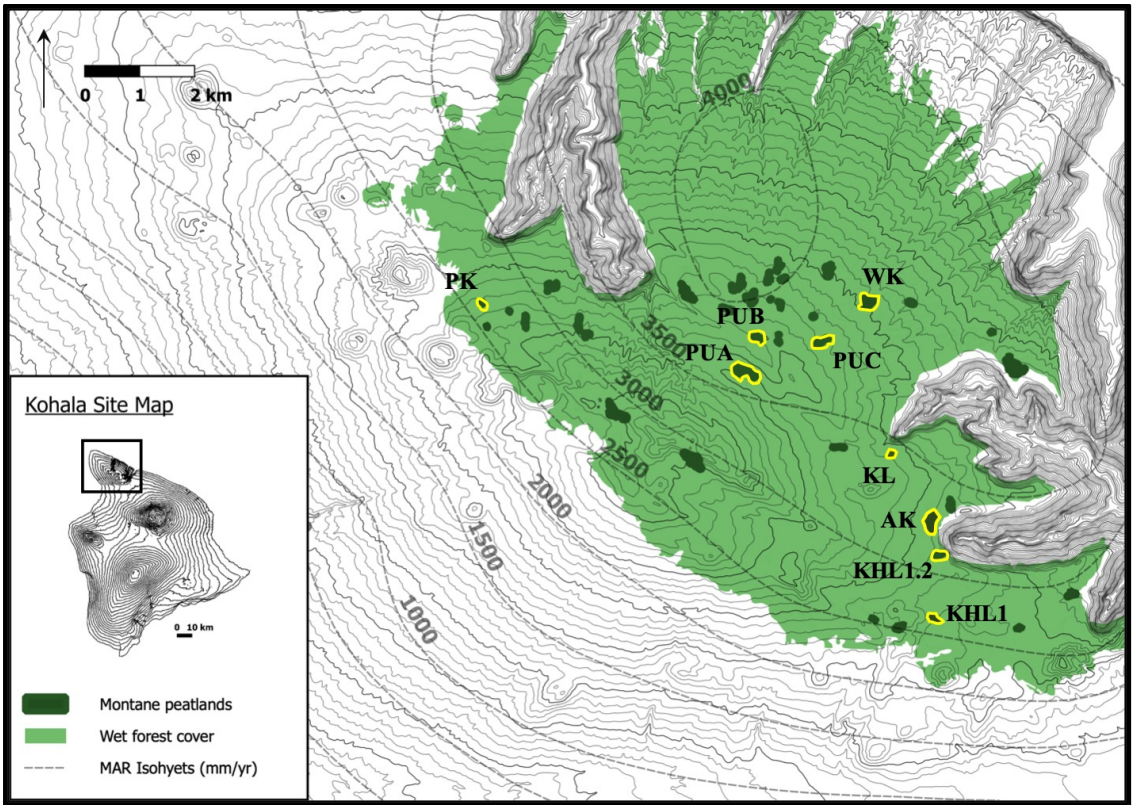

Figure 1: Site map of Kohala wet forest-peatland complex indicating locations of the nine peatland locations in this study (highlighted in yellow). Light green shows the extent of wet forest vegetation cover, and dark green polygons indicate montane peatland vegetation cover. Solid grey contours are 100 ft (30.3 m) elevation contours and dashed grey contours are the interpolated mean annual rainfall contours (mm/yr). Vegetation and elevation GIS layers downloaded from HI Statewide GIS Program (geoportal.hawaii.gov). Rainfall contours are from Giambelluca *et al*. (2013).

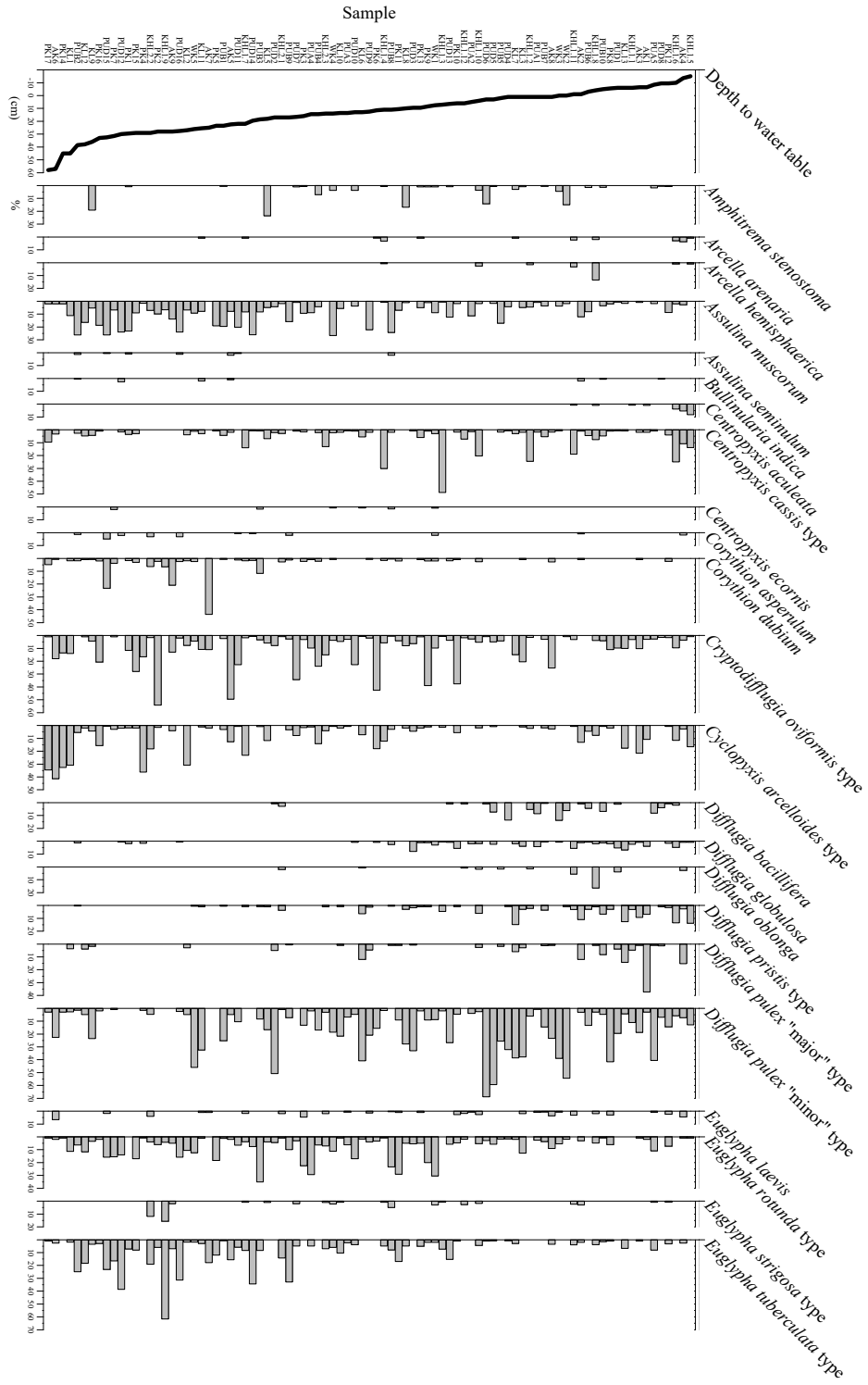

Figure 2: Surface sample testate amoebae and Cladocera relative abundances (%) arranged according to depth to water table at each sampling location. (1/2)

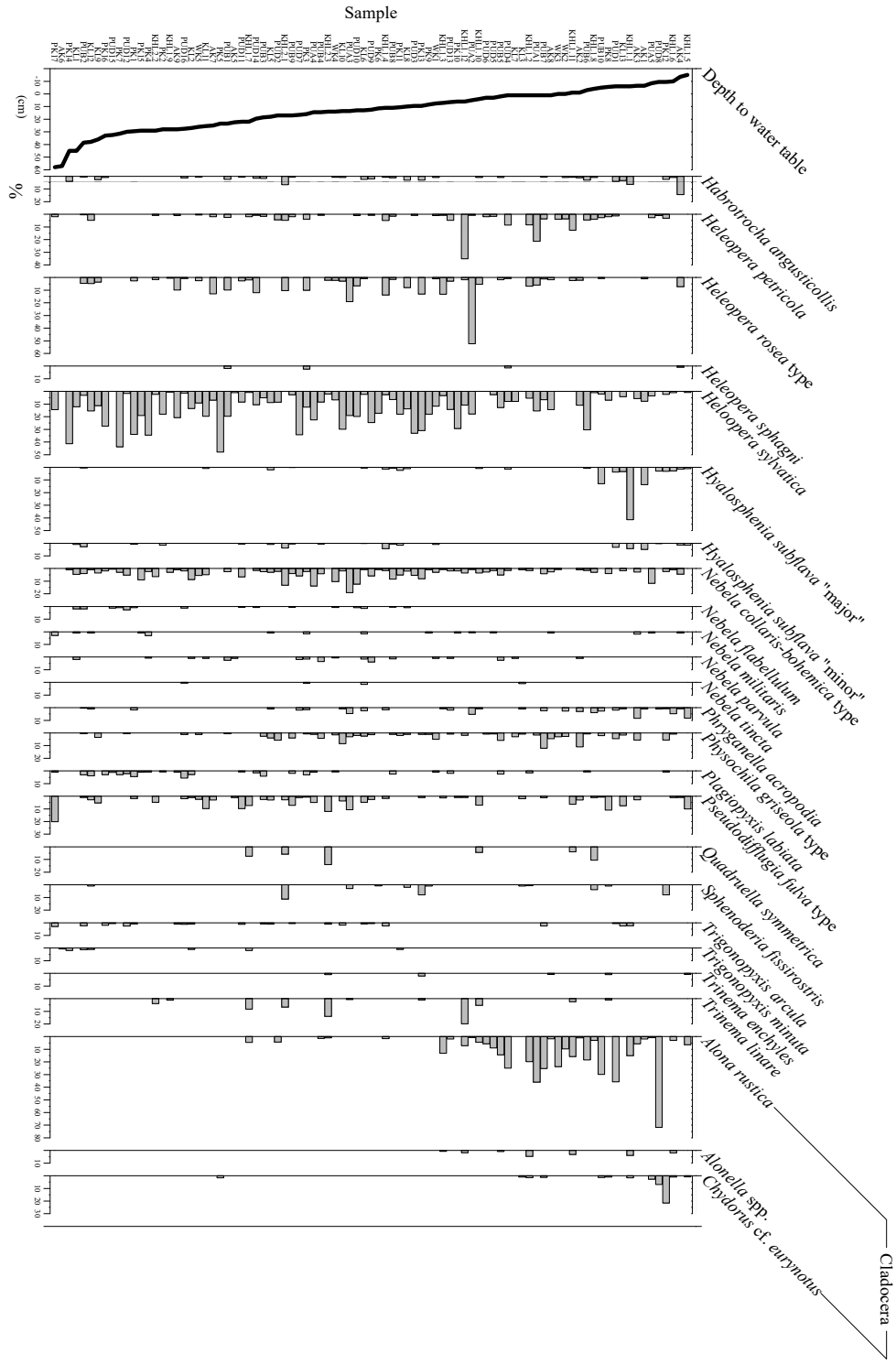

Figure 2: Surface sample testate amoebae and Cladocera relative abundances (%) arranged according to depth to water table at each sampling location. (2/2)

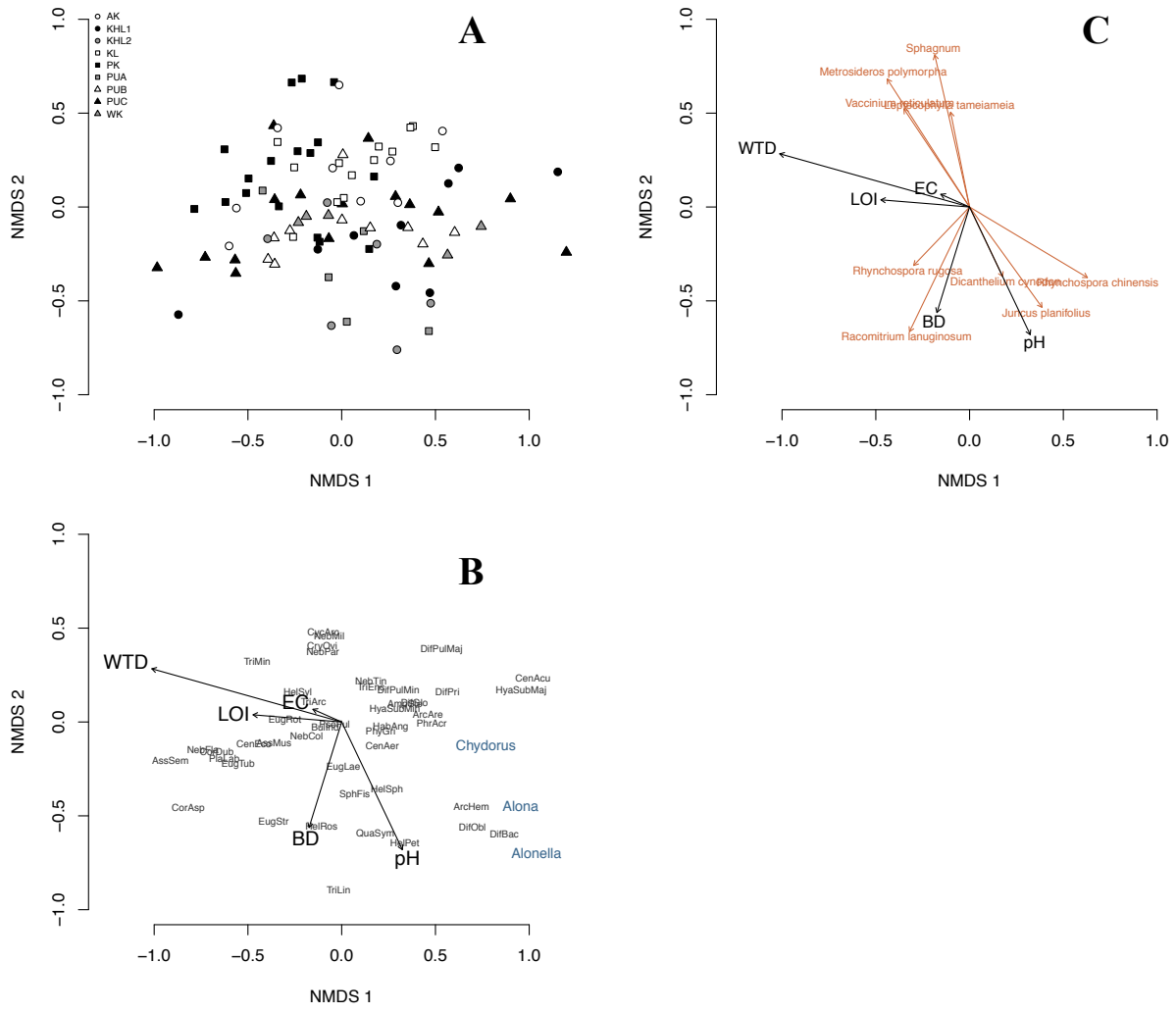

Figure 3: First two axes of a 3-dimensional NMDS of surface sample assemblages using Sørenson dissimilarity metric. **A)** Sample scores for the nine peatlands (codes link to table of descriptions of the nine peatlands). **B)** Species scores for testate amoebae taxa (black text) and Cladocera taxa (blue text) with environmental vectors overlain. WTD = depth to water table, BD = bulk density, LOI = loss-on-ignition, EC = conductivity. **C)** Vectors representing fine-resolution vegetation cover (orange) and environmental variables (black).

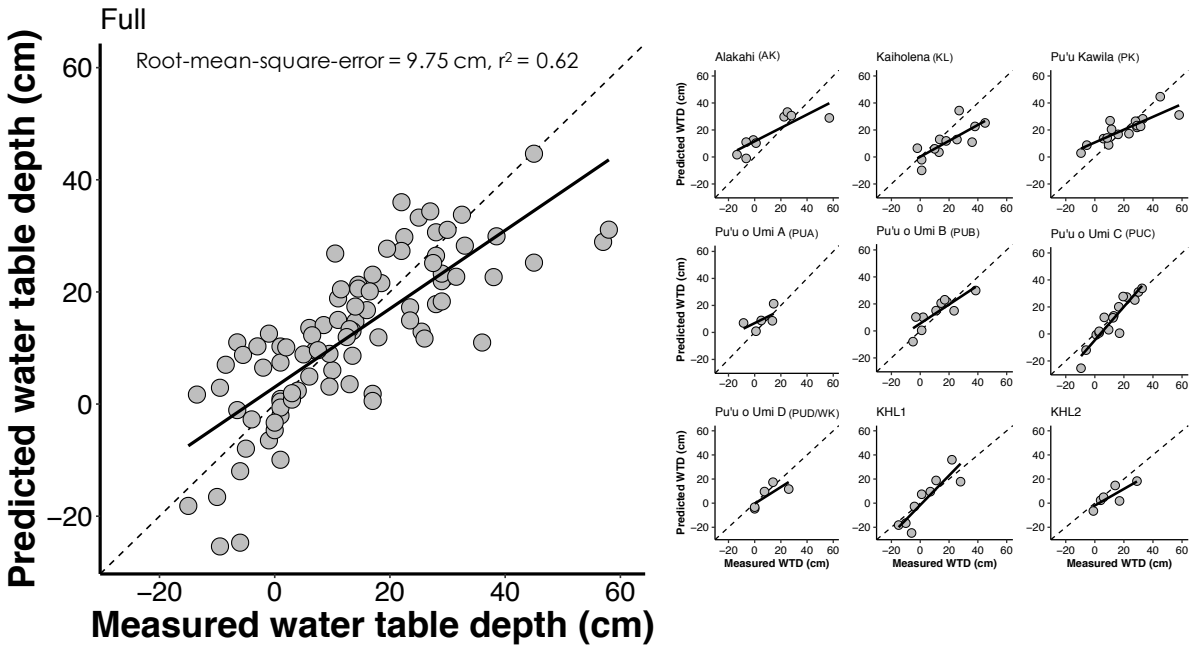

Figure 4: Leave-one-site-out cross-validation of a weighted average partial least-squares regression transfer function (2nd component). Plots on the right show the results of predicting water-table depth from biological assemblage data at each peatland from a calibration dataset that excludes that peatland. Plot on the left shows all samples from leave-one-site-out cross-validation. Dashed line is a 1:1 realtionship. Solid black line is the linear trend of the data points.

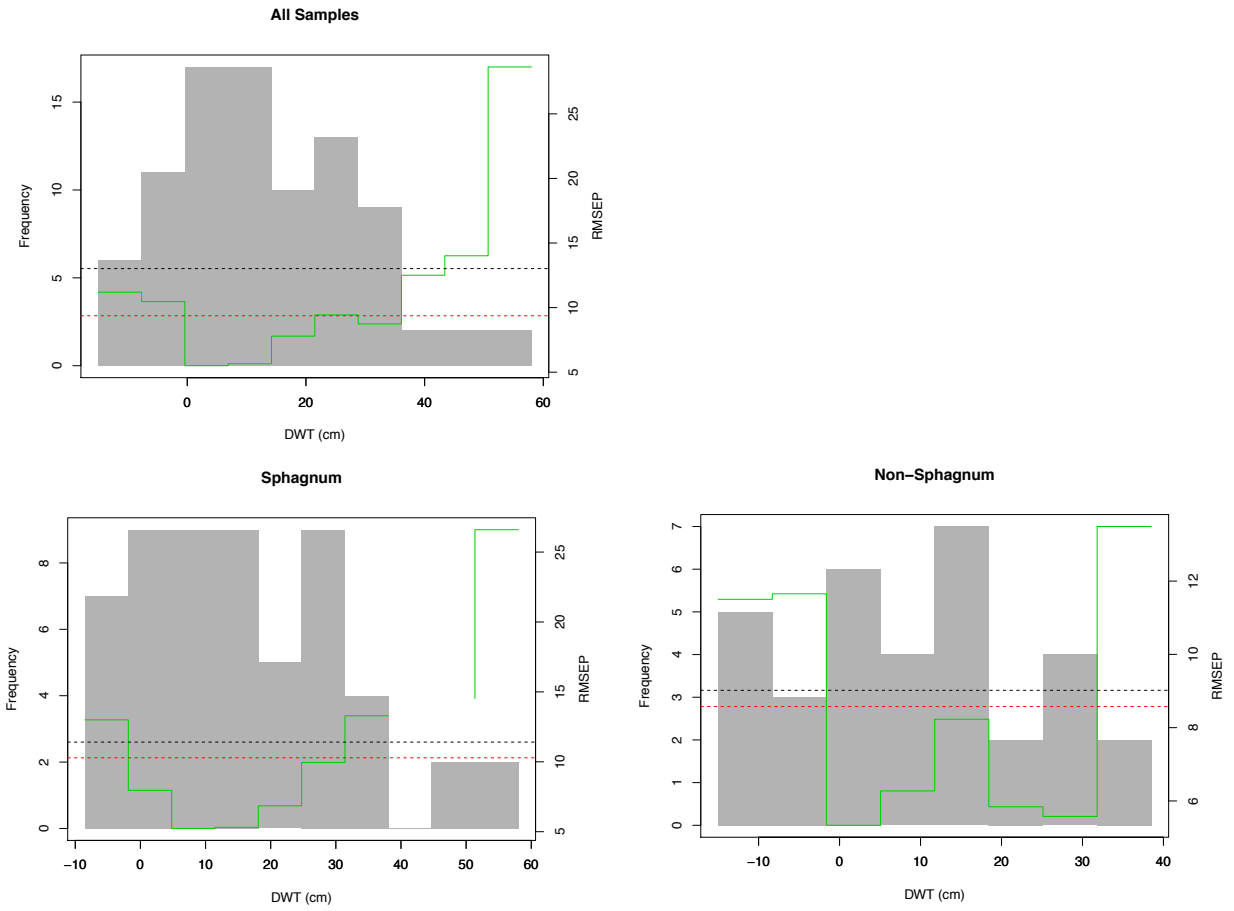

Figure 5: Sampling bias evaluated by dividing the water table depth gradient into 10 equal segments and calculating RMSEP for each segment. Gray bars represent the frequency of samples in the gradient segment, green lines represent the RMSEP for the segment, red dashed line is the $RMSEP_{LOO}$ for the entire gradient length, and the black dashed line is the average of the RMSEP values of each segment along the gradient, also called the segment-wise RMSEP.

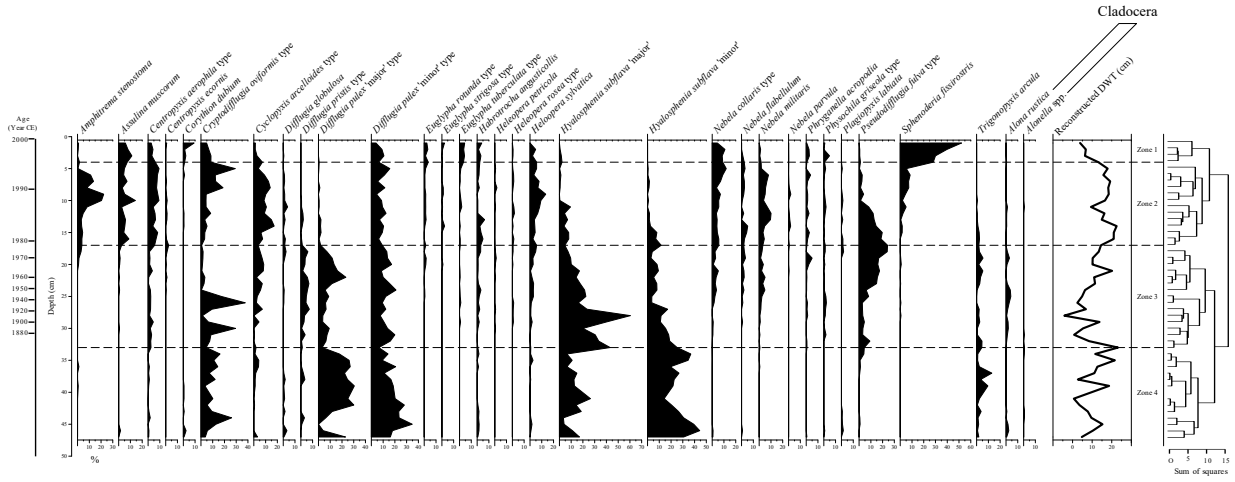

Figure 6: Stratigraphic diagram of testate amoebae and Cladocera assemblages in fossil core WK plotted against depth with ^{210}Pb age of the peat. Taxa present in fewer than three samples are excluded from the plot. Zonation is based on stratigraphically constrained cluster analysis (CONISS) and is derived from Euclidean distances.

-Chapter 3-

A 4000-year ecohydrological record from a Hawaiian peatland

Kevin D. Barrett[1], Patricia Sanford[2], Sara C. Hotchkiss[1,2]

University of Wisconsin-Madison, Botany[1]

University of Wisconsin-Madison, Center for Climatic Research[2]

Abstract

Here we present a detailed analysis and paleohydrological interpretation of the subfossil remains of testate amoebae and Cladocera in a Hawaiian montane peatland. Subfossils were analyzed in a ~4 ka peat core from an open peatland in the wet forest-montane bog complex on Kohala Mountain, Hawai‘i Island. A transfer function based on weighted averaging with partial least-squares regression was developed for Kohala and used to reconstruct past water-table depth from fossil assemblages. Subfossil concentrations were low in the core; however the taxa preserved were well-defined paleoenvironmental indicators. Peatland conditions were wetter than present between 3.4 and 2.7 ka (calendar years BP) and 1.6 to 1.2 ka. A pronounced dry period and poor-preservation environment occurred 2.7 to 1.6 ka. These results provide evidence for a centuries-long period of increased aridity in Hawai‘i and point to the occurrence of statewide drought, likely associated with El Niño-like conditions in the North Pacific.

Introduction

Peatlands develop in areas where waterlogged conditions slow rates of decomposition, resulting in net accumulation of partially decomposed organic matter. Peatlands cover roughly 3% of the global land surface but store 25% of global soil carbon (Limpens *et al.* 2008). The vast majority of peatland area is in temperate to subarctic latitudes, particularly in the Northern Hemisphere (Yu 2012), where cool and wet climates promote peat development. However, peat can also form in the humid tropics under high-rainfall and high-temperature conditions (Andriesse 1988) at both lowland and montane altitudes. Most tropical peatlands occur in lowlands in Southeast Asia and the Amazon, where they are typically forested, ombrogenous (only rain inputs), and very large in size (Page *et al.* 2006). Tropical montane peatlands lie in depressions or on shallow slopes of the tropical humid highlands of continental (*e.g.* Northern Andes, Costa Rica, Uganda) and island (*e.g.* Galapagos, Hawaiian Islands, Caribbean Islands) locations. These peatlands tend to be smaller and dominated by herbaceous tussock plants and bryophytes, and may be ombrogenous or geogenous (surface water and/or groundwater inputs) (Canfield 1986, Chimner 2004, Squeo *et al.* 2006). Despite their small size, tropical montane peatlands can be numerous and are important players in the global carbon cycle (Chimner and Karberg 2008) and in local hydrological cycles for both montane and downstream regions (Buytaert *et al.* 2006).

In Hawai‘i, montane peatlands are found between 1000 and 2300 m elevation on all five major islands. These peatlands include some of the few remaining intact natural ecosystems in Hawai‘i (Loope *et al.* 1991, Van Reese & Reed 2014); however, continued pressure from feral ungulates, such as wild pigs (Loope *et al.* 1991), and climate change (Loope & Giambelluca 1998) threaten long-term peatland stability.

Descriptions of Hawaiian peatland history span over a half century, beginning with Selling's seminal work on Quaternary Hawaiian pollen (1948). Selling (1948) noted noted long peat sections composed of the principal Hawaiian peatland sedge, *Oreobolus furcatus*, with short intervals of dark, organic-rich layers derived from bryophytes. Burney & Burney (2003) described sediment lithology in radiocarbon-dated peat cores from Kaua'i that revealed alternating layers of humified peat, clay, and wood deposited throughout the Holocene. Burney *et al*. (1995) provided detailed peat lithology of an East Maui montane peatland that had transitions from organic-rich layers with diatoms to fibrous peat to fine-grained, organic-rich peat over the past 5000 years. A new peatland multi-proxy record from East Moloka'i found evidence for wet and stable peatland conditions in the early and mid Holocene, and a shift to dry conditions in the late Holocene (Beilman *et al*. 2019).

Peatland and lake sediment records of pollen (Selling 1948, Burney *et al*. 1995, Hotchkiss 1998, Hotchkiss & Juvik 1999, Pau *et al*. 2012, Crausbay *et al*. 2014) and biomarkers (Uchikawa *et al*. 2010, Crausbay *et al*. 2014, Beilman *et al*. 2019) across all five major Hawaiian Islands have revealed vegetation and climate change throughout the Holocene. In particular, records spanning the past few thousand years on Maui, Oahu, and Moloka'i show evidence of synchronous wetting and aridification (Burney *et al*. 1995, Uchikawa *et al*. 2010, Pau *et al*. 2012, Crasubay *et al*. 2014, Beilman *et al*. 2019). The hydroclimate of Hawai'i Island has not been investigated in detail.

Here we present the results from a detailed analysis of testate amoebae and Cladocera subfossils in a dated peat core from a montane peatland on Hawai'i Island. Testate amoebae are a group of single-celled protozoa that produce decay-resistant shells ("tests") that have been widely applied as paleoenvironmental and paeohydrological indicators in temperate and boreal

peatlands (Booth 2008, Lamarre *et al.* 2013, Amesbury *et al.* 2016), and increasingly in the tropics (Swindles *et al.* 2014, Liu *et al.* 2019). Analysts have routinely confirmed the sensitivity of testate amoebae assemblage composition to soil moisture conditions at the surface and near-surface of peatlands, and records of subfossil testate amoebae in peat cores have been useful for infering peatland surface moisture histories, especially when integrated within multi-proxy investigations (*e.g.* Booth *et al.* 2012, Swindles *et al.* 2018). Our recent research suggests that testate amoebae are distinctly distributed along gradients of depth to water table in Hawaiian montane peatlands and that fossil assemblages of tesate amoebae are preserved in downcore peat deposits (Chapter 2). We also determined that analysis of Cladocera (water flea) subfossils improved transfer functions relating depth-to-water-table estimates to species assemblage data (Chapter 2). We apply this transfer function to a fossil testate amoebae and Cladocera chronology from Kohala Mountain, Hawai‘i to infer a history of peatland environmental change and compare the reconstruction with paleoenvironmental records from other Hawaiian Islands.

Study site

Vegetation

The peatland site is “Kohala 1” (KHL1), a gently sloping, open montane peatland in the Kohala State Forest Reserve on Kohala Mountain, 5 km southeast of the summit. KHL1 sits atop 120-230 kya tephra-fall deposits from the Hāwī Volcanic Series (Wolfe & Morris 1996). The surrounding forest is composed of stunted *Metrosideros polymorpha* Gaudich., *Vaccinium reticulatum* Smith, and *Leptecophylla tameiamaeia* Schltdl., with some dense thickets of *Dicranopteris linearis* NL Burm. The forest understory is primarily a monotypic carpet of *Sphagnum palustre* L. KHL1, however, is one of the few *Sphagnum*-free peatlands on the

mountain. Surface vegetation is a lawn of *Juncus planifolius* R. Br., with *Machaerina angustifolia* Gaudich., *Rhynchospora chinensis* ssp. *spiciformis* Hillebr., and tussocks of *Rhynchospora rugosa* var. *lavarum* Gaudich. and the moss *Racomitrium lanuginosum* Hedwig. *J. planifolius* is a nonnative rush of temperate South American or Australian origin first recorded in Hawai‘i in 1930 (Wagner *et al.* 1990).

Hydrology

KHL1 is likely underlain by a clay hardpan that impedes water drainage (Fosberg 1961). The surrounding volcanic substrate is porous and rainfall quickly percolates through the surface. However, heavy and prolonged rain can inundate forest soils, and we have observed overland surface water flow into KHL1. The hydrologic budget is probably somewhere between ombrogenous and soligenous.

Climate

KHL1 has a high-elevation tropical climate with estimated annual rainfall at 2800 mm/yr and annual temperature of 15.7°C. KHL1 is frequently surrounded by cloud cover, so fog-driven moisture likely contributes substantially to the hydrological input (Scholl *et al.* 2004, Giambelluca *et al.* 2011). Local climate is heavily influenced by two major sources of moisture: northeast tradewinds that deliver orographically lifted rain year-round and large “Kona storms” derived from subtropical cyclones that occur more frequently during winter months (Chu *et al.* 1993). These broad climatic patterns are sensitive to modes of Pacific climate variability, particularly in the El Niño-Southern Oscillation and Pacific Decadal Oscillation systems (Chu and Chen 1995).

Methods

Collection, preparation, and identification

A 2.6-m-long peat core was collected from KHL1 in 2015 near the center of the peatland using a Russian peat-corer with a 50-cm-long barrel. Each core segment was stored frozen at the University of Hawai‘i-Mānoa until subsamping and analysis. Ninety surface peat samples were collected from nine Kohala peatlands, including 15 from KHL, in 2015, 2016 and 2018 for analysis of modern testate amoebae and Cladocera to produce a species-environment transfer function (Chapter 2).

For the peat core, one cm^3 of peat was subsampled every 2 cm from depths 0-100 cm below the peat surface and every 4 cm for 100-260 cm depth. Microfossils were isolated from peat following standard practices outlined in Booth *et al.* (2010). The peat sample was disaggregated in boiling water for 10 min. The boiled samples were filtered through 300- and 15-μm sieves and the fraction between the sieves was retained and stored in glycerine. Subsamples were mounted on microscope slides and examined under 100-400X magnification. Testate amoebae and cladoceran remains were tallied together on the same slides, along with the common peatland rotifer *Habrotrocha angusticollis* Murray. The most abundant category of cladoceran remains (*i.e.* head shields, carapaces, post abdomens, and postabdominal claws) for each taxon was used to calculate minimum number of individuals (Frey 1986). A minimum of 50 testate amoebae and Cladocera individuals was attempted for each sample, however very low subfossil concentrations at certain depth intervals impeded counting efforts and the minimum was occasionally unmet (undercounts marked below). A 50-count minimum has been shown to capture the broad environmental signal from testate amoebae assemblage data (Payne and Mitchell 2009), and assemblages were evaluated with species-area curves as subsamples were

counted to inspect relative abundance stability. Additional microfauna and invertebrate remains (*e.g.* chironomids) were tallied for added stratigraphic information.

Taxonomy of testate amoebae followed Charman, Hendon, & Woodland (2000), modified by Booth (2008), and identification was aided with guides by Siemensma (2019). We applied the morphospecies approach for classifying testate amoebae taxa following the procedure in Chapter 2, however *Hyalosphenia subflava* Cash & Hopkinson was lumped as a single taxon instead of separating the "minor" and "major" size classes. Cladoceran taxonomy followed Dodson and Frey (1991).

Core stratigraphy

To complement the subfossil record, qualitative descriptions of the peat-contributing vegetation were made by identifying plant macrofossils. This analysis did not follow the standard protocol for quantitative analysis of peatland macrofossils (Mauquoy *et al.* 2010), because subsample material was limited to 1 cm^3 of peat and because macrofossil remains were often decayed and in low abundance. Plant macrofossils that were collected on the 300 µm sieve during the subfossil protocol outlined above were transferred to a glass petri dish and viewed under a dissecting microscope at 10 – 20X magnification. The only plant macrofossils that were identified to the source material were moss leaves and *Oreobolus furcatus* H. Mann, which has a characteristic red hue (Selling 1948). Remains of monocot leaves were coded as "graminoids" and leaf remains that had sori were coded as "pteridophytes." Each layer of peat was then assigned to "moss", "*Oreobolus"*, "graminoid", or "pteridophyte" based on the category that had the most remains. However, many samples lacked identifiable plant macrofossils and were

therefore assigned to the category of the nearest stratigraphic neighbor that did have macrofossil remains.

Radiocarbon Dating and Age-Depth Modeling

Radiocarbon (^{14}C) analysis was performed on seven bulk peat samples (Table 1). Fine roots were picked out from peat subsamples, which were then treated with an Acid-Alkalic-Acid sequence to remove any added organic and inorganic carbon. Peat sample ^{14}C was analyzed at the Lawrence Livermore National Lab's Center for Accelerator Mass Spectrometry (LLNL-CAMS). ^{14}C ages were calibrated to calendar years BP using IntCal13 (Reimer *et al.* 2013) with year 0 BP = 1950 CE by convention. The age-depth model was produced by a Bayesian analysis on millions of Markov Chain-Monte Carlo simulations using the probability distributions of the ages with a precise surface age of -65 cal yr (BP), and a prior of 20 yr/cm for stratigraphic accumulation using the R package "rbacon" (Blaauw and Christen 2011).

Transfer function

The second component of a weighted-average with partial least-squares regression (WA-PLS) was the best-performing transfer function model from Chapter 2 and was chosen to reconstruct water-table depths from fossil assemblages in KHL1. This model has a leave-one-site-out cross-validated root-mean-square-error of prediction (RMSEP) = 9.75 cm and $r^2 = 0.62$. We interpreted stratigraphy of the profile using stratigraphically constrained hierarchical cluster analysis on Sørenson distances between assemblages (Grimm 1987). Determination of zonation was guided by the broken stick model.

Results

Stratigraphy and Chronology

The base of the peat (255 cm) is dated to 3.9 ka (calendar years before BP, Figure 2, Table 1). The underlying clay layer (265 cm) is dated to 9.8 ka and the radiocarbon date was discarded by Bacon as an outlier (Figure 2). The bottom ~10 cm of the peat core is predominantly composed of silt and clay (Figure 3). This zone (265 to 255 cm) likely reflects a period of soil development and slow sedimentation rate prior to the development of the peatland. Plant remains from pteridophytes and mosses were found in the silt-clay layer, as well as testate amoebae and cladoceran remains, but these were in low abundances. Between 255 and 220 cm, the abundance of preserved moss leaves increases, including taxa such as *Thuidium delicatulum* Hedwig., *Distichophyllum freycinetii* Schwägr., and cf. *Ectropothecium* spp. Sull, and peat accumulates at 1.13 mm/yr. Between 220 and 195 cm is a layer of graminoids, followed by a layer of mosses between 195 and 185 cm, and then another layer of graminoids between 185 and 155 cm. *Oreobolus* macrofossils increase at after 155 cm and then disappear by 140 cm. From 210 to 140 cm the peat core accumulates peat at the fastest rate in the record (1.27 mm/yr, Figure 3). The mosses cf. *Ectropothecium* spp. and *T. delicatulum* reappear between 130 cm and 110 cm, and accumulation rate decreases to the slowest rate in the record (0.25 mm/yr, Figure 3). Sedimentation rate increased above this interval, but was lower than rates in the lower portion of the record. Between 104 cm and 94 cm there were many remains of pteridophytes and woody fragments. Graminoids were the most common plant remains between 94 cm and the top of the core.

Subfossil testate amoebae and Cladocera

No undescribed taxa were encountered in the core compared with the calibration dataset from Chapter 2 (Figure 4). Testate amoebae in general were low in concentration, so it was often necessary to count multiple slides per sample. This may reflect an issue with preservation (Mitchell *et al.* 2008), which appears to be common in tropical peat (Swindles *et al.* 2014, Swindles *et al.* 2016). However, the preserved taxa have well-defined moisture optima (*e.g. Assulina muscorum* Greeff, *Trigonopyxis arcula* Penard, and Cladocera; Chapter 2). Cladocera were present throughout much of the core, including the surface. Four significant biostratigraphic zones were identified by the cluster analysis and broken-stick model (Figure 4). Zone composition is described below.

Zone 1 (255 – 133 cm): Zone 1 is characterized by high abundances of the cladocerans *Alona rustica* Scott and cf. *Alonella* spp. and the rotifer *Habrotrocha angusticollis* Murray (Figure 4). *Difflugia globulosa* (Dujardin) Penard was also present in this zone. *Centropyxis cassis* Wallich type, *Trigonopyxis arcula,* and *Cyclopyxis arcelloides* Penard type had greater abundances in the deeper portion of Zone 1 than in the upper portion of the Zone 1 (Figure 4), which are intermediate and dry-indicator taxa in Hawai‘i (see Chapter 2), suggesting that drier conditions occurred during that period. Reconstructed water table at the beginning of the zone was low below the surface (~ 20 cm, Figure 4) and then reached the highest level of the record in the upper portion of the zone (~ -13 cm), reflecting a period of saturated peatland conditions with standing water.

Zone 2 (132 – 103 cm): The beginning of Zone 2 is characterized by an abrupt decline in cladoceran abundance to near zero where it remained until Zone 3 (Figure 4). Subfossil concentrations were very low in this zone. Relative abundances of *Assulina muscorum* and *Trigonopyxis arcula* reached the highest values of the record in this zone. Relative abundance of *Hyalosphenia subflava* was high, but variable. Reconstructed water table abruptly dropped at the beginning of the zone to ~ 25 cm, stayed low below the peatland surface eventually dropping to the lowest depth in the record (~ 40 cm), and then abruptly increased at the end of Zone 2 (Figure 4).

Zone 3 (102 – 69 cm): Zone 3 is characterized by abundant and assemblages of cladocerans (Figure 4). Testate amoebae have low abundances. *Amphitrema stenostoma* Nüsslin occurs in small numbers alongside *Hyalosphenia subflava* and *Habrotrocha angusticollis*. The reconstructed water table curve is high for this zone (between 8 and -1 cm, Figure 4), suggesting that saturated conditions or long periods of standing water were common, similar to the upper portion of Zone 1.

Zone 4 (68 cm – surface): Zone 4 marks a reduction in cladoceran abundance to ~5-10%. Testate amoebae taxonomic diversity was highest in this zone (Figure 4). *Hyalosphenia subflava* and *Centropyxis cassis* type were the most abundant testate amoebae. Species of *Difflugia* and *Euglypha* also occurred, but their overall abundance was low. *Quadruella symmetrica* Wallich., an indicator of high pH, appeared at the surface of the core, but in low abundance. The water-table reconstruction indicates near-surface water table for most of the zone and moderate drying in the upper ~20 cm (Figure 4).

Other microfauna

Concentrations of chironomid mandibles and egg cases of copepods and tardigrades were related to zones defined by testate amoebae and Cladocera (Figure 5). Chironomids were most frequent in *Zone 1* and *Zone 3* and copepods were most frequent in *Zone 4* when the water table curve reflects wet conditions. Chironomids and copepods were rare in *Zone 2* when the water table was low, then spiked in occurrence at the transition to *Zone 3* (Figure 5). Tardigrades were abundant at the onset of *Zone 2* and *Zone* 4*,* and at the end of *Zone 3*.

Discussion

Peat began accumulating at KHL1 3.9 ka during a period of the Holocene that other Hawaiian paleovegetation records point to being anomalously wet (Burney *et al.* 1995, Crausbay *et al.* 2014). The testate amoebae and Cladocera assemblages suggest that this period was of "intermediate" surface wetness (Figure 4). From 4.0 to ~3.3 ka the peatland water table remained relatively low and mosses were common on the peatland surface. After ~3.3 ka cladocerans became more abundant and dry-intermediate testate amoebae taxa, such as *Centropyxis*, *Cyclopyxis* and *Assulina*, became less abundant. The highest reconstructed water tables occur ~3 ka in this record. This also when remains of chironomids and copepods are at a local maximum (Figure 5). Chironomids and copepods are semi-aquatic invertebrates and their presence in the peat record indicates flooding on the peatland surface. This is supported by coherent changes in abundance of Cladocera (Figure 4). Peat accumulation rate is also greatest during this lower portion of the record. A wet period between 3.3 to 2.7 ka has been observed in other Hawaiian paleorecords. Crausbay *et al.* (2014) observed a rapid increase in sedimentation rate in a high-

elevation lake core on Maui after 3.2 ka and a multi-proxy paleorecord from a montane peatland on Molokaʻi that sediment accumulation rate quickened between 3.5 to 2.5 ka, which they attribute to high and stable peatland water tables (Beilman *et al.* 2019).

There are several lines of evidence of peatland drying between 2.7 and 1.6 ka. Subfossils of testate amoebae were difficult to find in this section of the core; however, the taxa that were encountered were reliable indicators of dry conditions (*e.g. Assulina muscorum* and *Trigonopyxis arcula*, Chapter 2). A parsimonious explanation for low test concentrations is that lower average water table and oxidation of surface peat enhanced microbial activity that degraded tests. Conversely, cladoceran exoskeletons are composed of chitin and are very well-preserved in humified peat. Hence, absence of Cladocera likely reflects environmental filtering due to dry conditions rather than taphonomic loss. In addition, chironomids and copepods are rare during this interval. Tardigrades, on the other hand, reach their highest concentration. Tardigrades inhabit a wide array of environments but are particularly abundant in wet moss. This has support from the peat stratigraphy which suggests that mosses were abundant during this period (Figure 3). Vegetation change at KHL1 in response to peatland drying could involve mosses colonizing dried-up hollows between sedge tussocks. Peat accumulation rate slowed during this dry interval and then increased after 1.6 ka (Figure 3). On East Maui, a drought regime began ca. 2.5 ka that resulted in dieback of wet forest tree species (Crausbay *et al.* 2014). A second Maui pollen record suggests treeline altitude lowered after 2.2 ka and the altitudinal limits of wet rainforest species shifted below the position of the peatland (Burney *et al.* 1995, Crausbay 2011). A geochemical record from lowland Oahu likewise indicates that aridification increased after 2 ka (Uchikawa *et al*. 2010). Drying at KHL1 and other Hawaiian paleorecord locations coincided with a Holocene maximum of El Niño-Southern Oscialltion (ENSO) frequency, duration, and

severity between 2.2 and 1.5 ka (Conroy *et al.* 2008). El Niño drives the drought regime in Hawai‘i. El Niño events reduce precipitation, particularly in winter, by hindering the development of subtropical cyclones, and disrupting the origin and movement of mid-latitude frontal storm systems into the island chain (Chu and Chen 2005). A reduction in winter storm frequency in Hawai‘i between 2.2 and 1.5 ka has evidence from hydrogen stable isotopes in a Moloka‘i peat record that suggest a shift in contribution from winter storm-derived rain to tradewind-derived rain (Beilman *et al*. 2019).

Surface re-wetting at 1.6 ka appeared to have occurred rapidly, although it is possible that re-wetting was gradual, and the ecological response was non-linear. Re-wetting was accompanied by a pulse of chironomids and copepods. Cladoceran diversity increases, which suggests that saturated conditions and food availability supported a stable cladoceran community. Assemblages become more testate amoebae-dominated towards the top of the peat profile, reflecting a more or less stable water table close to the surface. Today, the surface of KHL1 is still quite wet, with water occasionally pooling after heavy rainfall. This record shows that the modern environment is following a longer trend of relatively wet peatland surface conditons for the history of this site, although current conditions are not as wet as it was from 3.3 to 2.7 ka. There is also a clear message in the archive that abrupt peatland drying can occur and has occurred in the past, resulting in a thousand year-long state shift and reductions in carbon accumulation rate. In the context of this record, Hawaiian montane peatland resilience to drivers of environmental change, such as drought, is not certain. The system eventually recovered, but only as drought conditions abated at other montane sites (Crausbay *et al.* 2014), and testate amoebae did not return to pre-drying levels of taxonomic diversity for another 400 years.

Conclusion

Testate amoebae and Cladocera subfossils were analyzed in a ~4 ka peat core from a Hawaiian montane peatland. Paleoenvironmental signals were extracted from the fossil assemblages despite low subfossil concentration. Cladocera were present throughout much of the core and are useful indicators of saturated peatland conditions, confirming the utility of including these data in peatland paleoenvironmental reconstructions. We found that, over 4000 years, peatland WTD was highest and most stable between 3.3 and 2.7 ka, corresponding to a regional Holocene wet period recorded in Maui and Molokaʻi paleorecords. This wet stage was followed by an abrupt shift to drier conditions and an oxidizing state between 2.7 and 1.6 ka. These results strengthen evidence of statewide drought during a Holocene maximum of ENSO event frequency and severity. This is the first use of testate amoebae and Cladocera proxies for peatland paleohydrology in Hawaiʻi and this method should be applied to peatland studies on other Hawaiian Islands, particularly as part of a multi-proxy approach, to better understand Hawaiian environment and climate history.

References

Amesbury, M. J., Swindles, G. T., Bobrov, A., Charman, D. J., Holden, J., Lamentowicz, M., Mallon, G., Mazei, Y., Mitchell, E. A., Payne, R. J. and T. P. Roland. 2016. Development of a new pan-European testate amoeba transfer function for reconstructing peatland palaeohydrology. Quaternary Science Reviews 152:132-151.

Andriesse, J. P. 1988. Nature and Management of Tropical Peat Soils. Tillage and Cultivation 8.

Beilman, D., Massa, C., Nichols, J., Elison Timm, O., Kallstrom, R., and S. Dunbar-Co. 2019. Dynamic Holocene vegetation and North Pacific Hydroclimate recorded in a mountain peatland, Molokaʻi, Hawaiʻi. Frontiers in Earth Science 7:188.

Blaauw, M. and J. A. Christen. 2011. Flexible paleoclimate age-depth models using an autoregressive gamma process. Bayesian analysis 6:457-474.

Booth, R. K. 2008. Testate amoebae as proxies for mean annual water-table depth in Sphagnum-dominated peatlands of North America. Journal of Quaternary Science 23:43-57.

Booth, R. K., Lamentowicz, M., and D. J. Charman. 2010. Preparation and analysis of testate amoebae in peatland palaeoenvironmental studies. Mires & Peat 7:1-7.

Booth, R. K., Brewer, S., Blaauw, M., Minckley, T. A., and S. T. Jackson. 2012. Decomposing the mid-Holocene Tsuga decline in eastern North America. Ecology 93:1841-1852.

Burney, D. A., DeCandido, R. V., Burney, L. P., Kostel-Hughes, F. N., Stafford, T. W., Jr., and H. F. James. 1995. A Holocene record of climate change, fire ecology, and human activity from montane Flat Top Bog, Maui. Journal of Paleolimnology 13**:**209-217.

Burney, L. P. and D. A. Burney. 2003. Charcoal stratigraphies for Kaua'i and the timing of human arrival. Pacific Science 57:211-226.

Buytaert, W., Célleri, R., De Bièvre, B., Cisneros, F., Wyseure, G., Deckers, J., and R. Hofstede. 2006. Human impact on the hydrology of the Andean páramos. Earth Science Reviews 79:53-72.

Canfield, J. E. 1986. The role of edaphic factors and plant water relations in plant distribution in the bog/wet forest complex of Alaka'i Swamp, Kaua'i, Hawai'i. Doctoral dissertation, University of Hawai'i-Manoa.

Charman, D. J., Hendon, D., and W. A. Woodland. 2000. The identification of testate amoebae (Protozoa: Rhizopoda) in peats. Technical Guide No. 9. Quaternary Research Association, London, 147.

Chimner, R. A. 2004. Soil respiration rates of tropical peatlands in Micronesia and Hawaiʻi. Wetlands 24:51.

Chimner, R. A. and J. M. Karberg. 2008. Long-term carbon accumulation in two tropical mountain peatlands, Andes Mountains, Ecuador. Mires & Peat 3.

Chu, P. S., Nash, A. J., and F. Y. Porter. 1993. Diagnostic studies of two contrasting rainfall episodes in Hawaii: Dry 1981 and wet 1982. Journal of Climate 6:1457-1462.

Chu, P. S. and H. Chen. 2005. Interannual and interdecadal rainfall variations in the Hawaiian Islands. Journal of Climate 18:4796-4813.

Conroy, J. L., Overpeck, J. T., Cole, J. E., Shanahan, T. M., and M. Steinitz-Kannan. 2008. Holocene changes in eastern tropical Pacific climate inferred from a Galápagos lake sediment record. Quaternary Science Reviews 27:1166-1180.

Crausbay, S. D. 2011. Vegetation-climate relationships across space and time at high elevation in Hawai‘i. Doctoral dissertation, University of Wisconsin-Madison.

Crausbay, S., Genderjahn, S., Hotchkiss, S., Sachse, D., Kahmen, A., and S. K. Arndt. 2014. Vegetation dynamics at the upper reaches of a tropical montane forest are driven by disturbance over the past 7300 years. Arctic, Antarctic, and Alpine Research 46:787-799.

Dodson, S. I., & Frey, D. G. (1991) Cladocera and other Branchiopoda. In: Thorp, J. H., & Covich, A. P. (Eds.). (2009). *Ecology and classification of North American freshwater invertebrates*. Academic press.

Fosberg, F. R. (Ed.). 1961. Guide to Excursion III: Tenth Pacific Science Congress. Published jointly by Tenth Pacific Science Congress and University of Hawaii.

Giambelluca, T. W., DeLay, J. K., Nullet, M. A., Scholl, M., and S. B. Gingerich. 2011. Interpreting canopy water balance and fog screen observations: separating cloud water from wind-blown rainfall at two contrasting forest sites in Hawai’i. Tropical Montane Cloud Forests: Science for Conservation and Management 342.

Grimm, E.C. 1987 CONISS: A FORTRAN 77 program for stratigraphically constrained cluster analysis by the method of incremental sum of squares. Computers & Geosciences 13:13-35.

Hotchkiss, S. C. and J. O. Juvik. 1999. A Late-Quaternary pollen record from Ka‘au Crater, O‘ahu, Hawai‘i. Quaternary Research 52:115-128.

Lamarre, A., Magnan, G., Garneau, M., and É. Boucher. 2013. A testate amoeba-based transfer function for paleohydrological reconstruction from boreal and subarctic peatlands in northeastern Canada. Quaternary International 306:88-96.

Limpens, J., F. Berendse, C. Blodau, J. G. Canadell, C. Freeman, J. Holden, N. Roulet, Håkan Rydin, and G. Schaepman-Strub. 2008. Peatlands and the carbon cycle: from local processes to global implications–a synthesis. Biogeosciences 5:1475-1491.

Liu, B., Booth, R. K., Escobar, J., Wei, Z., Bird, B. W., Pardo, A., Curtis, J. H., and J. Ouyang. 2019. Ecology and paleoenvironmental application of testate amoebae in peatlands of the high-elevation Colombian páramo. Quaternary Research 92:14-32.

Loope, L. L., Medeiros, A. C., and B. H. Gagne. 1991. Aspects of the history and biology of the montane bogs of Haleakala National Park. Cooperative Nat. Pk. Resources Studies Unit, University of Hawai‘i-Mānoa, Department of Botany, Technichal Reportt 76.

Loope, L. L. and T. W. Giambelluca. 1998. Vulnerability of island tropical montane cloud forests to climate change, with special reference to East Maui, Hawaii. *Potential Impacts of Climate Change on Tropical Forest Ecosystems*, pp. 363-377. Springer, Dordrecht.

Lyon, H. L. 1909. The forest disease on Maui. Hawaiian Planter's Record 1:151-159.

Mauquoy, D., Hughes, P. D. M., and B. Van Geel. 2010. A protocol for plant macrofossil analysis of peat deposits. Mires and Peat 7:1-5.

Mitchell, E. A., Payne, R. J., and M. Lamentowicz. 2008. Potential implications of differential preservation of testate amoeba shells for paleoenvironmental reconstruction in peatlands. Journal of Paleolimnology 40:603-618.

Mueller-Dombois, D. 2006. Long-term rain forest succession and landscape change in Hawai'i: The ‘Maui Forest Trouble’revisited. Journal of Vegetation Science 17:685-693.

Page, S. E., Rieley, J. O., and R. Wüst. 2006. Lowland tropical peatlands of Southeast Asia. Developments in Earth Surface Processes 9:145-172.

Pau, S., MacDonald, G. M., and T. W. Gillespie. 2012. A dynamic history of climate change and human impact on the environment from Keālia Pond, Maui, Hawaiian Islands. Annals of the Association of American Geographers 102:748-762.

Payne, R. J. and E. A. Mitchell. 2009. How many is enough? Determining optimal count totals for ecological and palaeoecological studies of testate amoebae. Journal of Paleolimnology 42:483-495.

Reimer, P. J., Bard, E., Bayliss, A., Beck, J. W., Blackwell, P. G., Ramsey, C. B., Buck, C. E., Cheng, H., Edwards, R. L., Friedrich, M., and P. M. Grootes. 2013. IntCal13 and Marine13 radiocarbon age calibration curves 0–50,000 years cal BP. Radiocarbon 55:1869-1887.

Scholl, M., Gingerich S, Loope, L., Giambulluca, T.M., and M. Nullet. 2004. Quantifying the importance of fog drip to ecosystem hydrology and water resources in windward and leeward tropical montane cloud forests on East Maui. Venture Capital Project Final Report.

Selling, O. H. 1948. Studies in Hawaiian Pollen Statistics. Part III. On the Late Quaternary History of the Hawaiian Vegetation. Bernice P. Bishop Museum Special Publication 39.

Siemensma, F. J. (2019). Microworld, world of amoeboid organisms. World-wide electronic publication, Kortenhoef, the Netherlands.

Squeo, F. A., Warner, B. G., Aravena, R., and D. Espinoza. 2006. Bofedales: turberas de alta montana de los Andes centrales. Revista chilena de historia natural 79:245-255.

Swindles, G. T., Reczuga, M., Lamentowicz, M., Raby, C. L., Turner, T. E., Charman, D. J., Gallego-Sala, A., Valderrama, E., Williams, C., Draper, F., and E. N. H. Coronado. 2014. Ecology of testate amoebae in an Amazonian peatland and development of a transfer function for palaeohydrological reconstruction. Microbial ecology 68:284-298.

Swindles, G. T., Lamentowicz, M., Reczuga, M., and J. M. Galloway. 2016. Palaeoecology of testate amoebae in a tropical peatland. European journal of protistology 55:181-189.

Swindles, G. T., Morris, P. J., Whitney, B., Galloway, J. M., Gałka, M., Gallego-Sala, A., Macumber, A. L., Mullan, D., Smith, M. W., Amesbury, M. J., and T. P. Roland. (2018b). Ecosystem state shifts during long-term development of an Amazonian peatland. Global change biology 24:738-757.

Uchikawa, J., Popp, B. N., Schoonmaker, J. E., Timmermann, A., and S. J. Lorenz. 2010. Geochemical and climate modeling evidence for Holocene aridification in Hawaii: dynamic response to a weakening equatorial cold tongue. Quaternary Science Reviews 29:3057-3066.

Van Rees, C. B., and J. M. Reed. 2014. Wetland loss in Hawai'i since human settlement. Wetlands 34:335-350.

Vogl, R. J. and J. Henrickson. 1971. Vegetation of an alpine bog on East Maui, Hawaii. Pacific Science 25.

Wagner, W. L., Herbst, D. R., and S. H. Sohmer. 1990. Manual of the flowering plants of Hawaii. University of Hawaii Press.

Wolfe, E. W. and J. Morris. 1996. Geologic map of the Island of Hawaii (No. 2524-A).

Yu, Z. C. 2012. Northern peatland carbon stocks and dynamics: a review. Biogeosciences 9:4071-4085.

Table 1: ^{14}C and calendar ages for KHL1. ^{14}C dates were obtained from bulk peat sediment and ages were calibrated using IntCal13 (Reimers *et al.* 2013)

Lab ID	Depth interval (cm)	^{14}C Age	Calibrated age (cal yr BP) median probability, 2σ
CAMS-175931	19-20	370 ± 30	463, 317-502
CAMS-175932	63-64	1165 ± 30	1112, 985-1177
CAMS-178952	105-106	1745 ± 30	1642, 1567-1716
CAMS-175933	139-140	2860 ± 30	2992, 2880-3066
CAMS-175934	208-209	3315 ± 30	3537, 3460-3613
CAMS-173294	254-255	3645 ± 35	3943, 3872-4083
CAMS-178953	264-265	8815 ± 40	9823, 9691-10146

Figure legends

Figure 1: Site map of Hawaiian peatlands surveyed for transfer function development (highlighted in yellow) and the location of the KHL1 peat core. Green polygon is extent of wet forest cover where the peatlands lie. Dark green polygons are locations of other peatlands within the wet forest – montane bog complex. Black lines are 100-ft (30.3 m) elevation contours and dashed lines are estimated mean annual rainfall (mm/yr) isohyets from Giambelluca *et al.* (2013). Land cover data were downloaded from the Hawai‘i Statewide GIS Program (geoportal.hawaii.gov)

Figure 2: Results of Bayesian Monte Carlo – Markov Chain using probability distributions of radiocarbon ages from IntCal13 curve (Reimers *et al.* 2013) using the R package “rbacon” (Blaauw and Christen 2011).

Figure 3: Age-depth model for KHL1 derived from Bayesian Monte Carlo – Markov Chain as shown in Figure 2 plotted with average acumulation rate estimates (mm/yr). Also plotted is the stratigraphy of peat-contributing plant macrofossils corresponding to depths on the y-axis.

Figure 4: Stratigraphic diagram of testate amoebae and Cladocera subfossils in a Hawaiian peat core with coarse assessment of peat-contributing vegetation. Assemblages are plotted as relative abundances (%) by depth (cm). Zonation was determined by constrained cluster analysis on Sørenson distances between fossil assemblages. Reconstructed depth to water table curve based on the second component of a weighted average partial-least-squares regression transfer function is plotted to the right of the stratigraphic diagram with RMSEP error depicted by gray lines.

Figure 5: Reconstructed depth to water table (cm) for the past 4ka based on testate amoebae and Cladocera subfossils and a weighted average partial-least-squares regression (2^{nd} component) transfer function developed in Chapter 2. Sample-level reconstructed water table estimates are plotted as points. Smooth line is a 10% span LOESS smoothing of water table estimates. The water table curve is plotted against age of sediment determined by the age-depth model. The following panels are, from left to right, testate amoebae plus the rotifer *Habrotrocha angusticollis* relative abundance versus Cladocera relative abundance (%), chironomid mandible segments (counts/microscope slide), copepod egg cases (counts/microscope slide), and tardigrade egg cases (counts/microscope slide). Dashed lines signify the zones in the testate amoebae and Cladocera stratigraphy (Figure 4).

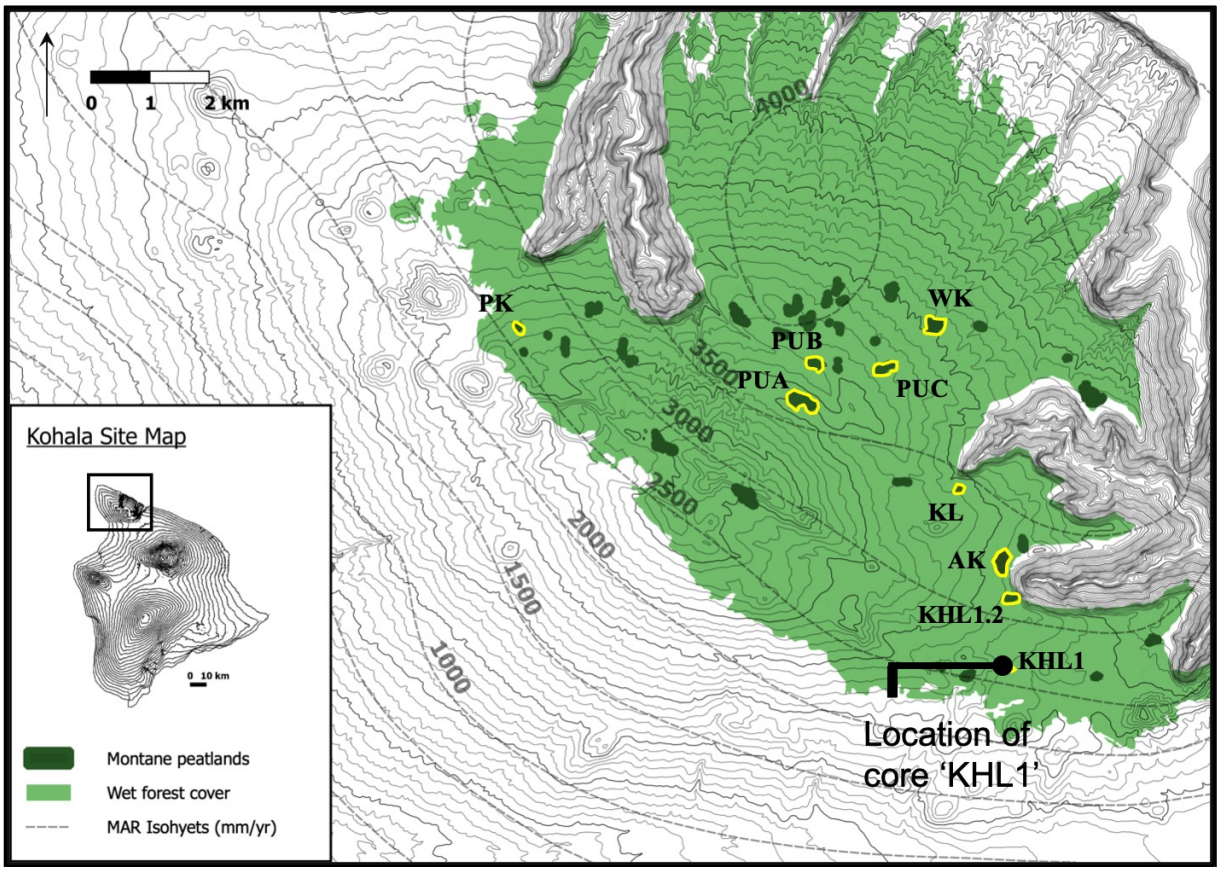

Figure 1: Site map of Hawaiian peatlands surveyed for transfer function development (highlighted in yellow) and the location of the KHL1 peat core. Green polygon is extent of wet forest cover where the peatlands lie. Dark green polygons are locations of other peatlands within the wet forest – montane bog complex. Black lines are 100-ft (30.3 m) elevation contours and dashed lines are estimated mean annual rainfall (mm/yr) isohyets from Giambelluca *et al.* (2013). Land cover data were downloaded from the Hawai‘i Statewide GIS Program (geoportal.hawaii.gov)

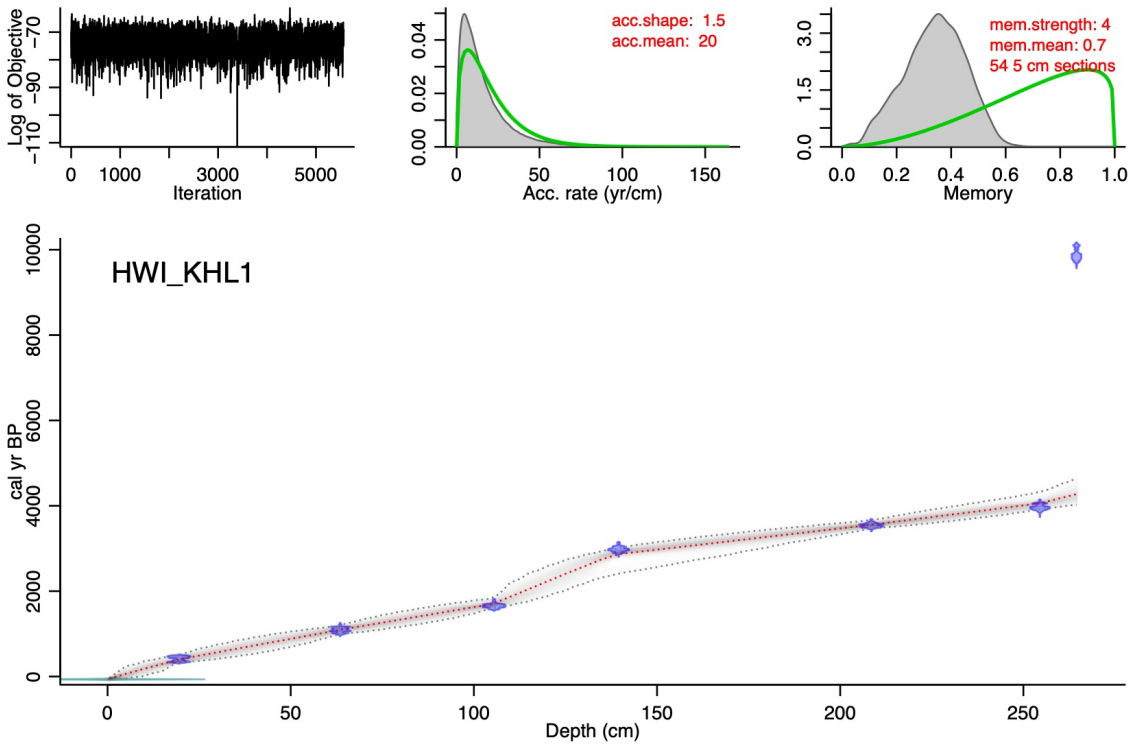

Figure 2: Results of Bayesian Monte Carlo – Markov Chain using probability distributions of radiocarbon ages from IntCal13 curve (Reimers *et al.* 2013). One date was flagged as an outlier by bacon.

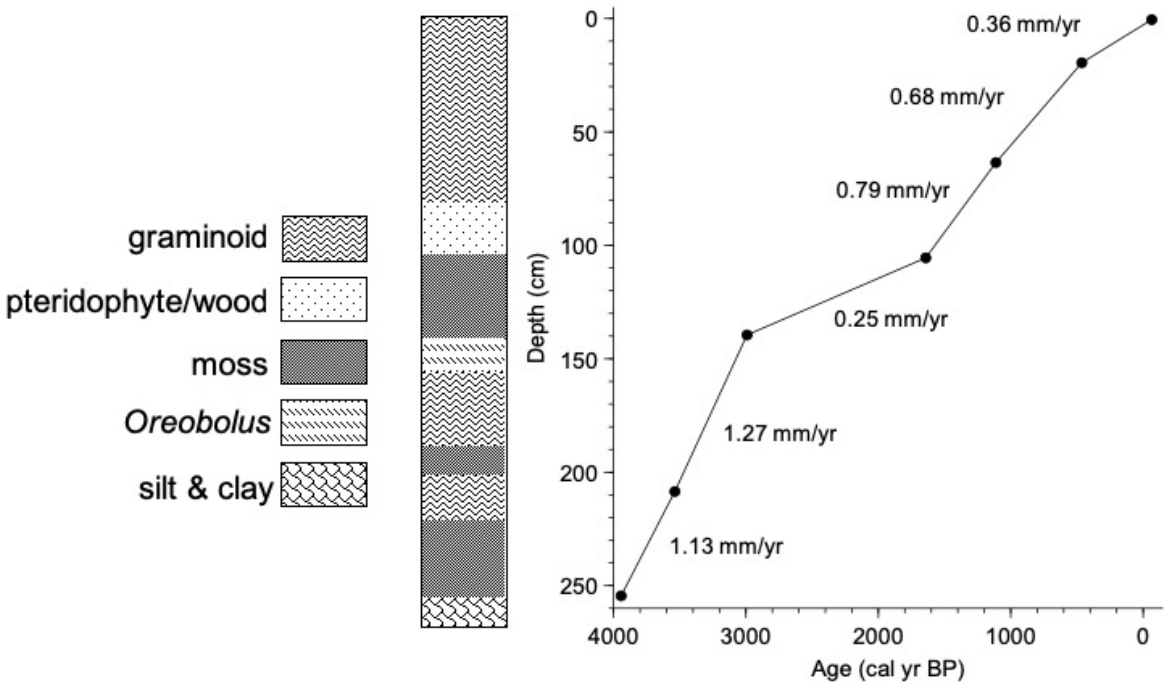

Figure 3: Age-depth model for KHL1 derived from Bayesian Monte Carlo – Markov Chain as shown in Figure 2 plotted with average acumulation rate estimates (mm/yr). Also plotted is the stratigraphy of peat-contributing plant macrofossils corresponding to depths on the y-axis.

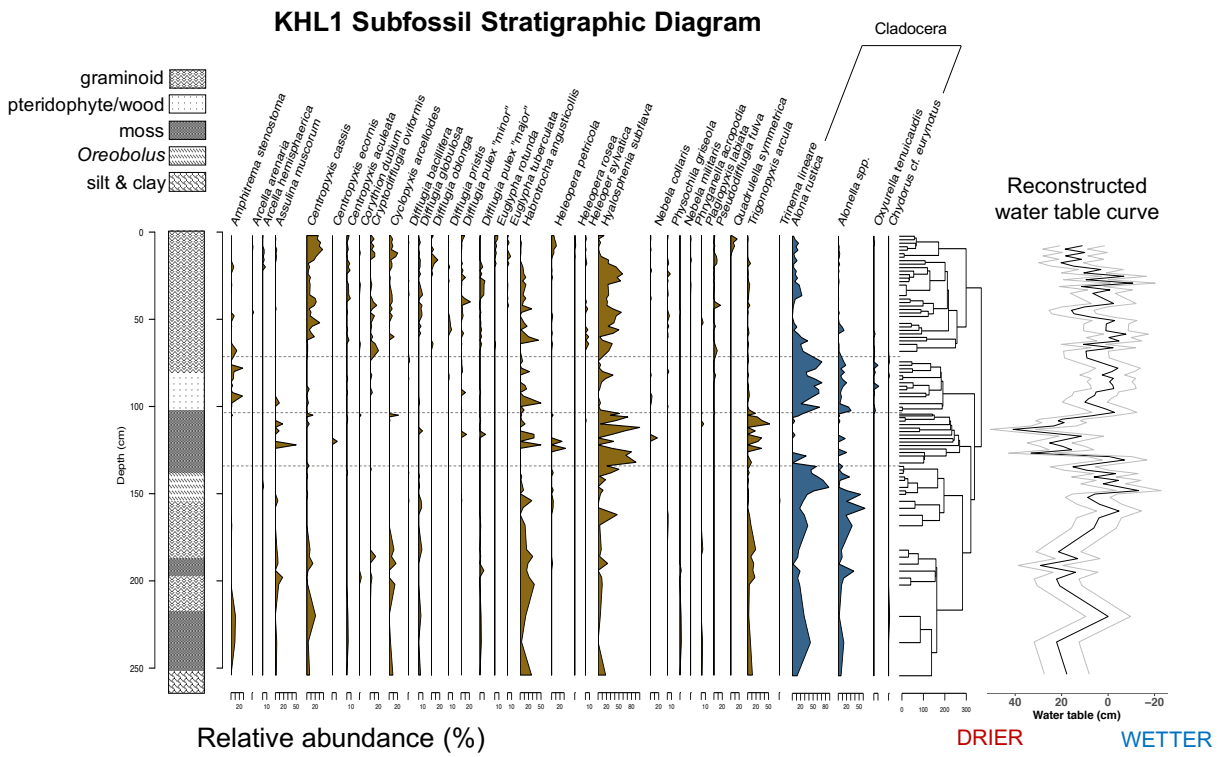

Figure 4: Stratigraphic diagram of testate amoebae and Cladocera subfossils in a Hawaiian peat core with coarse assessment of peat-contributing vegetation. Assemblages are plotted as relative abundances (%) by depth (cm). Zonation was determined by constrained cluster analysis on Sørenson distances between fossil assemblages. Reconstructed depth to water table curve based on the second component of a weighted average partial-least-squares regression transfer function is plotted to the right of the stratigraphic diagram with RMSEP error depicted by gray lines.

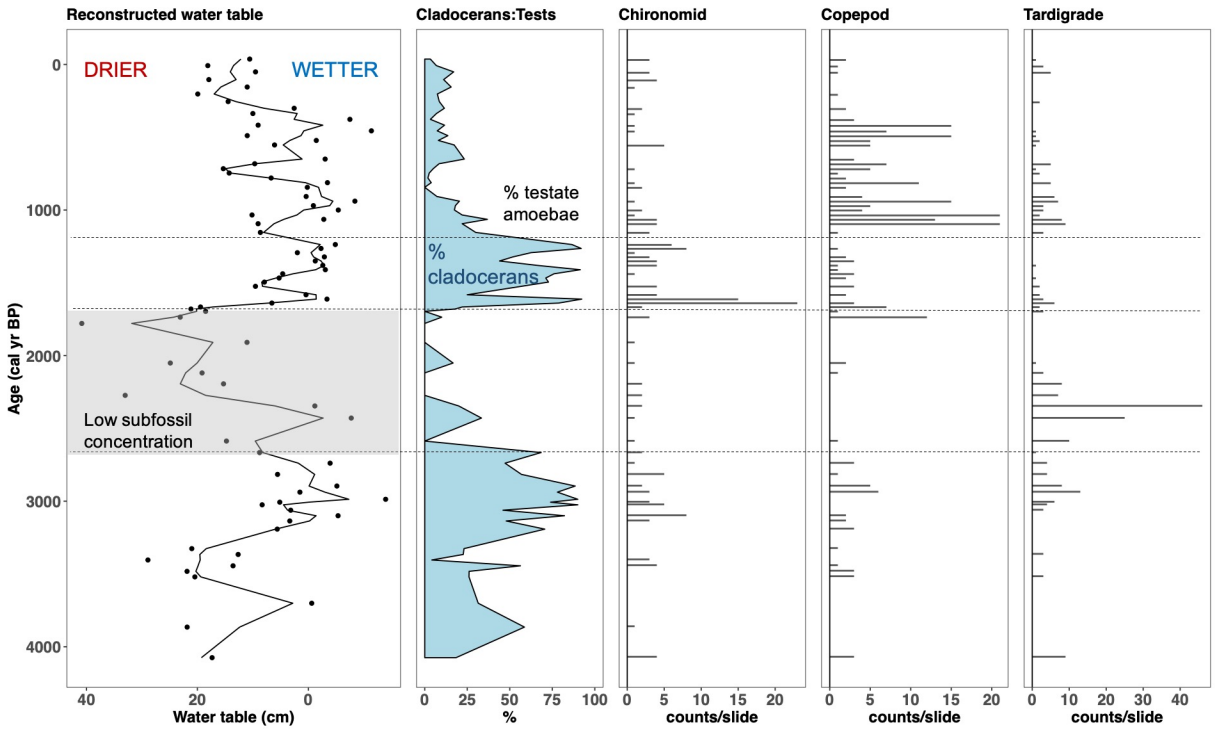

Figure 5: Reconstructed depth to water table (cm) for the past 4ka based on testate amoebae and Cladocera subfossils and a weighted average partial-least-squares regression (2nd component) transfer function developed in Chapter 2. Sample-level reconstructed water table estimates are plotted as points. Smooth line is a 10% span LOESS smoothing of water table estimates. The water table curve is plotted against age of sediment determined by the age-depth model. The following panels are, from left to right, testate amoebae plus the rotifer *Habrotrocha angusticollis* relative abundance versus Cladocera relative abundance (%), chironomid mandible segments (counts/microscope slide), copepod egg cases (counts/microscope slide), and tardigrade egg cases (counts/microscope slide). Dashed lines signify the zones in the testate amoebae and Cladocera stratigraphy (Figure 4).

Supplemental Information and Data

List of tables:

Appendix 1: Table of all testate amoebae taxa and notes on identification. * = taxa that were rare and removed from analysis. [1]*Hyalosphenia subflava* "major" was grouped with *Hyalosphenia subflava* "minor" in Chapters 1&3.

Species name	Notes	Authority
Amphitrema stenostoma		Nüsslin
Arcella arenaria		Greef
Arcella hemisphaerica		Perty
Argynnia dentistoma var. *laevis*		Cash & Hopkinson
Assulina muscorum		Greef
Assulina seminulum		Ehrenberg
Bullinularia indica		Penard
Centropyxis aculeata type	Any *Centropyxis* with spines	Ehrenberg
Centropyxis cassis type	*Centropyxis aerophila*, *Centropyxis sylvatica*, Charman et al. (2000)	Wallich
Centropyxis ecornis		Ehrenberg
**Centropyxis platystoma* type	Charman et al. (2000)	Penard
Corythion asperulum	Like *C. dubium*, but with spines	Schönborn
Corythion dubium		Taranek
Cryptodifflugia oviformis		Penard
Cyclopyxis arcelloides type	Following the description in Booth (2008)	Penard
Difflugia bacillifera		Penard
Difflugia globulosa	Following the description in Booth (2008)	(Dujardin) Penard
**Difflugia lucida*		Penard
Difflugia oblonga		Ehrenberg
Difflugia pristis type	Following the description in Charman et al. (2000)	Penard
Difflugia pulex "minor" type	Following the description in Charman et al. (2000)	Penard
Difflugia pulex "major" type	Like "minor," but > 45 μm in length	
**Difflugia pyriformis*		Perty
**Euglypha acanthophora*		Ehrenberg
**Euglypha cristata*		Leidy
**Euglypha filifera*		Penard
Euglypha laevis		Ehrenberg
Euglypha rotunda type	Following the description in Charman et al. (2000)	Ehrenberg
Euglypha strigosa type	Following the description in Charman et al. (2000)	Ehrenberg
Euglypha tuberculata type	Following the description in Charman et al. (2000)	Dujardin
**Gibbocarina gracilis*		Penard
Heleopera petricola		Leidy

Heleopera rosea	Likely includes *H. petricola* var. *amethystea*	Penard
Heleopera sphagni		Leidy
Heloopera sylvatica		Penard
**Hyalosphenia papilio*		Leidy
Hyalosphenia subflava "minor"		Cash & Hopkinson
[1]*Hyalosphenia subflava* "major"	Like "minor," but > 65 µm in length	
Nebela collaris type	*Nebela bohemica*	Ehrenberg
Nebela flabellulum		Leidy
Nebela militaris		Penard
Nebela parvula		Cash
Nebela tincta		Leidy
Phryganella acropodia type	Following the description in Booth (2008)	(Hertwig & Lesser) Hopkinson
Physochila griseola		Jung
Plagiopyxis labiata		Penard
Pseudodifflugia fulva type	Following the description in Charman et al. (2000)	Archer
Quadruella symmetrica type	Following the description in Charman et al. (2000)	Wallich
Sphenoderia fissirostris		Penard
**Tracheuglypha dentata*		Deflandre
Trigonopyxis arcula		Penard
Trigonopyxis minuta		Schönborn & Peschke
Trinema enchyles		Ehrenberg
Trinema lineare		Penard

Appendix 2: Table of testate amoebae functional functional traits. Aperture position, test shape, and test compression indices are from Fournier *et al*. (2012) and Fournier *et al*. (2015). Test biovolume and aperture diameter are from a combination of the above references and my own measurements.

Species name	Lobose/ Filose	Aperture position	Test shape	Test compression	Biovolume (μm^3)	Aperture diameter (µm)
Amphitrema stenostoma	F	2	4	2	53603	15
Arcella arenaria	L	1	2	2	194828	35
Arcella hemisphaerica	L	1	1	1	86590	37
Argynnia dentistoma var. *laevis*	L	2	4	3	260538	20
Assulina muscorum	F	2	2	4	15708	15
Assulina seminulum	F	2	2	4	43978	20
Bullinularia indica	L	3	4	3	932660	67
Centropyxis aculeata type	L	3	4	3	89316	62
Centropyxis cassis type	L	3	4	3	101137	40
Centropyxis ecornis	L	3	4	3	471239	54
Corythion asperulum	F	3	3	4	12435	13
Corythion dubium	F	3	3	4	12435	13
Cryptodifflugia oviformis	L	2	4	2	1047	5
Cyclopyxis arcelloides type	L	1	1	2	27143	35
Difflugia bacillifera	L	2	4	2	204753	31
Difflugia globulosa	L	2	1	1	110447	64
Difflugia oblonga	L	2	4	2	229074	23
Difflugia pristis type	L	2	4	2	26808	24
Difflugia pulex "minor" type	L	2	4	2	7854	18
Difflugia pulex "major" type	L	2	4	2	58316	23
Euglypha laevis	F	2	4	3	8252	10
Euglypha rotunda type	F	2	4	3	17999	12
Euglypha strigosa type	F	2	4	3	35736	16

Euglypha tuberculata type	F	2	4	2	45946	20
Heleopera petricola	L	2	4	3	77493	37
Heleopera rosea	L	2	4	3	90569	41
Heleopera sphagni	L	2	4	3	175824	43
Heloopera sylvatica	L	2	4	3	45643	23
Hyalosphenia subflava	L	2	4	2	12763	14
Nebela collaris type	L	2	4	3	128506	30
Nebela flabellulum	L	2	4	3	265301	32
Nebela militaris	L	2	4	3	76718	17
Nebela parvula	L	2	4	3	160810	26
Nebela tincta	L	2	4	3	126241	26
Phryganella acropodia type	L	1	1	2	28953	31
Physochila griseola	L	2	4	2	147781	21
Plagiopyxis labiata	L	3	4	4	58434	25
Pseudodifflugia fulva type	L	2	4	3	9687	13
Quadruella symmetrica type	L	2	4	3	62492	20
Sphenoderia fissirostris	F	3	3	3	12435	10
Trigonopyxis arcula	L	1	1	2	207738	31
Trigonopyxis minuta	L	1	1	2	67348	25
Trinema enchyles	F	3	3	3	34472	16
Trinema lineare	F	3	3	3	6809	12

References:

Fournier, B., Lara, E., Jassey, V. E., and E. A. Mitchell, E. A. 2015. Functional traits as a new approach for interpreting testate amoeba palaeo-records in peatlands and assessing the causes and consequences of past changes in species composition. The Holocene 25: 1375-1383.

Fournier, B., Malysheva, E., Mazei, Y., Moretti, M., and E. A. Mitchell. 2012) Toward the use of testate amoeba functional traits as indicator of floodplain restoration success. European Journal of Soil Biology 49: 85-91.

Appendix 3: Table of testate amoebae count data for all microsites. Chapter 2 transfer function excludes count data from all PO (Pu'u O'o) microsites.

Microsite	*Amphitrema stenostoma*	*Arcella arenaria*	*Arcella hemisphaerica*	*Argynnia dentistoma* var. *laevis*	*Assulina muscorum*	*Assulina seminulum*	*Bullinularia indica*	*Centropyxis aculeata* type	*Centropyxis cassis* type	*Centropyxis ecornis*	*Corythion asperulum*
AK1	0	0	0	0	0	0	0	1	2	0	0
AK2	0	0	0	0	12	0	2	0	3	0	1
AK3	0	0	0	0	1	0	0	0	5	0	0
AK4	0	4	0	0	3	0	0	6	11	0	2
AK5	0	0	0	0	8	2	1	0	2	0	0
AK6	0	0	0	0	3	0	0	0	5	0	0
AK7	0	0	0	0	0	0	0	0	0	0	0
AK8	0	0	0	0	0	0	0	0	2	0	0
AK9	0	0	0	0	14	0	0	0	0	0	0
KHL1.1	0	0	0	0	0	0	0	1	1	0	0
KHL1.2	0	0	2	0	6	0	0	0	33	0	0
KHL1.3	0	0	0	0	1	0	0	0	73	0	0
KHL1.4	1	4	1	0	1	0	0	0	43	0	0
KHL1.5	0	1	1	0	0	0	0	9	9	0	0
KHL1.6	0	3	1	0	2	0	0	4	28	0	0
KHL1.7	0	1	0	0	9	0	0	0	15	0	0
KHL1.8	0	2	14	0	0	0	0	1	8	0	0
KHL1.9	0	0	0	0	11	0	0	0	0	0	0
KHL2.1	4	0	3	0	2	0	0	0	23	0	0
KHL2.2	0	3	4	0	0	0	0	1	24	0	0
KHL2.3	0	0	0	0	0	0	0	0	8	0	0
KHL2.4	0	0	0	0	2	0	0	0	3	0	0
KHL2.5	0	0	0	0	9	0	0	0	0	0	4
KHL2.6	0	0	0	0	0	0	0	0	14	0	0
KL1	0	0	0	0	12	0	0	0	0	0	0
KL10	0	0	0	0	6	0	0	0	1	0	0
KL11	0	1	0	0	8	0	2	0	3	0	0
KL12	0	0	0	0	17	0	0	0	5	0	0
KL13	0	0	0	0	2	0	0	0	1	0	0
KL2	0	0	0	0	7	0	0	0	4	0	0
KL3	1	0	0	0	5	0	0	0	2	0	0
KL4	0	0	0	0	2	0	0	0	6	0	0
KL5	24	0	0	0	5	0	0	0	7	0	0
KL6	0	0	0	0	0	0	0	0	7	1	0

KL7	3	1	0	0	0	0	0	0	3	0	0
KL8	17	0	0	0	1	0	0	0	0	0	0
KL9	22	0	0	0	6	0	0	0	5	0	0
PK1	1	0	0	0	26	1	0	0	4	0	0
PK10	0	0	0	0	2	0	0	0	2	0	0
PK11	0	0	0	0	7	0	0	0	0	0	0
PK12	1	0	0	0	11	0	0	0	5	0	0
PK13	1	1	0	0	5	0	0	0	6	0	0
PK14	0	0	0	0	2	0	0	0	0	0	0
PK15	0	0	0	0	9	0	0	0	3	0	0
PK16	0	0	0	0	19	0	0	0	1	0	0
PK17	0	0	0	0	2	0	0	0	10	0	0
PK2	0	0	0	0	13	0	0	0	0	0	0
PK3	1	0	0	0	12	0	0	0	2	0	0
PK4	0	0	0	0	2	0	0	0	0	0	0
PK5	0	0	0	0	24	0	0	0	1	0	0
PK6	0	1	0	0	0	0	0	0	0	0	0
PK7	0	0	0	0	7	0	0	0	0	2	0
PK8	0	0	0	0	2	0	0	0	1	0	0
PK9	1	0	0	0	1	0	0	0	1	0	0
PO1	0	0	0	0	11	3	0	0	3	0	0
PO10	0	0	0	0	13	0	0	0	2	0	0
PO11	0	0	0	0	8	1	0	0	2	0	0
PO12	0	0	0	0	28	12	0	0	13	0	0
PO13	0	1	0	0	2	0	1	0	5	0	0
PO14	0	0	0	1	57	0	0	0	6	0	0
PO15	0	0	0	0	23	1	0	0	3	0	0
PO16	0	0	0	1	17	1	0	0	4	0	0
PO17	0	0	0	1	13	0	0	0	4	0	0
PO2	0	0	0	0	26	0	2	0	5	1	0
PO3	0	0	1	0	20	1	1	0	4	0	0
PO4	0	0	0	0	37	3	0	0	11	0	0
PO5	0	0	0	0	17	2	0	0	0	0	0
PO6	0	0	0	0	7	0	1	0	0	0	0
PO7	0	0	0	0	26	2	0	0	0	0	0
PO8	0	0	0	2	47	13	0	0	0	0	0
PO9	0	0	0	3	12	4	0	0	6	0	0
PUA1	0	0	0	0	1	0	0	0	2	0	0
PUA2	0	0	0	0	17	0	0	0	0	0	0
PUA3	0	0	0	0	0	0	0	0	1	0	0
PUA4	0	0	0	0	9	0	0	0	0	0	0
PUA5	2	0	0	0	2	0	0	0	1	0	0
PUB1	1	0	0	0	32	0	0	0	7	0	0
PUB10	2	0	0	0	5	0	1	0	7	0	0
PUB2	0	0	0	4	58	3	1	0	6	0	3

PUB3	0	0	0	0	10	0	0	0	1	2	0
PUB4	10	0	0	0	6	0	0	0	3	0	0
PUB5	0	0	0	0	20	0	0	0	2	0	0
PUB6	2	0	0	0	11	0	0	0	6	0	0
PUB7	1	0	0	0	6	0	0	0	9	0	0
PUB8	0	0	0	0	49	4	0	0	4	3	0
PUB9	0	0	0	0	24	0	0	0	0	0	3
PUC1	0	0	0	0	1	0	0	0	1	0	0
PUC10	4	0	0	0	4	0	0	0	1	0	0
PUC11	0	0	0	0	32	1	0	0	0	0	1
PUC12	0	0	0	0	46	0	5	0	3	0	4
PUC13	1	0	0	0	13	0	0	0	0	0	0
PUC14	0	0	0	0	35	0	0	0	1	0	1
PUC15	0	0	0	0	43	1	0	0	0	0	8
PUC16	0	0	0	0	38	2	0	0	0	0	5
PUC2	0	0	0	0	6	0	0	0	3	0	0
PUC3	0	0	0	0	0	0	0	0	1	0	0
PUC4	0	0	0	0	6	0	0	0	1	0	0
PUC5	1	0	0	0	2	0	0	0	0	0	0
PUC6	15	0	0	0	0	0	0	0	0	0	0
PUC7	1	0	0	0	1	0	0	0	1	0	0
PUC8	1	0	0	0	0	0	1	0	0	0	0
PUC9	0	0	0	0	34	0	0	0	3	0	0
WK1	1	0	0	0	9	0	0	0	3	1	2
WK2	17	0	0	0	2	0	0	0	0	0	0
WK3	6	0	0	0	5	0	0	0	1	0	0
WK4	5	0	0	0	36	0	0	0	3	1	0
WK5	0	0	0	0	15	0	0	0	2	0	0

Microsite	*Corythion dubium*	*Cryptodifflugia oviformis*	*Cyclopyxis arcelloides* type	*Difflugia bacillifera*	*Difflugia globulosa*	*Difflugia oblonga*	*Difflugia pristis* type	*Difflugia pulex* "minor" type	*Difflugia pulex* "major" type	*Euglypha laevis*	*Euglypha rotunda* type
AK1	0	3	11	0	4	0	7	3	38	0	2
AK2	0	0	13	1	1	0	11	3	12	0	3
AK3	1	11	23	0	1	0	10	20	1	0	1
AK4	0	4	3	0	1	3	3	8	17	5	1
AK5	0	51	13	0	0	0	0	5	0	0	2
AK6	1	27	62	0	0	0	0	34	0	10	3
AK7	44	11	2	0	0	0	0	0	0	1	0

AK8	3	28	3	0	0	0	0	26	1	4	10
AK9	21	13	4	0	0	0	0	0	0	0	5
KHL1.1	0	4	0	0	3	0	4	14	6	0	0
KHL1.2	0	2	3	7	0	2	3	8	0	0	0
KHL1.3	0	1	2	0	1	0	7	3	0	0	0
KHL1.4	2	7	15	0	0	0	0	2	0	0	1
KHL1.5	0	1	18	0	1	0	15	14	0	0	1
KHL1.6	0	11	13	2	5	0	15	6	0	0	0
KHL1.7	2	2	25	0	0	0	1	0	0	2	4
KHL1.8	0	4	8	0	2	17	1	3	1	2	5
KHL1.9	11	0	0	0	0	0	0	0	0	0	7
KHL2.1	3	6	2	0	2	2	7	3	3	3	6
KHL2.2	0	4	1	0	7	7	4	0	0	4	0
KHL2.3	0	2	0	1	0	1	0	0	0	2	2
KHL2.4	3	1	0	3	0	2	4	1	0	2	1
KHL2.5	8	2	23	0	0	0	0	6	0	5	5
KHL2.6	0	16	4	0	0	0	1	3	0	2	7
KL1	2	15	33	0	0	0	0	3	4	0	12
KL10	0	5	2	0	0	0	1	23	1	0	1
KL11	0	11	1	0	0	0	1	33	0	1	1
KL12	1	1	2	0	0	0	0	5	4	0	12
KL13	0	12	21	0	8	0	15	5	17	0	0
KL2	2	8	32	0	0	0	0	5	3	0	11
KL3	1	21	1	0	4	0	3	39	3	2	13
KL4	0	11	9	0	2	0	9	29	17	0	4
KL5	0	6	12	0	0	0	1	17	0	0	4
KL6	0	1	9	0	0	1	8	51	15	0	2
KL7	0	15	0	0	2	0	15	39	6	0	2
KL8	0	8	2	0	0	0	3	28	0	0	5
KL9	1	5	5	0	0	0	0	27	2	0	4
PK1	2	13	2	0	2	0	0	0	0	0	0
PK10	1	41	6	0	6	0	1	5	0	3	5
PK11	2	4	0	0	0	0	0	9	1	1	29
PK12	3	2	1	1	2	0	2	18	0	3	9
PK13	1	1	2	0	1	0	1	2	0	1	5
PK14	0	14	34	0	0	0	0	3	0	0	1
PK15	3	28	2	0	0	0	0	0	0	0	17
PK16	2	21	16	0	0	0	0	2	0	0	2
PK17	5	1	36	0	0	0	0	3	0	0	1
PK2	3	72	2	0	0	0	0	0	0	0	8
PK3	3	4	2	0	0	0	0	17	0	6	29
PK4	0	21	46	0	2	0	0	2	0	0	1
PK5	0	0	0	0	0	0	0	0	0	0	23
PK6	0	52	22	0	1	0	0	19	0	0	4
PK7	4	1	3	0	0	0	0	1	0	0	16

PK8	0	11	2	0	2	0	3	42	0	3	6
PK9	2	39	1	0	1	0	1	9	0	0	20
PO1	0	0	1	1	1	0	0	0	0	0	2
PO10	5	1	0	0	3	0	0	0	0	2	14
PO11	2	2	0	0	0	0	2	0	0	0	0
PO12	7	3	3	0	0	0	0	0	0	0	5
PO13	0	0	0	1	0	0	0	0	0	0	0
PO14	3	0	1	0	1	0	0	0	0	0	6
PO15	1	1	4	0	0	0	0	0	0	0	0
PO16	6	3	24	0	0	0	0	0	0	0	0
PO17	3	0	0	0	1	0	0	0	0	7	3
PO2	0	1	0	0	0	0	0	0	0	0	1
PO3	0	0	2	0	0	0	0	0	0	0	2
PO4	2	0	1	0	2	0	0	0	0	0	0
PO5	2	1	0	0	0	0	0	0	0	0	0
PO6	0	0	0	0	0	0	0	0	0	0	0
PO7	0	0	5	0	0	0	0	0	0	0	0
PO8	0	0	13	0	0	0	0	0	0	0	0
PO9	1	0	0	0	0	0	0	0	0	0	4
PUA1	0	0	0	10	5	0	0	1	0	1	3
PUA2	0	4	0	0	3	0	0	6	0	1	0
PUA3	0	4	1	0	0	0	0	9	0	1	8
PUA4	1	10	1	0	0	0	0	2	0	0	30
PUA5	0	3	0	9	0	0	0	46	1	1	12
PUB1	1	4	5	0	0	0	1	41	0	0	2
PUB10	0	6	1	10	2	0	10	7	12	0	1
PUB2	4	0	12	0	3	0	1	3	0	0	14
PUB3	14	4	1	0	0	0	1	10	0	0	42
PUB4	3	34	20	0	0	0	0	24	0	0	9
PUB5	0	5	0	0	0	2	0	30	2	0	2
PUB6	0	0	6	6	1	0	4	18	0	0	0
PUB7	0	5	3	1	1	0	6	24	2	1	6
PUB8	1	1	6	0	5	0	1	0	2	1	47
PUB9	2	4	5	0	0	0	0	11	1	0	15
PUC1	0	15	0	2	8	6	0	30	6	0	0
PUC10	0	24	0	0	1	0	0	5	0	0	18
PUC11	2	36	1	0	0	0	0	16	0	0	10
PUC12	0	0	4	0	1	0	0	0	0	0	27
PUC13	2	4	0	1	1	0	0	28	0	0	6
PUC14	2	1	0	0	0	0	0	0	0	0	10
PUC15	38	0	1	0	0	0	0	0	0	3	26
PUC16	4	3	0	0	1	0	0	4	0	0	25
PUC2	0	11	0	1	0	0	0	72	7	0	6
PUC3	0	7	5	0	9	0	2	37	1	0	6
PUC4	0	0	0	19	0	0	1	45	0	0	2

PUC5	0	6	1	9	3	0	0	73	0	0	7
PUC6	0	1	0	1	0	0	0	73	0	0	3
PUC7	0	35	8	0	0	0	0	0	0	0	3
PUC8	0	3	0	8	0	0	2	14	3	0	0
PUC9	1	3	0	0	0	0	2	32	7	2	6
WK1	2	10	0	0	3	0	0	9	0	0	31
WK2	0	1	0	7	0	0	1	62	0	0	2
WK3	0	0	0	18	1	0	0	51	0	1	7
WK4	1	5	1	0	0	0	0	25	0	0	15
WK5	4	7	0	0	0	0	1	75	0	0	20

Microsite	*Euglypha strigosa* type	*Euglypha tuberculata* type	*Heleopera petricola*	*Heleopera rosea*	*Heleopera sphagni*	*Heleopera sylvatica*	*Hyalosphenia subflava*	*Nebela collaris-bohemica* type	*Nebela flabellulum*	*Nebela militaris*	*Nebela parvula*
AK1	0	0	0	1	0	8	19	0	0	0	0
AK2	3	2	0	2	0	11	0	1	0	0	1
AK3	0	1	0	0	0	6	1	3	0	2	0
AK4	0	3	0	8	1	0	3	5	0	1	0
AK5	0	16	0	0	0	1	0	0	0	0	1
AK6	0	4	0	0	0	0	0	0	0	0	0
AK7	0	18	2	13	0	7	0	0	0	0	0
AK8	0	4	0	2	0	16	0	3	0	1	0
AK9	2	7	1	10	0	21	0	1	0	0	0
KHL1.1	0	0	0	0	0	0	58	0	0	0	0
KHL1.2	0	0	11	9	0	7	1	2	0	0	0
KHL1.3	1	11	1	20	0	5	0	1	0	0	0
KHL1.4	1	6	6	17	0	3	7	2	0	0	0
KHL1.5	0	0	0	0	0	1	3	0	0	0	0
KHL1.6	0	0	0	0	0	1	3	1	0	0	0
KHL1.7	1	9	2	2	0	1	0	0	0	0	0
KHL1.8	0	4	4	0	0	1	0	3	0	0	0
KHL1.9	26	103	0	1	0	1	0	5	0	0	0
KHL2.1	2	5	0	6	0	0	1	4	0	0	0
KHL2.2	3	5	16	3	0	0	0	0	0	0	0
KHL2.3	3	0	39	2	0	12	0	4	0	0	0
KHL2.4	0	15	5	11	0	0	4	14	0	0	0
KHL2.5	15	24	1	2	0	3	0	8	0	0	0
KHL2.6	1	7	0	2	0	2	0	0	0	0	0

KL1	0	2	0	0	0	13	1	5	2	1	2
KL10	1	11	0	3	0	32	0	2	0	0	0
KL11	0	3	0	0	0	20	1	5	0	0	1
KL12	0	19	5	5	0	16	0	1	0	1	0
KL13	0	8	0	0	0	5	4	2	0	0	0
KL2	0	2	0	0	0	14	0	9	0	0	1
KL3	0	0	0	0	0	0	1	1	0	0	0
KL4	0	0	0	0	0	2	2	0	0	0	1
KL5	1	0	0	0	0	9	3	3	0	1	0
KL6	0	0	0	1	0	3	1	1	2	2	2
KL7	0	3	0	0	0	8	0	0	0	0	1
KL8	0	5	0	8	0	14	1	2	1	0	0
KL9	0	4	0	4	0	13	0	4	0	0	0
PK1	0	8	0	3	0	38	1	0	1	0	0
PK10	0	1	0	0	0	32	0	2	0	1	0
PK11	0	17	0	0	0	18	4	5	0	0	0
PK12	1	5	4	0	0	3	4	3	0	0	0
PK13	0	5	0	13	0	31	0	8	0	0	0
PK14	0	0	0	0	0	43	0	1	0	0	0
PK15	0	8	0	0	0	19	0	9	0	1	0
PK16	0	3	0	0	0	28	0	2	0	0	0
PK17	0	1	2	0	0	15	0	0	0	3	0
PK2	0	8	0	0	0	24	0	0	0	0	0
PK3	1	0	5	13	3	16	0	3	0	2	2
PK4	0	0	0	0	0	44	0	3	0	4	1
PK5	0	15	0	0	0	60	0	0	0	0	0
PK6	0	0	0	0	0	21	0	1	0	0	0
PK7	0	17	0	0	0	45	0	3	1	0	0
PK8	0	1	2	0	0	7	0	4	0	0	0
PK9	0	2	0	0	0	18	0	1	0	1	0
PO1	19	24	0	0	0	0	0	0	0	0	0
PO10	15	20	0	0	0	1	0	1	0	0	0
PO11	0	2	6	2	1	0	1	0	0	0	0
PO12	0	15	6	13	0	3	0	3	0	0	0
PO13	3	2	13	0	0	0	0	0	0	0	0
PO14	1	0	24	0	0	0	0	1	0	0	0
PO15	1	5	6	0	0	0	0	0	0	0	0
PO16	0	6	3	0	0	5	0	7	0	0	0
PO17	2	6	3	0	0	0	0	3	0	0	0
PO2	11	8	0	0	0	3	1	0	0	0	0
PO3	18	18	0	0	0	3	0	1	0	0	0
PO4	7	10	0	0	0	0	0	0	0	0	0
PO5	2	3	0	0	3	4	1	2	0	0	0
PO6	17	11	0	0	0	2	0	0	0	0	0
PO7	0	0	5	0	2	3	3	2	0	0	0

PO8	1	1	0	0	0	2	0	1	0	0	0
PO9	5	5	11	1	0	4	0	3	0	0	0
PUA1	0	0	25	7	0	18	0	0	0	0	0
PUA2	0	0	1	79	0	27	0	1	0	1	0
PUA3	0	3	0	25	0	25	0	25	0	0	0
PUA4	0	5	0	0	0	23	0	14	0	0	0
PUA5	1	9	3	0	0	4	0	13	0	1	0
PUB1	0	1	4	16	3	32	0	4	0	0	4
PUB10	0	2	4	1	0	3	19	0	0	0	0
PUB2	4	58	1	10	0	7	7	9	4	0	0
PUB3	1	10	2	0	0	6	0	3	0	0	0
PUB4	0	0	1	0	0	12	1	6	0	0	5
PUB5	0	0	0	2	0	15	0	6	0	0	3
PUB6	0	0	6	0	0	41	1	2	0	0	0
PUB7	0	0	6	2	0	11	0	7	0	0	0
PUB8	10	18	3	3	0	13	3	17	1	0	3
PUB9	0	50	3	0	0	4	1	6	1	0	0
PUC1	0	0	2	0	0	0	11	0	0	0	0
PUC10	0	4	1	7	0	21	0	13	1	0	0
PUC11	0	9	0	4	0	13	1	10	1	0	0
PUC12	0	74	0	0	0	3	0	10	5	0	0
PUC13	0	16	5	3	0	15	0	2	0	0	1
PUC14	0	46	1	16	0	14	0	2	1	0	0
PUC15	0	38	0	0	0	0	0	1	2	0	0
PUC16	0	50	0	1	0	2	0	3	2	0	0
PUC2	0	0	6	0	0	12	0	3	0	0	0
PUC3	0	0	1	0	0	37	0	6	0	0	0
PUC4	0	1	12	1	2	11	2	2	0	0	0
PUC5	0	1	2	0	0	3	0	2	0	1	0
PUC6	0	1	2	0	0	0	0	3	0	0	0
PUC7	2	5	0	0	0	35	0	6	0	0	2
PUC8	0	0	2	0	0	0	7	0	0	0	0
PUC9	0	0	1	0	0	38	0	9	0	0	6
WK1	3	2	1	1	0	12	1	3	0	0	1
WK2	0	0	4	0	0	0	0	0	0	0	0
WK3	0	0	5	0	0	0	0	1	0	0	0
WK4	3	8	0	3	0	9	0	14	1	0	1
WK5	0	3	1	4	0	15	0	9	0	0	0

Microsite	*Nebela tincta*	*Phryganella acropodia* type	*Physochila griseola* type	*Plagiopyxis labiata*	*Pseudodifflugia fulva* type	*Quadruella symmetrica* type	*Sphenoderia fissirostris*	*Trigonopyxis arcula*	*Trigonopyxis minuta*	*Trinema enchyles*	*Trinema lineare*
AK1	0	1	0	0	0	0	0	0	0	0	0
AK2	0	3	11	0	3	0	0	0	0	0	1
AK3	0	9	6	0	3	0	0	0	0	0	0
AK4	0	1	0	0	1	0	0	0	0	0	0
AK5	0	0	0	0	1	0	0	0	0	0	0
AK6	0	0	0	0	0	0	0	0	1	0	0
AK7	0	0	0	0	3	0	0	0	0	0	0
AK8	0	0	5	0	0	0	0	0	0	1	0
AK9	0	0	0	1	0	0	0	1	0	0	0
KHL1.1	0	0	0	0	0	0	0	3	0	0	0
KHL1.2	0	0	0	2	0	0	1	0	0	0	0
KHL1.3	0	1	0	0	2	0	0	0	0	0	0
KHL1.4	0	2	0	0	2	0	0	3	0	0	0
KHL1.5	0	9	0	0	11	0	0	0	0	1	0
KHL1.6	0	5	1	0	1	0	0	0	0	0	0
KHL1.7	0	0	0	0	8	8	0	0	2	0	9
KHL1.8	0	4	0	0	1	11	4	0	0	0	0
KHL1.9	0	0	0	0	0	0	0	0	0	0	2
KHL2.1	0	1	0	0	8	5	0	0	0	0	6
KHL2.2	0	0	0	0	8	5	0	0	0	0	3
KHL2.3	0	0	2	0	1	0	0	0	0	0	22
KHL2.4	0	0	0	0	3	6	12	0	0	0	7
KHL2.5	0	0	0	0	6	0	0	0	0	0	5
KHL2.6	0	0	0	0	13	15	0	1	0	1	15
KL1	0	0	0	0	0	0	0	0	0	0	0
KL10	0	1	9	0	4	0	0	2	0	0	0
KL11	0	0	0	0	10	0	0	0	0	0	0
KL12	0	1	0	4	3	0	1	0	1	0	0
KL13	0	1	2	0	9	0	0	3	0	0	0
KL2	0	0	0	3	1	0	0	1	1	0	0
KL3	1	1	1	0	2	0	1	0	0	0	0
KL4	0	1	0	0	0	0	0	1	0	0	0
KL5	0	1	4	0	3	0	0	1	0	0	0
KL6	2	3	3	0	6	0	0	1	0	0	0
KL7	0	0	3	0	0	0	0	0	0	0	0
KL8	0	0	1	0	0	0	2	0	0	0	0

KL9	0	0	4	0	6	0	0	0	0	0	0
PK1	0	2	0	5	2	0	0	1	0	0	0
PK10	0	0	0	0	1	0	0	0	0	0	0
PK11	0	0	2	0	0	0	0	0	1	0	0
PK12	0	1	7	1	0	0	10	0	0	0	0
PK13	0	0	1	0	1	0	8	0	0	2	1
PK14	0	0	0	0	0	0	0	0	2	0	0
PK15	0	0	0	1	0	0	0	0	0	0	0
PK16	0	0	0	3	0	0	0	2	0	0	0
PK17	0	0	0	1	21	0	0	3	0	0	0
PK2	0	0	0	1	0	0	0	0	0	0	0
PK3	1	2	1	4	1	0	0	0	0	0	0
PK4	0	0	0	1	0	0	0	0	0	0	0
PK5	0	0	0	0	0	0	0	0	0	0	0
PK6	0	0	0	0	0	0	1	0	0	0	0
PK7	0	0	0	3	0	0	0	0	0	0	0
PK8	0	0	0	0	11	0	1	0	0	1	1
PK9	0	0	1	0	0	0	1	0	0	0	0
PO1	0	0	0	0	0	0	0	0	0	0	0
PO10	0	0	0	0	0	0	0	0	0	0	8
PO11	0	0	0	0	2	0	0	1	0	0	1
PO12	0	0	0	0	0	0	2	1	1	0	0
PO13	0	0	0	0	0	0	1	0	0	0	0
PO14	0	0	0	0	0	0	0	0	0	0	0
PO15	0	0	0	0	0	0	0	0	0	0	1
PO16	0	0	0	0	0	0	2	3	0	0	0
PO17	0	0	0	2	0	0	1	0	0	0	0
PO2	0	0	0	1	0	0	1	0	0	0	0
PO3	0	0	0	0	2	0	0	0	0	0	9
PO4	0	0	0	0	0	0	0	2	0	0	2
PO5	0	0	0	0	0	0	0	0	0	0	0
PO6	0	0	0	0	0	0	0	0	0	0	2
PO7	0	2	0	0	0	0	0	0	0	0	0
PO8	0	1	0	0	0	0	0	2	1	0	0
PO9	0	0	0	0	0	0	1	0	1	0	0
PUA1	0	0	2	0	0	0	0	0	0	0	0
PUA2	0	8	0	0	0	0	0	0	0	0	0
PUA3	0	6	4	0	14	0	4	0	0	0	1
PUA4	0	0	1	1	5	0	0	0	0	0	0
PUA5	0	0	0	0	0	0	0	0	0	0	0
PUB1	0	0	1	0	0	0	0	0	0	0	0
PUB10	0	4	3	0	1	0	0	0	0	0	0
PUB2	0	1	1	7	2	0	0	5	3	0	0
PUB3	0	0	3	5	3	0	0	1	0	0	0
PUB4	0	0	6	0	0	0	0	0	0	0	0

PUB5	0	0	7	3	0	0	0	0	0	0	0
PUB6	0	0	1	1	0	0	0	0	0	0	0
PUB7	0	4	20	0	2	0	0	4	0	0	0
PUB8	0	0	2	5	0	0	0	0	0	0	0
PUB9	0	0	6	3	11	0	0	1	0	0	0
PUC1	0	3	7	0	0	0	0	1	0	0	0
PUC10	0	0	2	0	0	0	0	0	0	0	0
PUC11	0	0	0	1	15	0	0	2	0	0	0
PUC12	0	0	1	4	0	0	0	5	0	0	0
PUC13	0	2	1	2	0	0	0	0	0	0	0
PUC14	0	0	0	2	0	0	0	0	0	0	0
PUC15	0	0	0	2	0	0	0	1	0	0	0
PUC16	1	0	2	9	3	0	0	2	0	0	0
PUC2	0	0	8	0	0	0	0	0	0	0	0
PUC3	0	0	0	0	0	0	0	0	0	0	0
PUC4	0	0	0	0	0	0	0	0	0	0	0
PUC5	0	0	1	0	0	0	0	0	0	0	0
PUC6	0	0	1	0	0	0	0	0	0	0	0
PUC7	0	2	0	0	1	0	0	0	0	0	0
PUC8	0	2	0	0	0	0	0	0	0	0	0
PUC9	0	0	2	0	4	0	0	1	0	0	0
WK1	0	0	5	1	0	0	0	0	0	0	0
WK2	0	3	3	0	0	0	0	0	0	0	0
WK3	0	0	4	0	0	0	0	0	0	0	0
WK4	0	0	2	1	0	0	0	0	0	0	0
WK5	0	0	2	0	4	0	0	0	0	0	0

Appendix 4: Table of non-testate amoebae remains. *Habrotrocha angusticollis* is a common peatland rotifer. *Alona rustica*, *Chydorus* cf. *eurynotus*, and cf. *Alonella* spp. are cladocerans. Number of cladoceran individuals was determined by the maximum tally of cladoceran remains of either carapaces, postabdomens, or head shields for that taxa.

Microsite	*Habrotrocha angusticollis*	*Alona rustica*	*Chydorus* cf. *eurynotus*	cf. *Alonella* spp.
AK1	0	2	0	0
AK2	1	1	0	0
AK3	0	6	0	0
AK4	16	0	0	0
AK5	0	0	0	0
AK6	0	0	0	0
AK7	0	0	0	0
AK8	0	2	0	0
AK9	0	0	0	0
KHL1.1	8	19	2	5
KHL1.2	0	26	2	6
KHL1.3	0	20	0	1
KHL1.4	1	2	0	0
KHL1.5	0	7	1	0
KHL1.6	1	3	1	2
KHL1.7	0	5	0	0
KHL1.8	1	3	0	0
KHL1.9	0	0	0	0
KHL2.1	1	5	0	0
KHL2.2	1	20	0	4
KHL2.3	0	8	0	2
KHL2.4	7	0	0	0
KHL2.5	0	0	0	0
KHL2.6	0	1	0	0
KL1	0	0	0	0
KL10	1	0	0	0
KL11	0	0	0	0
KL12	0	0	0	0

KL13	4	0	0	0
KL2	0	0	0	0
KL3	0	0	1	0
KL4	4	0	2	0
KL5	0	0	0	0
KL6	3	0	0	0
KL7	0	0	0	0
KL8	3	0	0	0
KL9	3	0	0	0
PK1	0	0	0	0
PK10	0	0	0	0
PK11	0	0	0	0
PK12	3	0	27	0
PK13	3	0	0	0
PK14	4	0	0	0
PK15	0	0	0	0
PK16	1	0	0	0
PK17	0	0	0	0
PK2	0	0	0	0
PK3	0	0	0	0
PK4	0	0	0	0
PK5	0	0	2	0
PK6	0	0	0	0
PK7	0	0	0	0
PK8	0	0	1	0
PK9	0	0	0	0
PO1	0	3	0	0
PO10	1	4	6	0
PO11	8	0	0	0
PO12	20	0	0	0
PO13	1	16	6	0
PO14	7	3	0	0
PO15	13	3	0	0
PO16	18	1	0	0
PO17	2	0	0	0
PO2	6	0	0	0
PO3	2	0	0	0
PO4	1	0	0	0
PO5	5	3	0	0
PO6	0	3	0	0
PO7	9	0	0	0
PO8	4	0	0	0
PO9	5	0	0	0
PUA1	0	42	0	0
PUA2	0	1	0	0

PUA3	0	0	0	0
PUA4	0	0	0	0
PUA5	0	1	3	0
PUB1	4	0	0	0
PUB10	0	44	2	0
PUB2	1	0	0	0
PUB3	2	0	0	0
PUB4	0	2	0	0
PUB5	1	17	0	1
PUB6	4	25	0	0
PUB7	1	42	2	0
PUB8	2	0	0	0
PUB9	1	0	0	0
PUC1	6	55	0	0
PUC10	0	0	0	0
PUC11	1	0	0	0
PUC12	0	0	0	0
PUC13	0	2	0	0
PUC14	2	0	0	0
PUC15	0	0	0	0
PUC16	2	0	0	0
PUC2	0	6	0	0
PUC3	0	0	0	0
PUC4	0	35	0	0
PUC5	0	11	0	0
PUC6	0	6	0	0
PUC7	0	0	0	0
PUC8	0	145	14	0
PUC9	3	0	0	0
WK1	1	0	0	0
WK2	1	11	0	0
WK3	0	31	0	0
WK4	1	0	0	0
WK5	1	0	0	0

Appendix 5: Table of environmental measurements for all microsites

Microsite	WTD (cm)	pH	Conductivity (mS)	Bulk Density (g/cm^3)	Loss-on-ignition (%)
AK1	-6.5	4	1.7	0.096	89.6
AK2	-1	3.9	0.08	0.105	97.1
AK3	-6.5	4	0.07	0.077	97.4
AK4	-13.5	5.9	0.09	0.088	86.4
AK5	22.5	3.5	0.55	0.047	93.6
AK6	57	3.4	0.8	0.031	100
AK7	25	3.8	0.85	0.099	92.9
AK8	1	4.1	0.17	0.071	87.3
AK9	28	3.9	0.13	0.118	97.5
KHL1.1	-6	4.5	0.01	0.082	75.6
KHL1.2	1	4.2	0.01	0.09	91.1
KHL1.3	7	4.9	0.02	0.107	80.4
KHL1.4	11	5.5	0.3	0.109	77.1
KHL1.5	-15	5.7	0.02	0.114	76.3
KHL1.6	-10	5.1	0.02	0.119	68.9
KHL1.7	22	5.4	0.03	0.126	81
KHL1.8	-4	5.6	0.05	0.089	77.5
KHL1.9	28	5.2	0.01	0.16	95.6
KHL2.1	4	5.5	0.23	0.147	90.5
KHL2.2	-1	5.5	0.05	0.082	78
KHL2.3	6	4.1	0.94	0.145	94.5
KHL2.4	17	5	0.22	0.098	88.8
KHL2.5	29	4.1	3.84	0.199	90.5
KHL2.6	14	4.6	0.92	0.108	78.7
KL1	45	3.3	0.06	0.092	91.3
KL10	13.5	4.1	0.02	0.138	85.5
KL11	25.5	4	0.04	0.107	94.4
KL12	38	4.2	0.32	0.084	98.8
KL13	-2	4.5	0.02	0.097	96.9
KL2	27	3.4	0.03	0.096	90.6
KL3	1	3.5	0.02	0.094	86.2
KL4	-27	3.3	0.02	0.093	96.8
KL5	18	3.5	0.04	0.096	92.7
KL6	13	3.7	0.03	0.145	91
KL7	1	3.9	0.03	0.131	96.9
KL8	10	3.7	0.02	0.122	91.8
KL9	36	3.9	0.03	0.101	91.1
PK1	29.5	3.7	0.06	0.077	100
PK10	6	3.9	0.09	0.078	75.6

PK11	10.5	4.8	0.11	0.085	96.5
PK12	-9.5	3.7	0.09	0.143	92.3
PK13	9.5	3.9	0.06	0.089	100
PK14	45	3.6	0.35	0.064	96.9
PK15	29	3.8	0.22	0.083	92.8
PK16	33	3.4	0.48	0.085	94.1
PK17	58	3.3	0.34	0.105	89.5
PK2	28	3.8	0.13	0.075	98.7
PK3	16	3.4	0.25	0.07	92.9
PK4	29	3.3	0.14	0.072	93.1
PK5	23.5	3.8	0.16	0.064	96.9
PK6	11.5	3.2	0.16	0.065	100
PK7	31.5	3.4	0.18	0.065	98.5
PK8	-5.5	4.1	0.15	0.069	81.2
PK9	8.5	3.5	0.11	0.078	91
PO1	-6.5	4.3	0.11	0.136	82.4
PO10	0	4.6	0.09	0.152	86.2
PO11	32	4.4	0.05	0.134	86.6
PO12	21	4.6	0.01	0.194	74.7
PO13	5	4.5	0.07	0.271	73.4
PO14	9	4.3	0.07	0.167	73.7
PO15	12	4.4	0.09	0.167	80.2
PO16	28	4.7	0.03	0.194	74.7
PO17	12	4.2	0.31	0.156	81.8
PO2	2	4.4	0.09	0.159	81.8
PO3	5	4.5	0.1	0.138	77.5
PO4	17	4.5	0.11	0.125	79.2
PO5	-6	4.5	0.05	0.13	90.8
PO6	-7	4.5	0.04	0.159	76.1
PO7	13	4.5	0.05	0.167	80.2
PO8	22	4.4	0.04	0.14	76.4
PO9	14	4.6	0.03	0.205	78.5
PUA1	1	4.6	0.01	0.096	93.8
PUA2	5	4.5	0.01	0.099	96
PUA3	13.5	4.2	0.01	0.118	91.5
PUA4	14.5	3.8	0.01	0.071	93
PUA5	-8.5	3.7	0.01	0.071	91.5
PUB1	23.5	4	0.02	0.138	96.4
PUB10	-5	4.2	0.01	0.118	94.9
PUB2	38.5	3.6	0.01	0.19	95.8
PUB3	18.5	4.1	0.03	0.163	96.9
PUB4	14.5	4.1	0.01	0.107	95.3
PUB5	2	4	0.01	0.071	97.2
PUB6	-3	3.7	0.01	0.083	95.2
PUB7	1	4.4	0.01	0.1	97

PUB8	11	3.9	0.01	0.144	95.1
PUB9	17	3.9	0.01	0.143	95.8
PUC1	-6	4.7	0.02	0.121	96.7
PUC10	13	3.5	0.01	0.123	96.7
PUC11	22	4	0.02	0.118	96.6
PUC12	30	4.1	0.01	0.158	96.2
PUC13	6.5	4	0.02	0.108	96.3
PUC14	19.5	4.1	0.01	0.071	97.2
PUC15	32.5	4	0.01	0.228	97.8
PUC16	27.5	4.1	0.01	0.192	96.9
PUC2	17	4.3	0.03	0.179	96.1
PUC3	9.5	4.2	0.01	0.129	98.4
PUC4	1	4.1	0.01	0.163	97.5
PUC5	3	4	0.01	0.122	98.4
PUC6	3	4	0.01	0.056	94.6
PUC7	16.5	4	0.01	0.103	94.2
PUC8	-9.5	4	0.01	0.085	95.3
PUC9	12.5	4.2	0.01	0.087	96.6
WK1	7.5	4.1	0.01	0.078	97.4
WK2	0	4	0.01	0.068	94.1
WK3	0	4.2	0.02	0.088	94.3
WK4	14	4.2	0.02	0.135	97
WK5	26	4	0.02	0.096	95.8

Appendix 6: Table of vegetation proportion cover for all microsites.

Microsite	*Sphagnum palustre*	*Deschampsia nubigena*	*Rhynchospora rugosa* var. *lavarum*	*Rhynchospora chinensis* subsp. *spiciformis*	*Racomitrium lanuginosum*	*Oreobolus furcatus*	*Juncus planifolius*	*Machaerina angustifolia*	*Dicanthelium cynodon*	*Panicum* spp.	*Metrosideros polymorpha*
AK1	1	0	0	0	0	0	0	0	0	0	0
AK2	1	0	0	0	0	0	0	0	0	0	0
AK3	0.8	0	0	0	0	0	0	0	0	0	0
AK4	0	0	0	0.8	0	0	0	0	0	0	0
AK5	0.8	0	0	0	0	0	0	0	0	0	0.1
AK6	1	0	0	0	0	0	0	0	0	0	0
AK7	0.4	0.4	0	0	0	0	0	0	0	0	0.05
AK8	0.5	0.5	0	0	0	0	0	0	0	0	0
AK9	0.6	0.3	0	0	0	0	0	0	0	0	0
KHL1.1	0	0	0.3	0	0	0	0.4	0	0	0	0
KHL1.2	0.8	0	0	0	0	0	0.2	0	0	0	0
KHL1.3	0	0	0	0	0	0	0.8	0	0	0.2	0
KHL1.4	0	0	0	0	0	0	0.8	0.2	0	0	0
KHL1.5	0	0	0	0.6	0	0	0.4	0	0	0	0
KHL1.6	0	0	0	0	0	0	1	0	0	0	0
KHL1.7	0	0	0	0.2	0	0	0	0	0	0	0
KHL1.8	0	0	0	0.5	0	0	0.5	0	0	0	0
KHL1.9	0	0	0	0	0.8	0	0	0.2	0	0	0
KHL2.1	0	0	0	0	0	0	0.8	0	0.2	0	0
KHL2.2	0	0	0	0	0	0	0.2	0	0.8	0	0
KHL2.3	0	0	0	0	0.6	0	0.4	0	0	0	0
KHL2.4	0	0	0	0	0	0	1	0	0	0	0
KHL2.5	0	0.2	0	0	0.8	0	0	0	0	0	0
KHL2.6	0	0	0	0	0	0	0	0	0	0	0
KL1	0.9	0	0	0	0	0	0	0	0	0	0.1
KL10	0.2	0.7	0	0	0	0	0	0	0	0	0
KL11	0.2	0.6	0	0	0	0	0	0	0	0	0.1
KL12	0.8	0	0	0	0	0	0	0	0	0	0.2
KL13	0.2	0.6	0	0	0.2	0	0	0	0	0	0
KL2	1	0	0	0	0	0	0	0	0	0	0
KL3	1	0	0	0	0	0	0	0	0	0	0
KL4	1	0	0	0	0	0	0	0	0	0	0
KL5	1	0	0	0	0	0	0	0	0	0	0
KL6	0	0	0	0.8	0.2	0	0	0	0	0	0

KL7	0.2	0.6	0	0	0.2	0	0	0	0	0	0
KL8	0.2	0.6	0	0	0	0	0	0	0	0	0
KL9	0.2	0.7	0	0	0	0	0	0	0	0	0
PK1	0.9	0	0	0	0	0	0	0	0	0	0
PK10	1	0	0	0	0	0	0	0	0	0	0
PK11	0.8	0	0	0.2	0	0	0	0	0	0	0
PK12	0	0	0	1	0	0	0	0	0	0	0
PK13	0.8	0	0	0	0	0	0	0	0	0	0
PK14	0.8	0	0	0	0	0	0	0	0	0	0.1
PK15	0.75	0	0	0	0	0	0	0	0	0	0.1
PK16	0.75	0	0	0	0	0	0	0	0	0	0.1
PK17	0.8	0	0	0	0	0	0	0	0	0	0.05
PK2	0.9	0	0	0	0	0	0	0	0	0	0
PK3	0.9	0	0	0	0	0	0	0	0	0	0
PK4	0.9	0	0	0	0	0	0	0	0	0	0.05
PK5	0.9	0	0	0	0	0	0	0	0	0	0
PK6	0.8	0	0	0	0	0	0	0	0	0	0.1
PK7	0.8	0	0	0	0	0	0	0	0	0	0
PK8	0.7	0	0	0	0	0	0	0	0	0	0
PK9	1	0	0	0	0	0	0	0	0	0	0
PO1	0	0	0.4	0.4	0.2	0	0	0	0	0	0
PO10	0	0	0.3	0.7	0	0	0	0	0	0	0
PO11	0	0.6	0.1	0	0.3	0	0	0	0	0	0
PO12	0	0.3	0.1	0	0.6	0	0	0	0	0	0
PO13	0	0	0	1	0	0	0	0	0	0	0
PO14	0	0	0.3	0.7	0	0	0	0	0	0	0
PO15	0	0.1	0.1	0.4	0.4	0	0	0	0	0	0
PO16	0	0.5	0	0	0.5	0	0	0	0	0	0
PO17	0	0.1	0	0.7	0.2	0	0	0	0	0	0
PO2	0	0.1	0.9	0	0	0	0	0	0	0	0
PO3	0	0	0.4	0.4	0	0	0	0	0	0	0.2
PO4	0	0.3	0.5	0	0.2	0	0	0	0	0	0
PO5	0	0	0.2	0.8	0	0	0	0	0	0	0
PO6	0	0.5	0	0.5	0	0	0	0	0	0	0
PO7	0	0.25	0.2	0.45	0.3	0	0	0	0	0	0
PO8	0	0.2	0.4	0	0.4	0	0	0	0	0	0
PO9	0	0	0.25	0.75	0	0	0	0	0	0	0
PUA1	0.2	0	0	0.8	0	0	0	0	0	0	0
PUA2	0.2	0	0	0.8	0	0	0	0	0	0	0
PUA3	0.2	0	0	0	0	0	0	0	0	0	0
PUA4	1	0	0	0	0	0	0	0	0	0	0
PUA5	1	0	0	0	0	0	0	0	0	0	0
PUB1	0.3	0	0.6	0	0	0	0	0	0	0	0
PUB10	0.8	0	0	0.2	0	0	0	0	0	0	0
PUB2	0	0	0.7	0	0.3	0	0	0	0	0	0

PUB3	0	0	0	0	0.2	0.8	0	0	0	0	0
PUB4	0	0	0	0	0	0.9	0	0	0	0	0
PUB5	0.2	0	0	0	0.8	0	0	0	0	0	0
PUB6	0.4	0	0	0	0	0.4	0	0.2	0	0	0
PUB7	0	0	0	1	0	0	0	0	0	0	0
PUB8	0.2	0	0.6	0	0.2	0	0	0	0	0	0
PUB9	0	0	0.6	0	0.4	0	0	0	0	0	0
PUC1	0.6	0	0	0	0	0	0	0.2	0	0	0
PUC10	0.3	0	0.7	0	0	0	0	0	0	0	0
PUC11	0.2	0	0.7	0	0	0	0	0	0	0	0.1
PUC12	0	0	0	0	0.75	0.15	0	0	0	0	0.1
PUC13	0.2	0	0.6	0	0.2	0	0	0	0	0	0
PUC14	0.2	0	0.6	0	0.2	0	0	0	0	0	0
PUC15	0	0	0.3	0	0.7	0	0	0	0	0	0
PUC16	0	0	0	0	0.7	0	0	0	0	0	0
PUC2	0	0	0	0	0.8	0	0	0.15	0	0	0
PUC3	0	0	0	0	0	0.8	0	0	0	0	0
PUC4	0.1	0	0	0	0.8	0	0.1	0	0	0	0
PUC5	0	0	0	0	0.2	0.8	0	0	0	0	0
PUC6	0.8	0	0	0	0	0	0	0.2	0	0	0
PUC7	0	0	0	0	0	1	0	0	0	0	0
PUC8	0	0	0	1	0	0	0	0	0	0	0
PUC9	0.2	0	0.8	0	0	0	0	0	0	0	0
WK1	1	0	0	0	0	0	0	0	0	0	0
WK2	1	0	0	0	0	0	0	0	0	0	0
WK3	0	0	0	1	0	0	0	0	0	0	0
WK4	0.4	0	0.5	0	0	0	0	0	0	0	0.05
WK5	0.2	0	0.8	0	0	0	0	0	0	0	0

Microsite	*Lycopodiella cernua*	*Leptecophylla tameiameia*	*Vaccinium reticulatum*	*Juncus effusus*	*Carex alligata*	*Holcus lanatus*	*Dicranopteris linearis*	*Cibotium* spp.	*Hedychium gardnerium*	*Cheirodendron trigynum*
AK1	0	0	0	0	0	0	0	0	0	0
AK2	0	0	0	0	0	0	0	0	0	0
AK3	0	0	0	0	0	0	0	0.2	0	0
AK4	0	0	0	0	0	0.2	0	0	0	0
AK5	0	0.1	0	0	0	0	0	0	0	0
AK6	0	0	0	0	0	0	0	0	0	0

AK7	0	0	0.05	0	0	0	0	0.05	0.05	0
AK8	0	0	0	0	0	0	0	0	0	0
AK9	0	0	0	0	0	0	0.1	0	0	0
KHL1.1	0	0	0	0	0	0.3	0	0	0	0
KHL1.2	0	0	0	0	0	0	0	0	0	0
KHL1.3	0	0	0	0	0	0	0	0	0	0
KHL1.4	0	0	0	0	0	0	0	0	0	0
KHL1.5	0	0	0	0	0	0	0	0	0	0
KHL1.6	0	0	0	0	0	0	0	0	0	0
KHL1.7	0	0	0	0	0	0.8	0	0	0	0
KHL1.8	0	0	0	0	0	0	0	0	0	0
KHL1.9	0	0	0	0	0	0	0	0	0	0
KHL2.1	0	0	0	0	0	0	0	0	0	0
KHL2.2	0	0	0	0	0	0	0	0	0	0
KHL2.3	0	0	0	0	0	0	0	0	0	0
KHL2.4	0	0	0	0	0	0	0	0	0	0
KHL2.5	0	0	0	0	0	0	0	0	0	0
KHL2.6	0	0	0	1	0	0	0	0	0	0
KL1	0	0	0	0	0	0	0	0	0	0
KL10	0	0	0	0	0	0.1	0	0	0	0
KL11	0	0.1	0	0	0	0	0	0	0	0
KL12	0	0	0	0	0	0	0	0	0	0
KL13	0	0	0	0	0	0	0	0	0	0
KL2	0	0	0	0	0	0	0	0	0	0
KL3	0	0	0	0	0	0	0	0	0	0
KL4	0	0	0	0	0	0	0	0	0	0
KL5	0	0	0	0	0	0	0	0	0	0
KL6	0	0	0	0	0	0	0	0	0	0
KL7	0	0	0	0	0	0	0	0	0	0
KL8	0	0	0.1	0	0.1	0	0	0	0	0
KL9	0.1	0	0	0	0	0	0	0	0	0
PK1	0.05	0	0.05	0	0	0	0	0	0	0
PK10	0	0	0	0	0	0	0	0	0	0
PK11	0	0	0	0	0	0	0	0	0	0
PK12	0	0	0	0	0	0	0	0	0	0
PK13	0	0	0	0	0.2	0	0	0	0	0
PK14	0	0	0.1	0	0	0	0	0	0	0
PK15	0.1	0.05	0	0	0	0	0	0	0	0
PK16	0.1	0	0.05	0	0	0	0	0	0	0
PK17	0	0	0.1	0	0	0	0	0	0	0.05
PK2	0.05	0	0.05	0	0	0	0	0	0	0
PK3	0.05	0	0.05	0	0	0	0	0	0	0
PK4	0	0	0.05	0	0	0	0	0	0	0
PK5	0.05	0	0.05	0	0	0	0	0	0	0

PK6	0	0.1	0	0	0	0	0	0	0	0
PK7	0	0	0	0	0.2	0	0	0	0	0
PK8	0	0	0	0	0.3	0	0	0	0	0
PK9	0	0	0	0	0	0	0	0	0	0
PO1	0	0	0	0	0	0	0	0	0	0
PO10	0	0	0	0	0	0	0	0	0	0
PO11	0	0	0	0	0	0	0	0	0	0
PO12	0	0	0	0	0	0	0	0	0	0
PO13	0	0	0	0	0	0	0	0	0	0
PO14	0	0	0	0	0	0	0	0	0	0
PO15	0	0	0	0	0	0	0	0	0	0
PO16	0	0	0	0	0	0	0	0	0	0
PO17	0	0	0	0	0	0	0	0	0	0
PO2	0	0	0	0	0	0	0	0	0	0
PO3	0	0	0	0	0	0	0	0	0	0
PO4	0	0	0	0	0	0	0	0	0	0
PO5	0	0	0	0	0	0	0	0	0	0
PO6	0	0	0	0	0	0	0	0	0	0
PO7	0	0	0	0	0	0	0	0	0	0
PO8	0	0	0	0	0	0	0	0	0	0
PO9	0	0	0	0	0	0	0	0	0	0
PUA1	0	0	0	0	0	0	0	0	0	0
PUA2	0	0	0	0	0	0	0	0	0	0
PUA3	0	0	0	0	0	0.8	0	0	0	0
PUA4	0	0	0	0	0	0	0	0	0	0
PUA5	0	0	0	0	0	0	0	0	0	0
PUB1	0	0.05	0.05	0	0	0	0	0	0	0
PUB10	0	0	0	0	0	0	0	0	0	0
PUB2	0	0	0	0	0	0	0	0	0	0
PUB3	0	0	0	0	0	0	0	0	0	0
PUB4	0	0.1	0	0	0	0	0	0	0	0
PUB5	0	0	0	0	0	0	0	0	0	0
PUB6	0	0	0	0	0	0	0	0	0	0
PUB7	0	0	0	0	0	0	0	0	0	0
PUB8	0	0	0	0	0	0	0	0	0	0
PUB9	0	0	0	0	0	0	0	0	0	0
PUC1	0.1	0	0	0	0	0	0.1	0	0	0
PUC10	0	0	0	0	0	0	0	0	0	0
PUC11	0	0	0	0	0	0	0	0	0	0
PUC12	0	0	0	0	0	0	0	0	0	0
PUC13	0	0	0	0	0	0	0	0	0	0
PUC14	0	0	0	0	0	0	0	0	0	0
PUC15	0	0	0	0	0	0	0	0	0	0
PUC16	0	0	0	0	0	0	0.3	0	0	0

PUC2	0	0	0	0	0	0.05	0	0	0	0
PUC3	0	0	0	0	0	0	0.2	0	0	0
PUC4	0	0	0	0	0	0	0	0	0	0
PUC5	0	0	0	0	0	0	0	0	0	0
PUC6	0	0	0	0	0	0	0	0	0	0
PUC7	0	0	0	0	0	0	0	0	0	0
PUC8	0	0	0	0	0	0	0	0	0	0
PUC9	0	0	0	0	0	0	0	0	0	0
WK1	0	0	0	0	0	0	0	0	0	0
WK2	0	0	0	0	0	0	0	0	0	0
WK3	0	0	0	0	0	0	0	0	0	0
WK4	0	0	0	0	0	0	0.05	0	0	0
WK5	0	0	0	0	0	0	0	0	0	0